

# Nanoscale Imaging and Polarization Dynamics in Relaxor Ferroelectrics

**Andrei Kholkin**

*Department of Ceramics and Glass Engineering &  
Center for Research in Ceramic and Composite Materials,  
University of Aveiro (Portugal)*

**3<sup>rd</sup> Piezoresponse Force Microscopy Workshop  
Oak Ridge National Laboratory  
22-24 of September, 2008**

# Acknowledgements

- S. Kalinin, S. Jesse, ORNL, USA
- V. Shvartsman, University of Duisburg-Essen, Germany
- D. Kiselev, I. Bdikin, University of Aveiro, Portugal
- B. Dkhil, Ecole Centrale Paris, France
- A. Safari, Rutgers University, USA
- A. Sternberg, K. Bormanis, Institute of Physics, Latvia
- M. Tjunina, University of Oulu, Finland
- S. Vakhrushev, Ioffe Institute, Russia



User proposal CNMS 2007-265



**FCT** Fundação para a Ciência e a Tecnologia  
MINISTÉRIO DA CIÊNCIA, TECNOLOGIA E ENSINO SUPERIOR



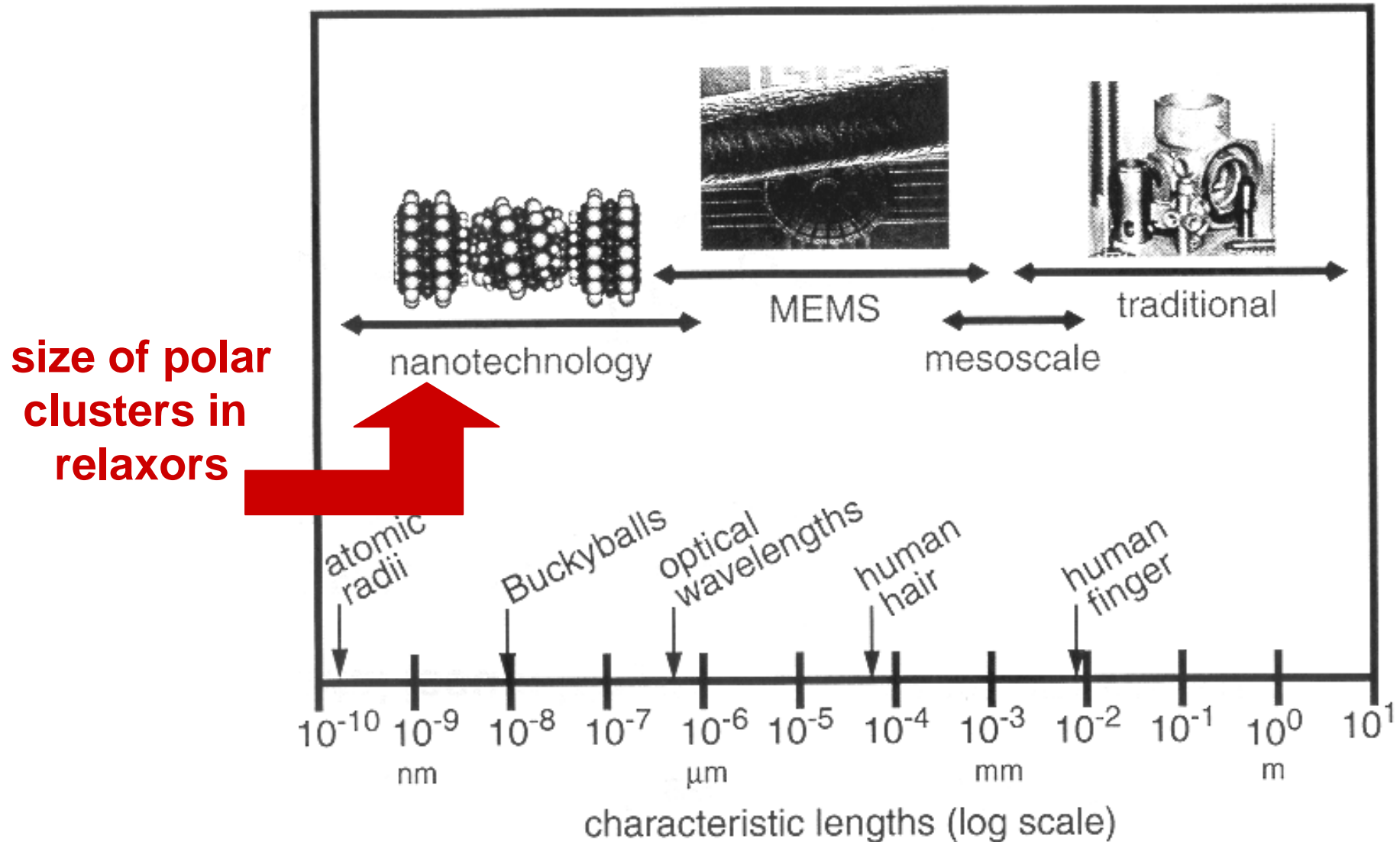
**Agilent Technologies**

Joint Agilent-CICECO Laboratory

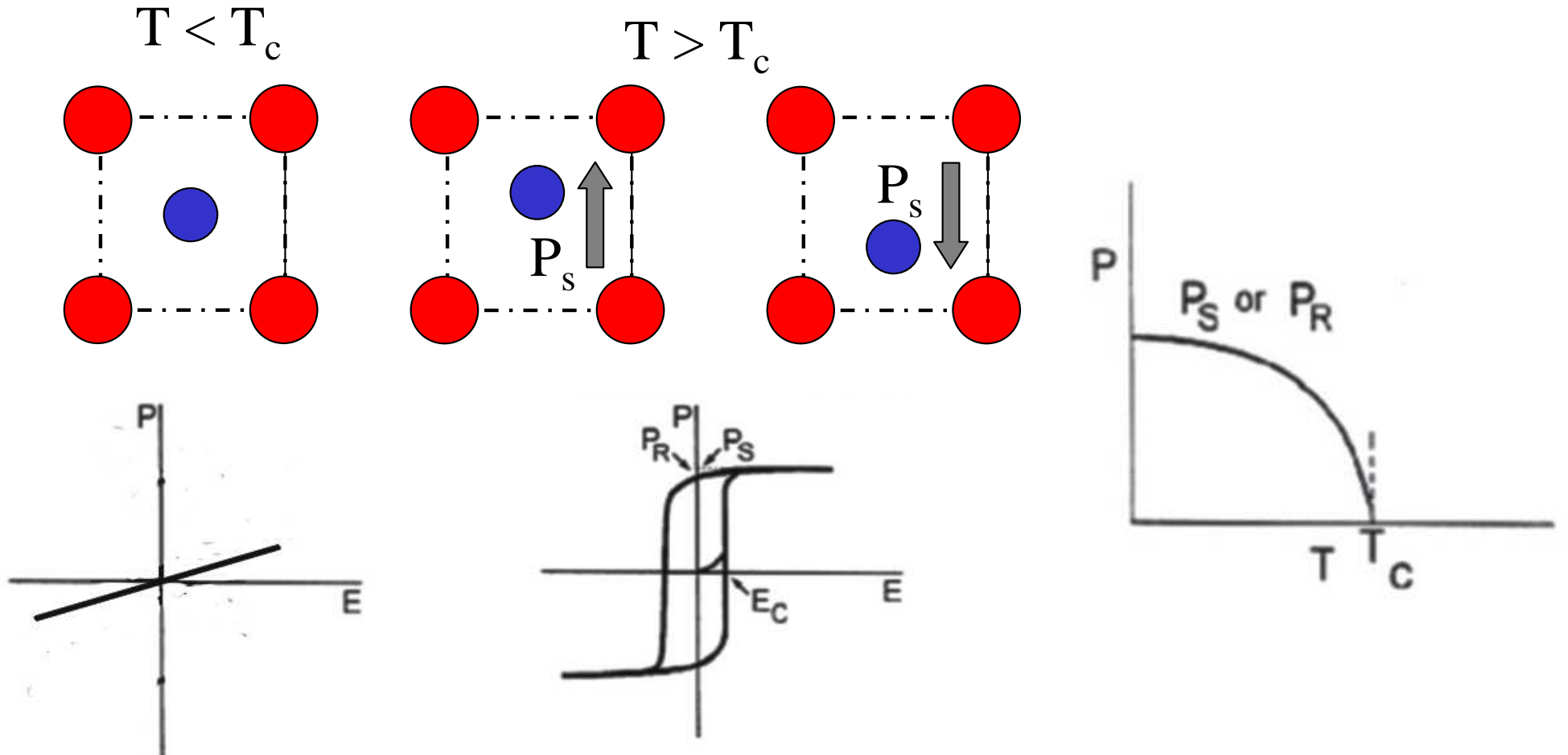
# Outline

- Introduction to relaxors
- $\text{Sr}_x\text{Ba}_{1-x}\text{Nb}_2\text{O}_6$  uniaxial system with positional disorder
- PMN and its solid solutions with  $\text{PbTiO}_3$
- PZN-PT single crystals with giant piezoresponse
- Relaxor ceramics (PMN, PLZT) at the nanoscale
- Relaxor thin films as natural nanocomposites
- Conclusions

# *Future of Piezoelectric Transduction - Nanoscale Sensors and Actuators*



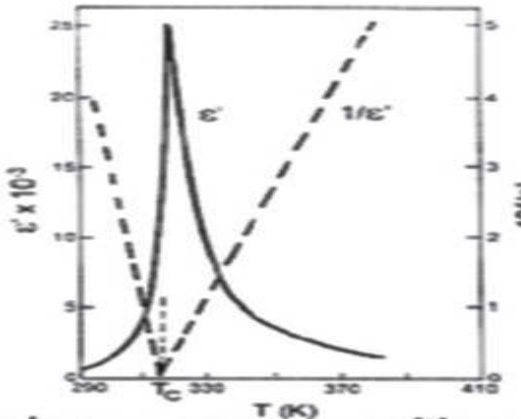
# Ferroelectrics



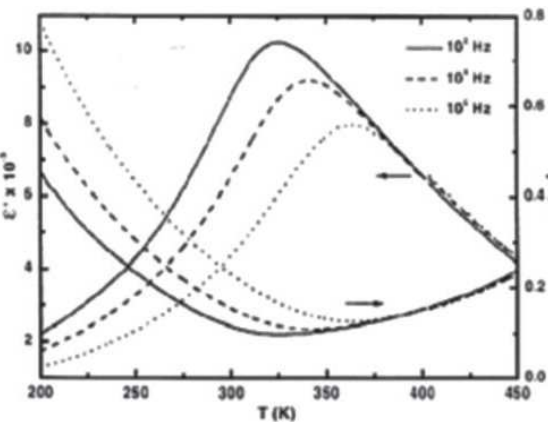
Ferroelectrics – materials with spontaneous polarization,  $P_s$ , which can be switched by an external electric field.

$P_s$  arises at  $T_c$  as the results of structural phase transition with the loss of inversion center.

# Ferroelectrics vs. Relaxors



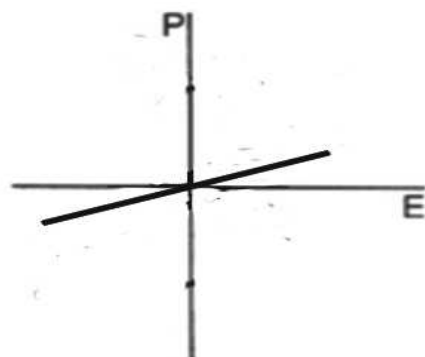
$$T > T_m, \epsilon^{-1} = \frac{C}{T - T_0}$$



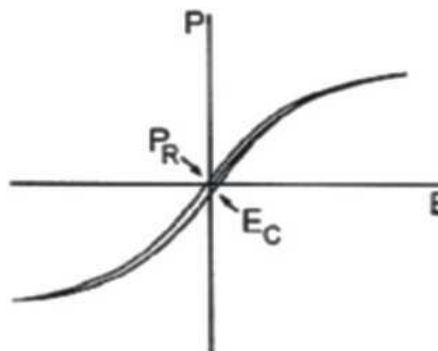
$$T > T_m, \epsilon^{-1} \neq \frac{C}{T - T_0}$$

❖ A sharp narrow maximum of  $\epsilon(T)$  at  $T_c$

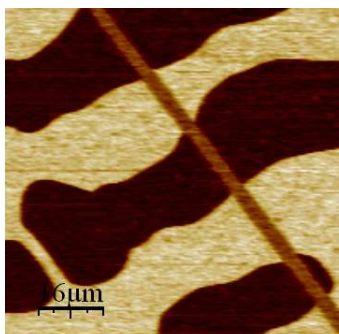
❖ A broad frequency dependent maximum on  $\epsilon(T)$ , not related to a phase transition.



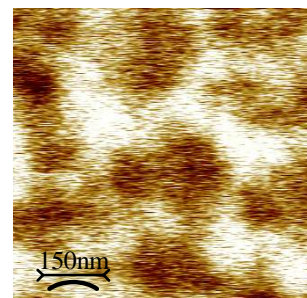
❖ Linear  $P(E)$ , no hysteresis above  $T_c$



❖ Non-linear  $P(E)$ , „slim“ hysteresis loops above  $T_m$ .



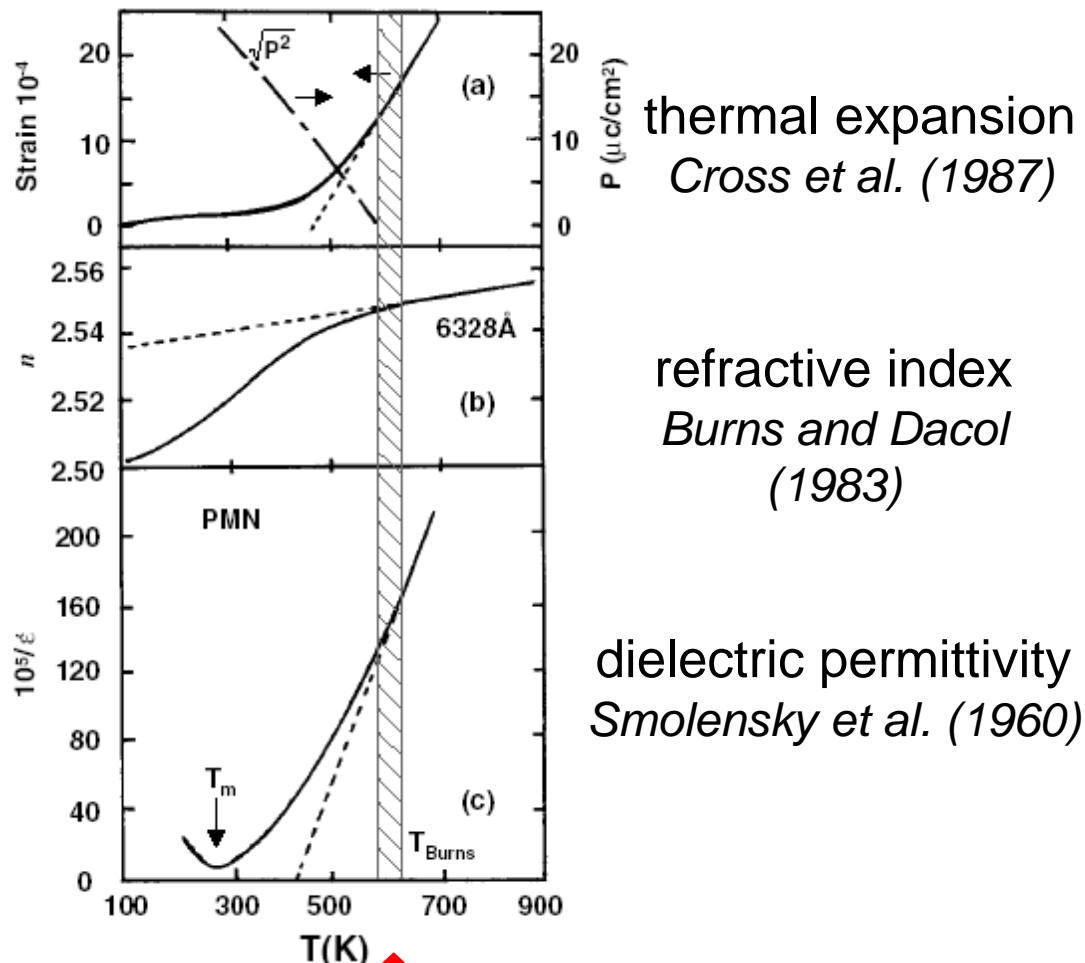
❖ Long-range polar order, macrosized domains below  $T_c$



❖ Short-range ordered polar regions at  $T \gg T_m$

# Manifestation of PNRs

sensitive to  $\overline{P^2}$



Burns temperature –  
appearance of PNRs

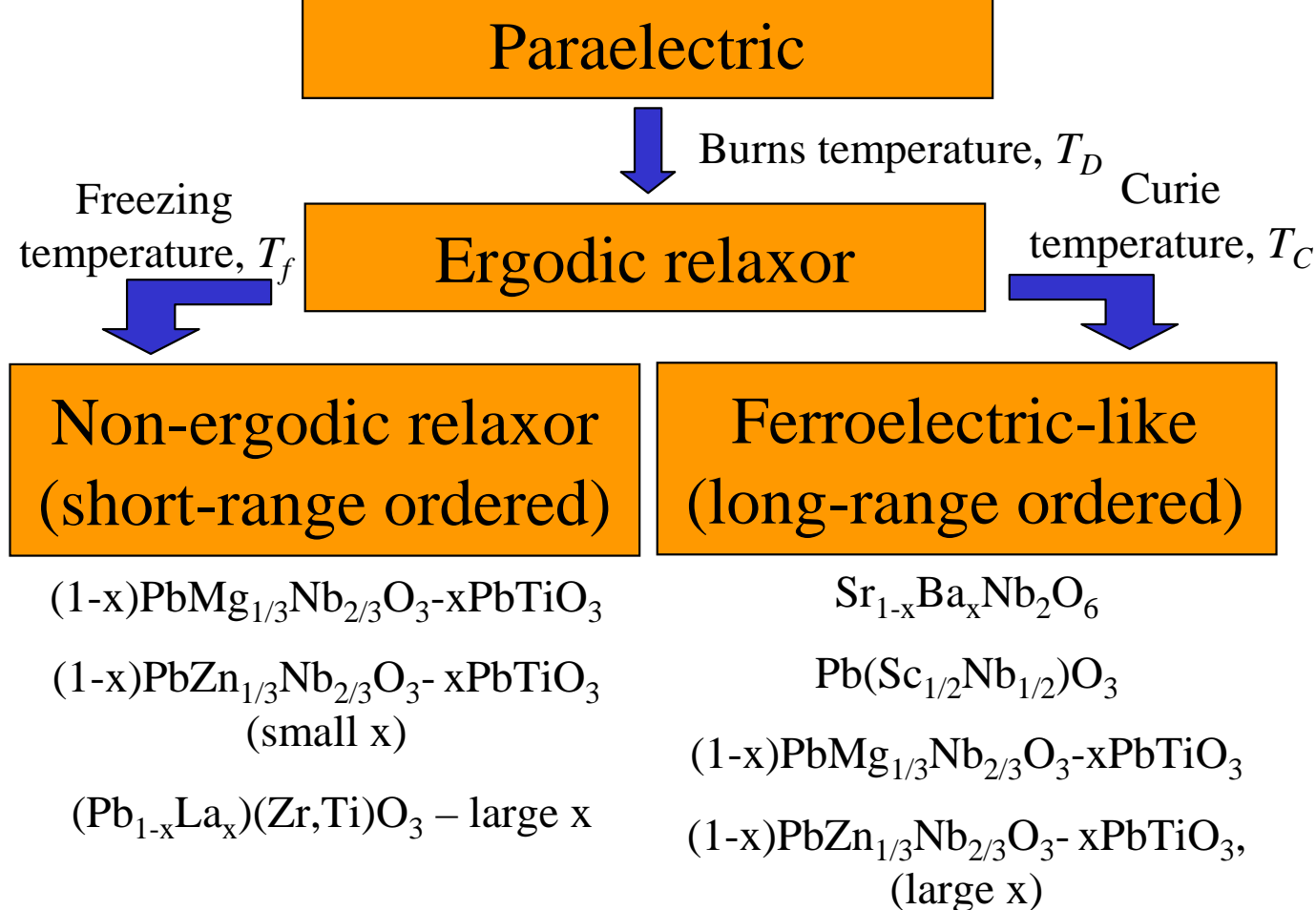
From Samara, JPCM 15, R367 (2003)

- Relaxors – materials with lattice disorder.
- Disorder is a source of random fields
- Random fields destroy long-range ordered ground state
- Fluctuations of random fields promote nucleation of PNRs

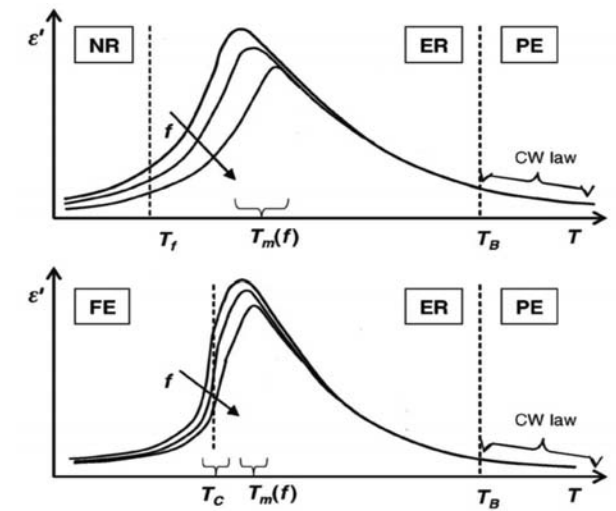
- excellent properties for multilayer capacitors and electro mechanical actuators:

$\epsilon \sim 10^4$ ,  $d_{33} \sim 10^3 \text{ pC/N}$   
(used, e.g. in Hubble telescope)

# Relaxors: evolution of polar structures



Bokov & Ye, JMS **41**, 31 (2006)

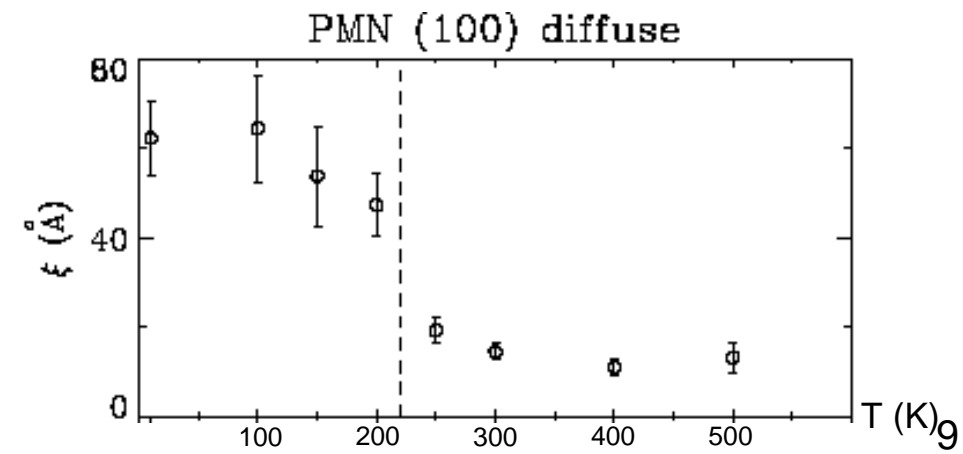
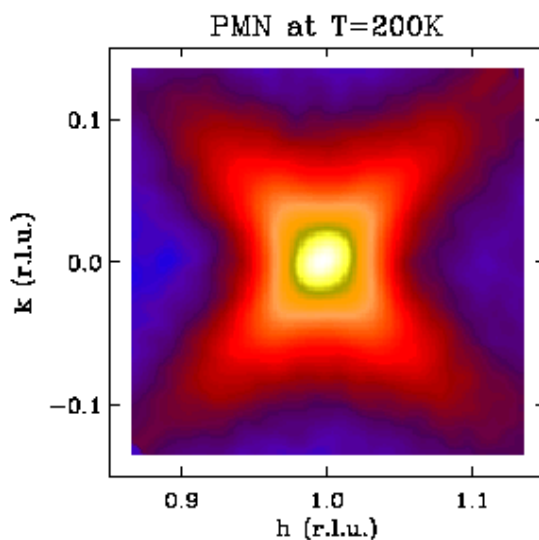


- ❖ In ergodic state ( $T_C$  ( $T_f$ )  $< T < T_D$ ) - highly mobile PNRs of size of several nm
- ❖ Increase of number of PNRs on cooling from  $T_D$ ; Growth of PNRs in vicinity of  $T_f$
- ❖ At  $T_f$  ( $T_C$ ) – slowing down of PNRs dynamic and transition into nonergodic relaxor (glassy-like) or ferroelectric state.

# Models of relaxors

- Smolensky model (local composition inhomogeneity)
- Superparaelectric model
- Dipole glass model
- Random field model (frustrated ferroelectric)
- Spherical random-bond-random-field model

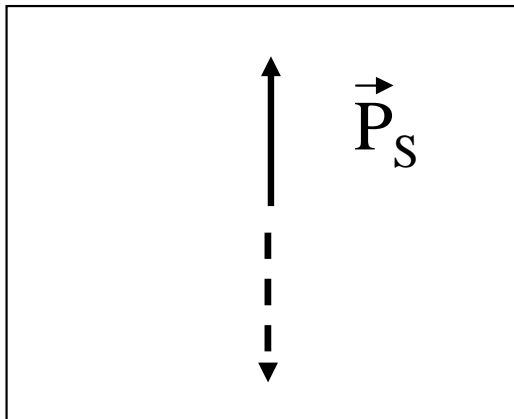
Most agree on existence of polar reorientable units  
**(Polar Nano Regions – PNRs) with the size of 2-10 nm!**  
However, only average size/concentration  
could be measured until recently.



# Ground state of relaxors

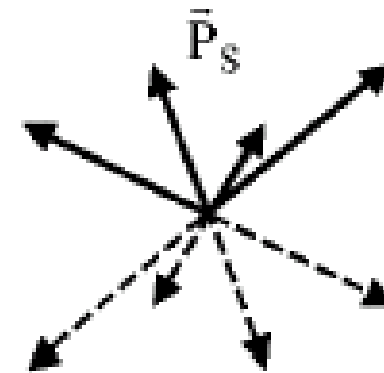
## Uniaxial relaxor

$\text{SrBaNb}_2\text{O}_6$  (SBN)



## Cubic relaxors

$\text{PbMg}_{1/3}\text{Nb}_{2/3}\text{O}_3 - \text{PbTiO}_3$



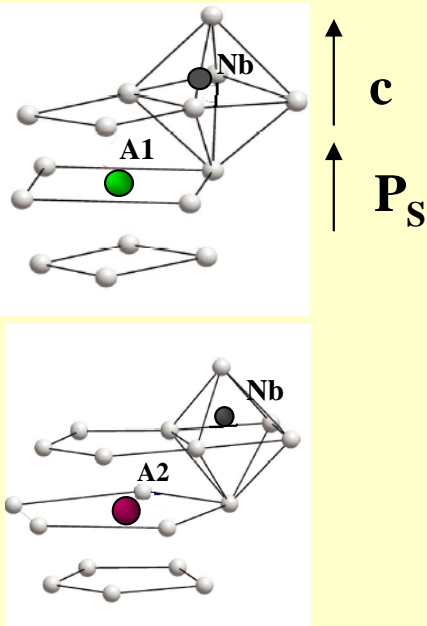
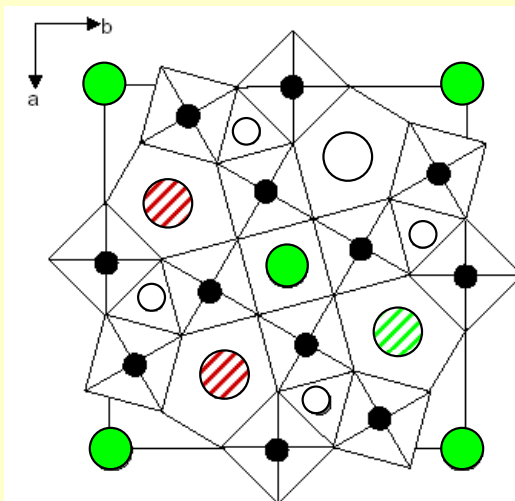
- ❖ One-component order parameter.  
Long-range ordered ground state

- ❖ Quasi-continuous order parameter. Short-range ordered (glassy like) ground state

Therefore, we will start with SBN !

# $(\text{Sr}_x\text{Ba}_{1-x})\text{Nb}_2\text{O}_6$ (SBN)

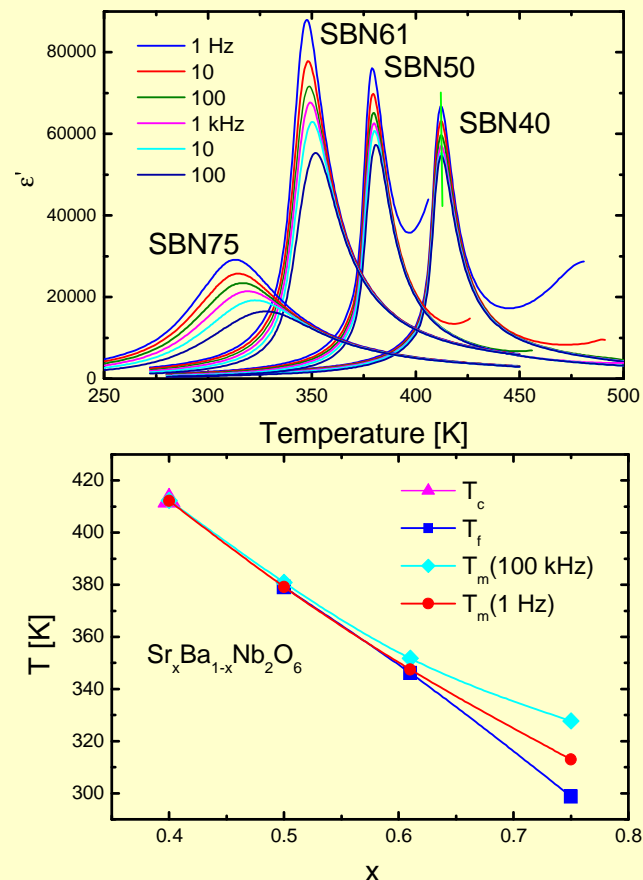
Tungsten bronze structural class. General formula of the unit cell  $[\text{A}_1_2\text{A}_2_4\text{A}_3_4][\text{B}_1_2\text{B}_2_8]\text{O}_{30}$



○ A3 – empty      ● A1-occupied by  $\text{Sr}^{2+}$

● A2 – occupied by both  $\text{Ba}^{2+}$  and  $\text{Sr}^{2+}$

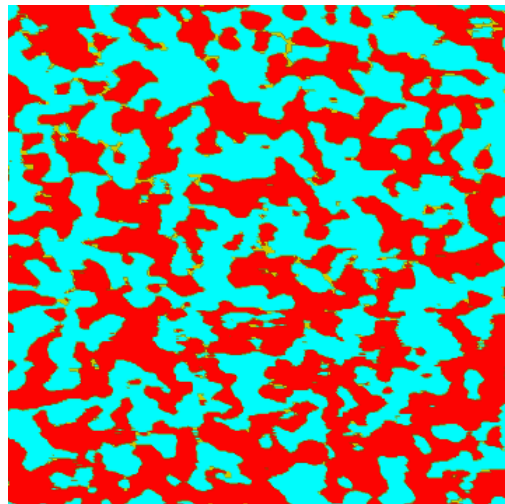
- From available six A1 and A2 positions only five are occupied
- Frozen random fields due to randomly distributed A-site vacancies



- Transformation from the ferroelectric to relaxor behavior at  $x \sim 0.60$
- Belongs to the 3D random-field Ising model universality class. Ground state is a long-range ordered state

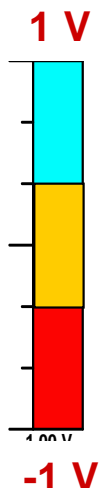
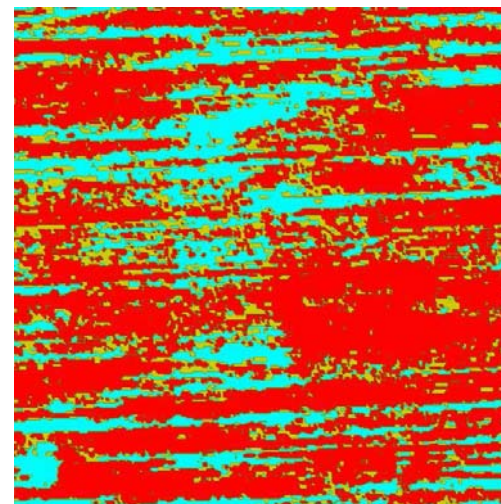
# SBN40: Domain structure at RT

c-cut, Vertical PFM



• [001]  $\frac{1}{\mu\text{m}}$

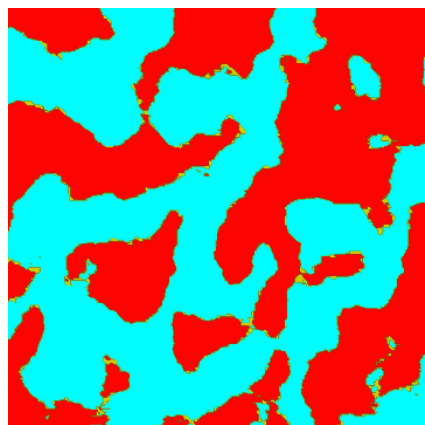
a-cut, Lateral PFM



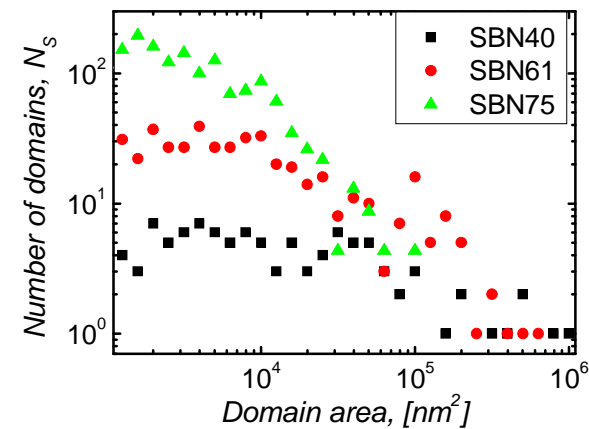
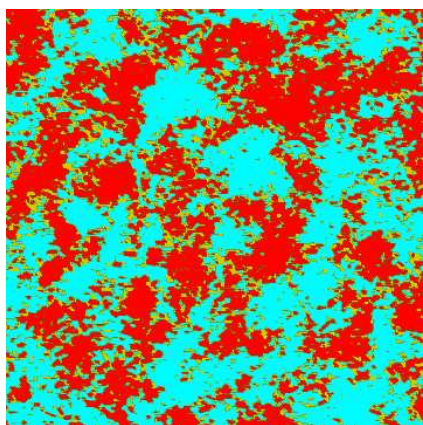
- Complex maze-type domain patterns for c-cut, irregular shape of domain walls
- Domain structure is strongly anisotropic

# SBN: Domain structure vs. composition

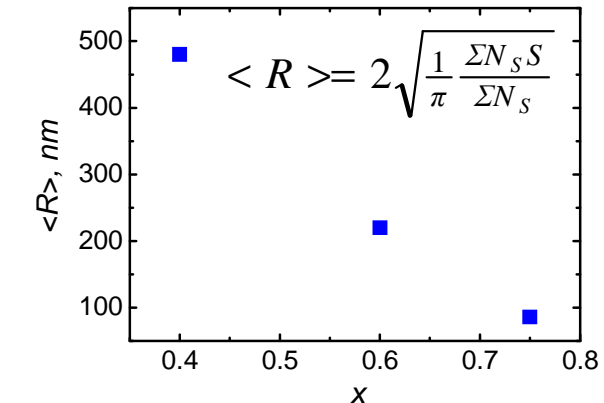
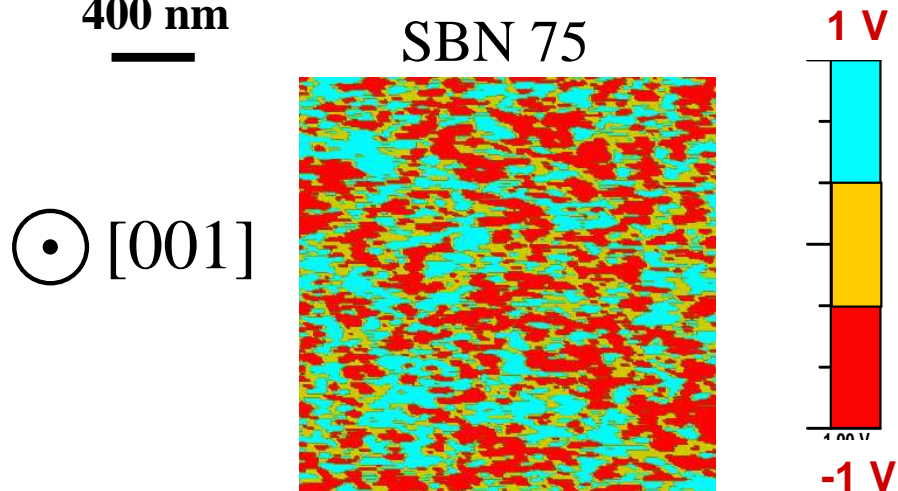
SBN 40



SBN 61



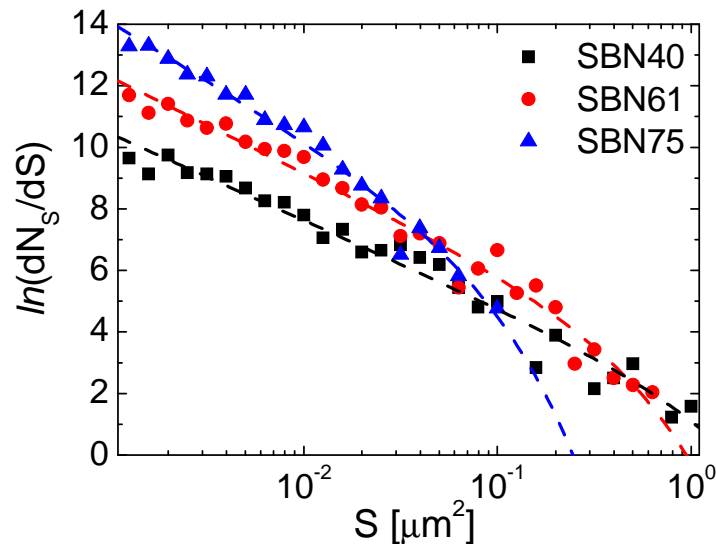
400 nm



Shvartsman et al. Phys. Rev. B 77, 054105 (2008)

- Domain walls become more jagged with increasing Sr content
- Decrease of domain size - transformation to a typical relaxor behaviour

# Domain distributions in SBN



$$\frac{dN_s}{dS} \sim S^{-\delta} \exp\left(-\frac{S}{S_0}\right)$$

	$\delta$	$S_0$
SBN40	$1.2 \pm 0.1$	$1.1 \pm 0.1 \mu\text{m}^2$
SBN61	$1.3 \pm 0.1$	$0.7 \pm 0.2 \mu\text{m}^2$
SBN75	$1.6 \pm 0.15$	$0.05 \pm 0.02 \mu\text{m}^2$

For 3D RFIM  $\delta=1.8$  is predicted

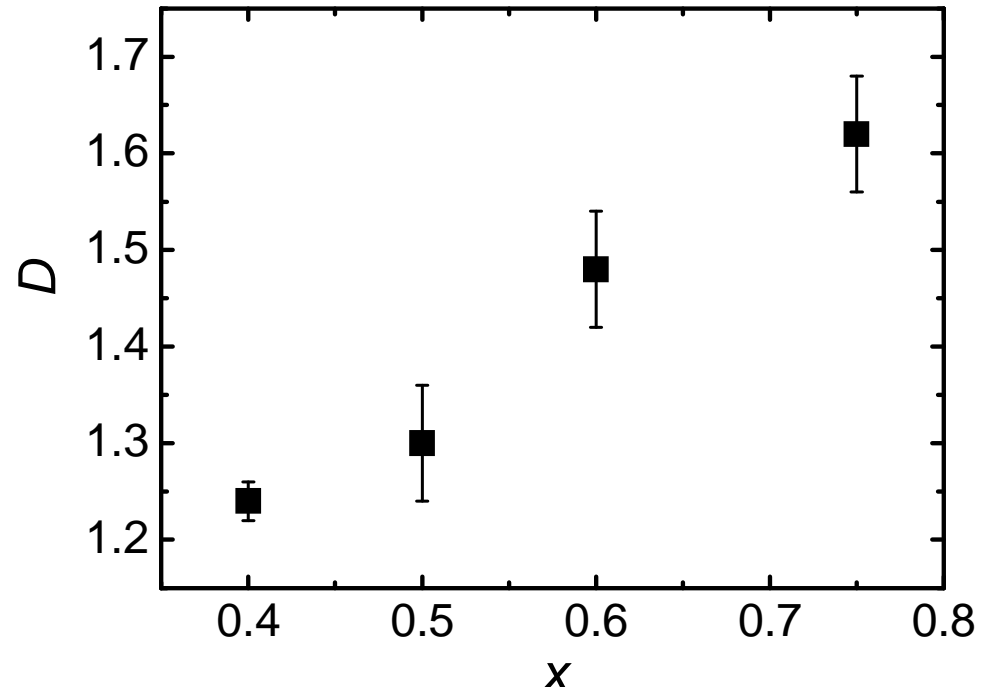
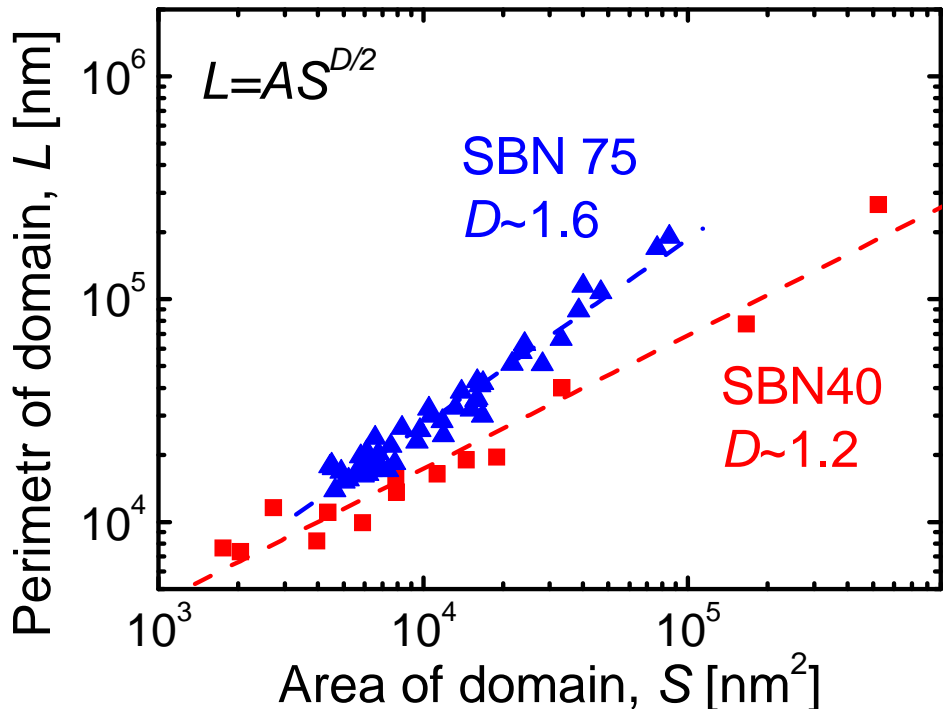
Nowak et al. Phys. A 232, 40 (1996)

- Domain size distribution is described by a power law with exponential cut-off

# Domain analysis using fractals

$$L^{1/D} S^{1/2} = \text{const} \quad (D - \text{fractal dimension})$$

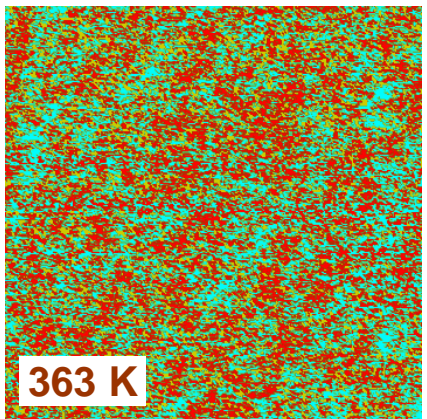
(J. Feder, *Fractals*, Plenum Press, New York, 1988)



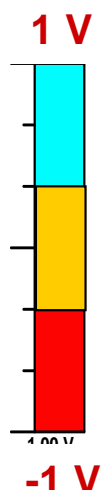
- Irregular shape of domain boundaries is observed even in ferroelectric SBN40 (inherent structural disorder).
- Fractal dimension of domain boundaries increases with increasing %Sr

# SBN: Evolution of polar structure with T

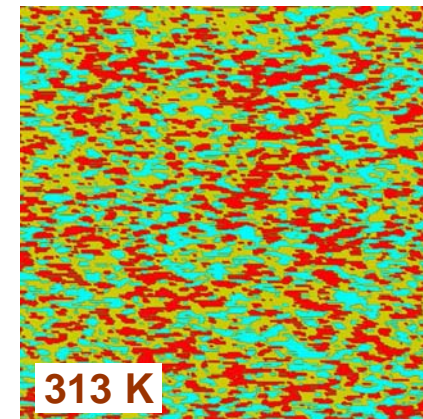
SBN61  $T_C=346$  K



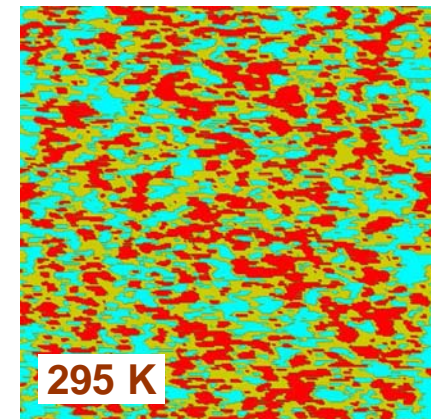
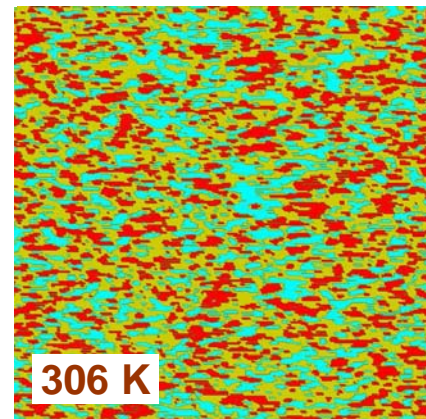
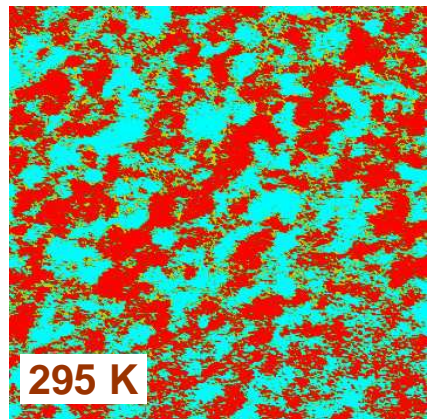
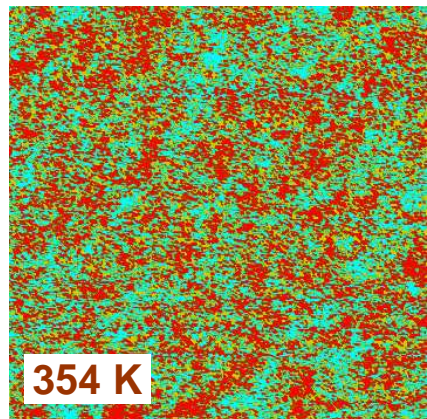
1  $\mu\text{m}$



SBN75  $T_C=298$  K



500 nm



Kleemann *et al.* PRL 97, 065702 (2006), Shvartsman *et al.* Phys. Rev. B 77, 054105 (2008)

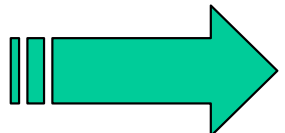
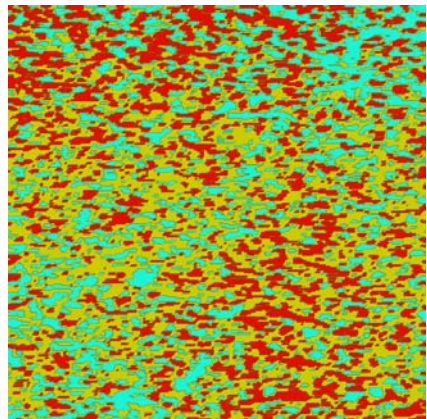
- Stable regions of correlated polarization are observed 15 K above  $T_C$
- They are less compact than the domains in ferroelectric state.
- Correspond to large PNRs „frozen“ on the experimental time scale

# SBN: Autocorrelation analysis

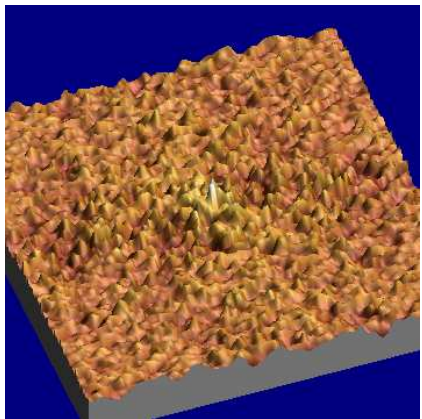
SBN61

$$C(r_1, r_2) = \sum_{x,y} D(x, y)D(x + r_1, y + r_2)$$

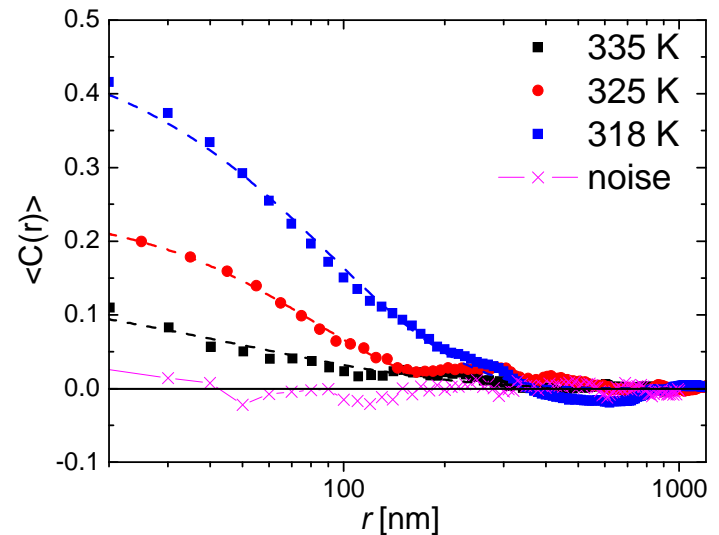
Piezoresponse,  $D(x,y)$



Autocorrelation,  $C(x,y)$



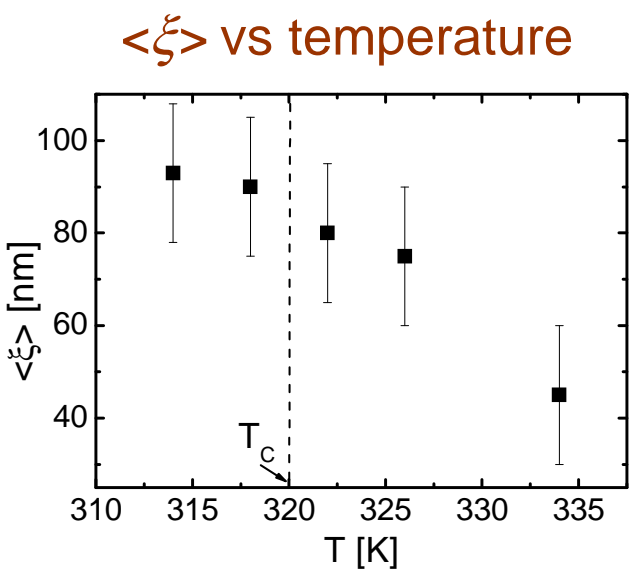
Averaged autocorrelation function



$$\langle C(r) \rangle = \sigma^2 \exp \left[ - \left( \frac{r}{\langle \xi \rangle} \right)^{2h} \right]$$

$\langle \xi \rangle$  - average correlation radius

- Width of the central peak is proportional to size of region of correlated piezoresponse
- Growth of quasi-static PNRs on cooling.

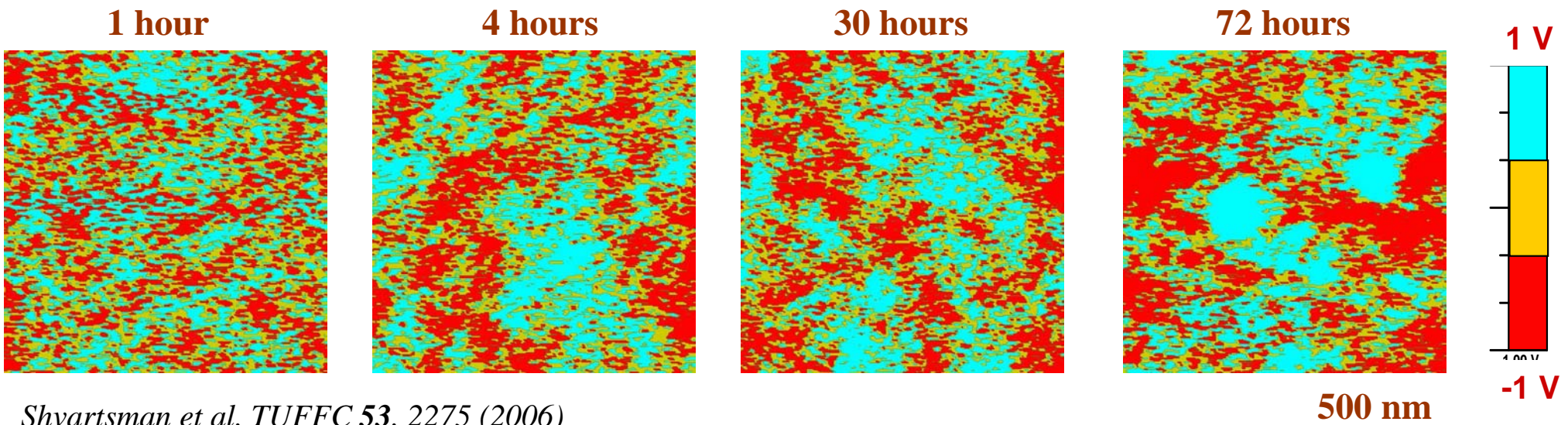


# Metastability of domains below the Curie temperature

Ce-doped SBN  $T_C \sim 320$  K

The sample was annealed during 2h at  $T = 420$  K and then cooled down to RT.

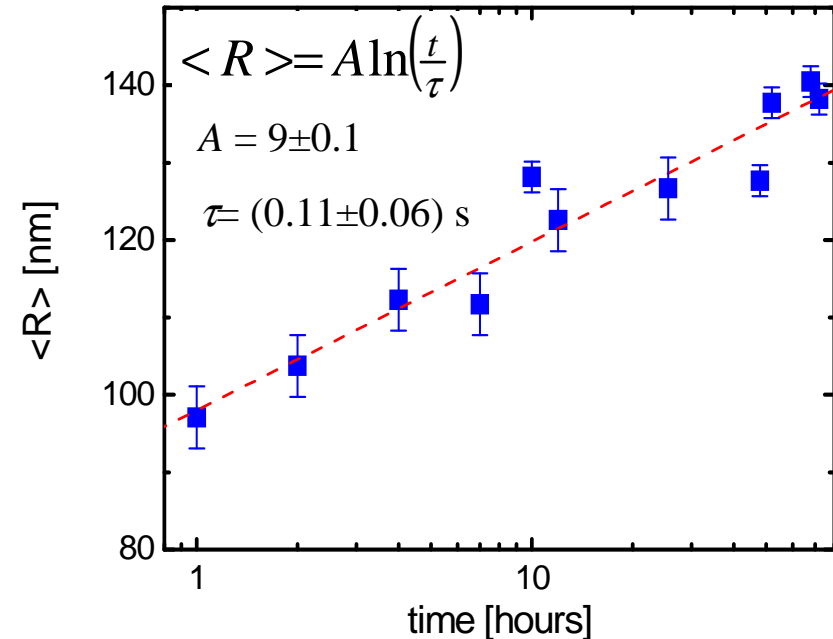
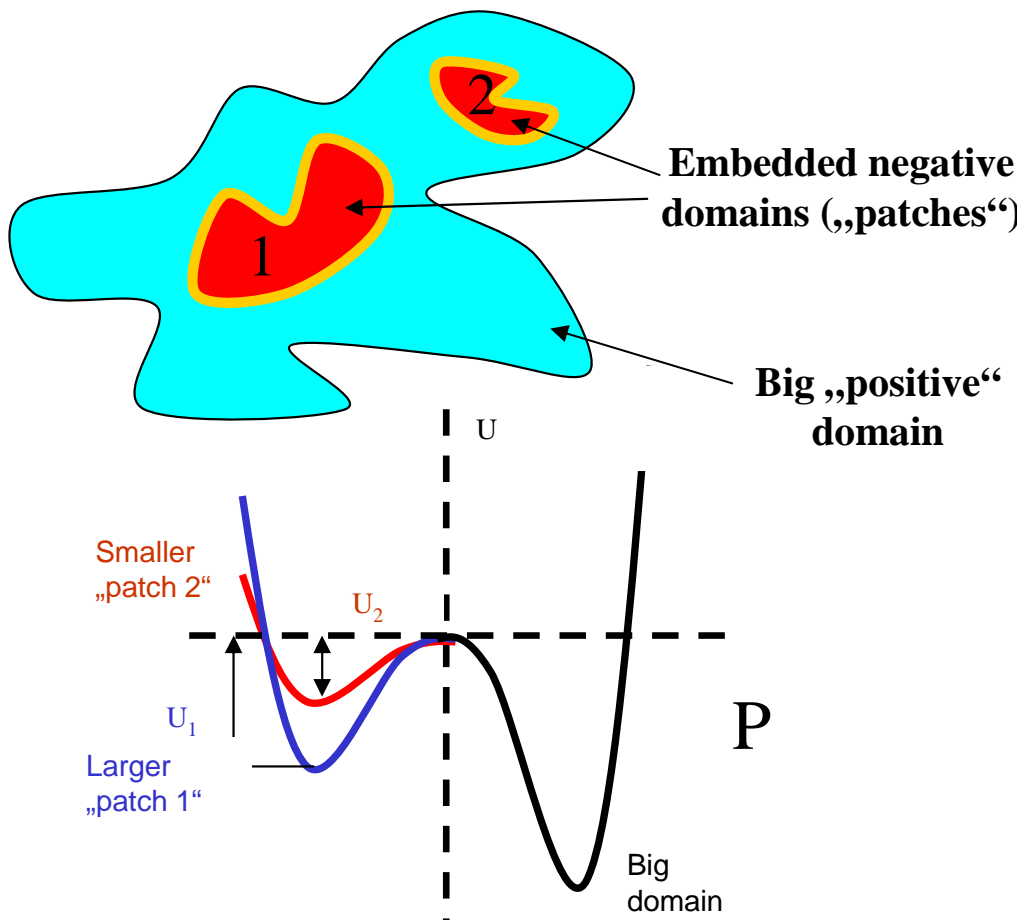
• [001]



*Shvartsman et al, TUFFC 53, 2275 (2006)*

- Just after the cooling domains are relatively small with strongly jagged borders. The domain polarity is determined by RFs distribution.
- Domains are coarsened and become more compact with time. The growth of the domains occurs at the expense of both embedded small “patches” of opposite polarity and interfaces with initially zero piezoresponse.

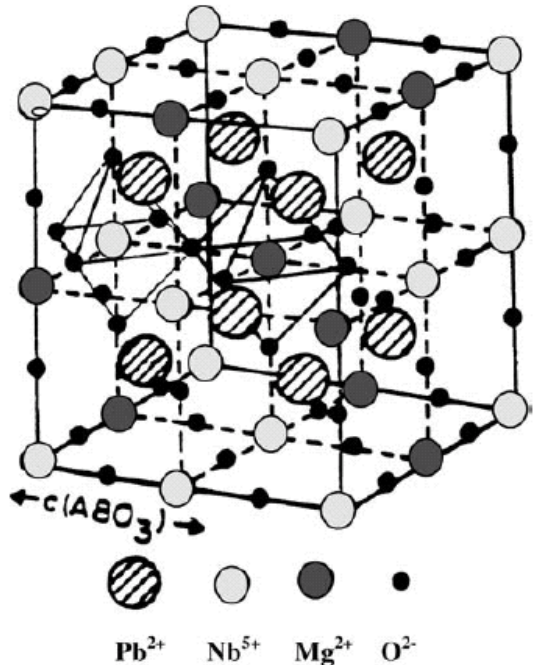
# Metastability of domains below $T_c$



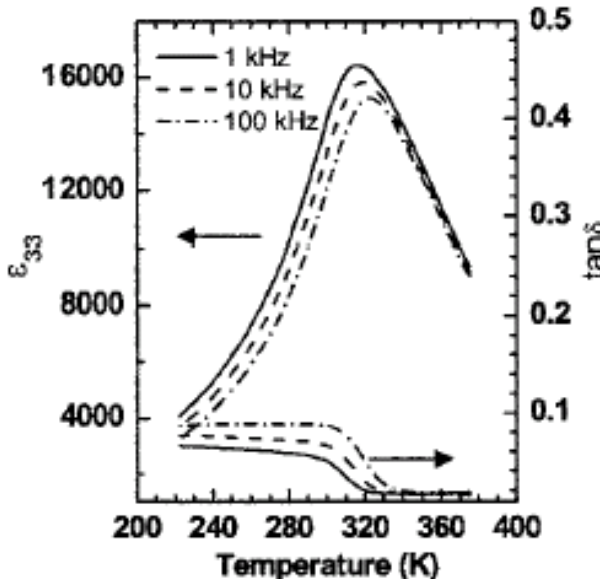
Shvartsman, TUFFC 53, 2275 (2006)

- To „take up“ a metastable RF-pinned domain a potential barrier proportional to the size of absorbing domains has to be overcome.
- Logarithmic dependence in accordance with predictions [Villain, PRL 52, 1543 (1984)].

# $(1-x)\text{PbMg}_{1/3}\text{Nb}_{2/3}\text{O}_3-x\text{PbTiO}_3$ (PMN-PT)



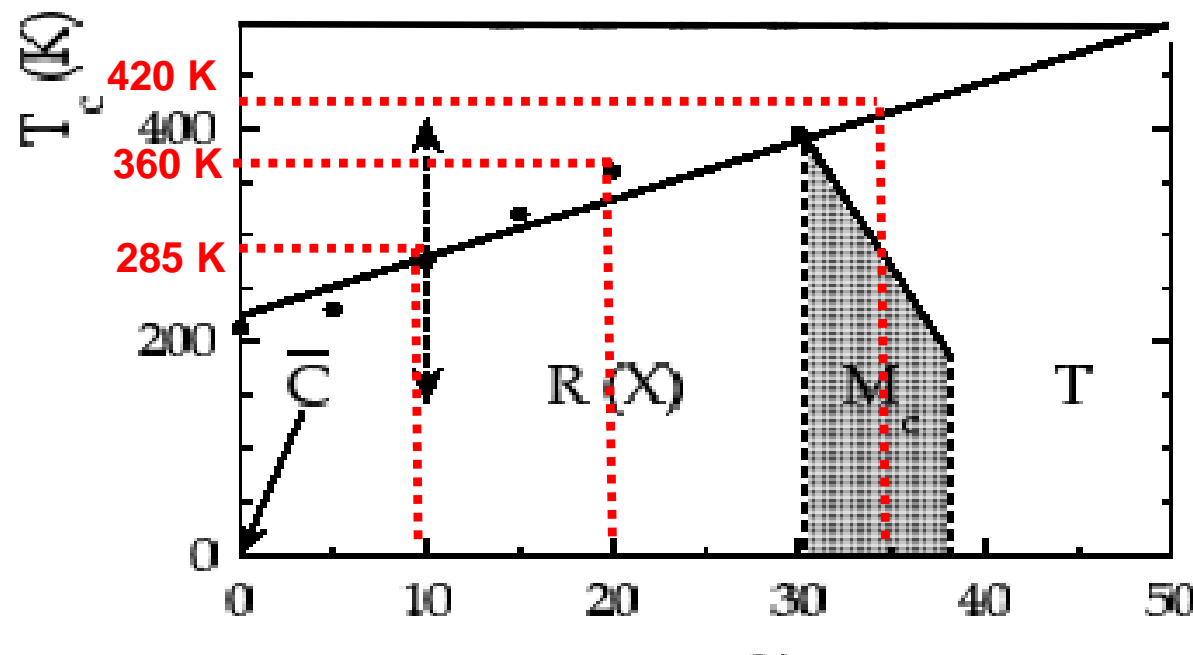
0.9PMN-0.1PT single crystal



Wang *et al. APL 88, 112909 (2006)*

- Relaxor behaviour is due to charge disorder.
- Solid solutions with  $0.05 < x < 0.25$  combine relaxor and ferroelectric properties:
- A spontaneous transition into long-range ordered state was reported for ceramics.
- In single crystal such a phase transition was found in a surface layer (thickness  $< 50 \mu\text{m}$ ), while the internal part remains short-range ordered.

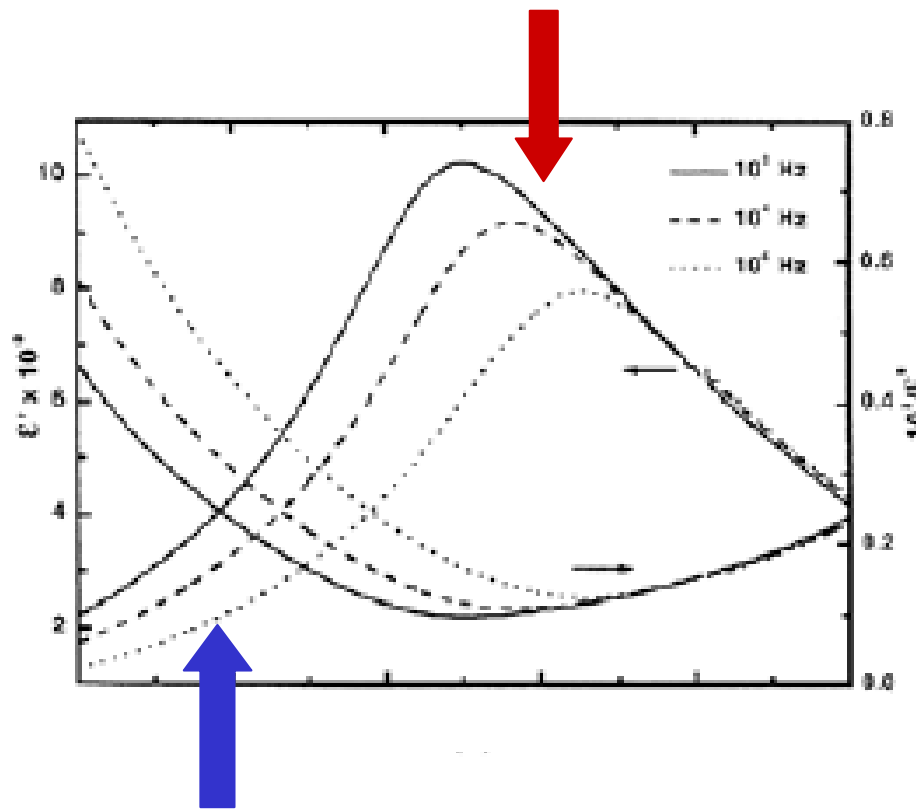
# Solid solutions $\text{PbMg}_{1/3}\text{Nb}_{2/3}\text{O}_3$ - $\text{PbTiO}_3$



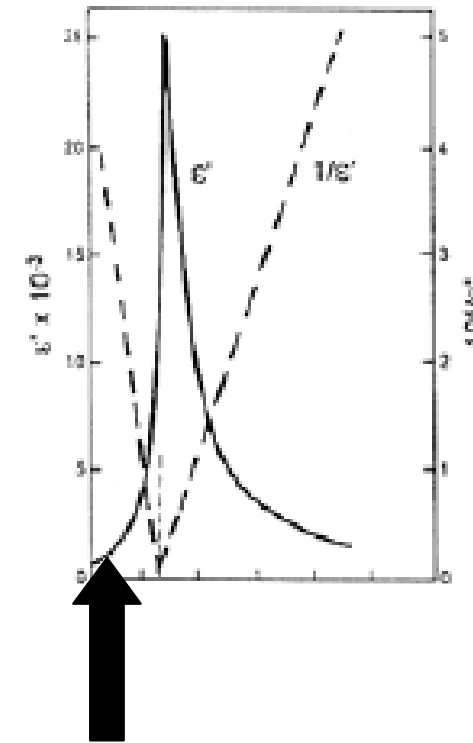
selected compositions  
of PMN-PT single crystals

# Expected domain states after ZFC at $T_{\text{room}}$

PMN-10%PT: polar clusters ( $>10$  nm)

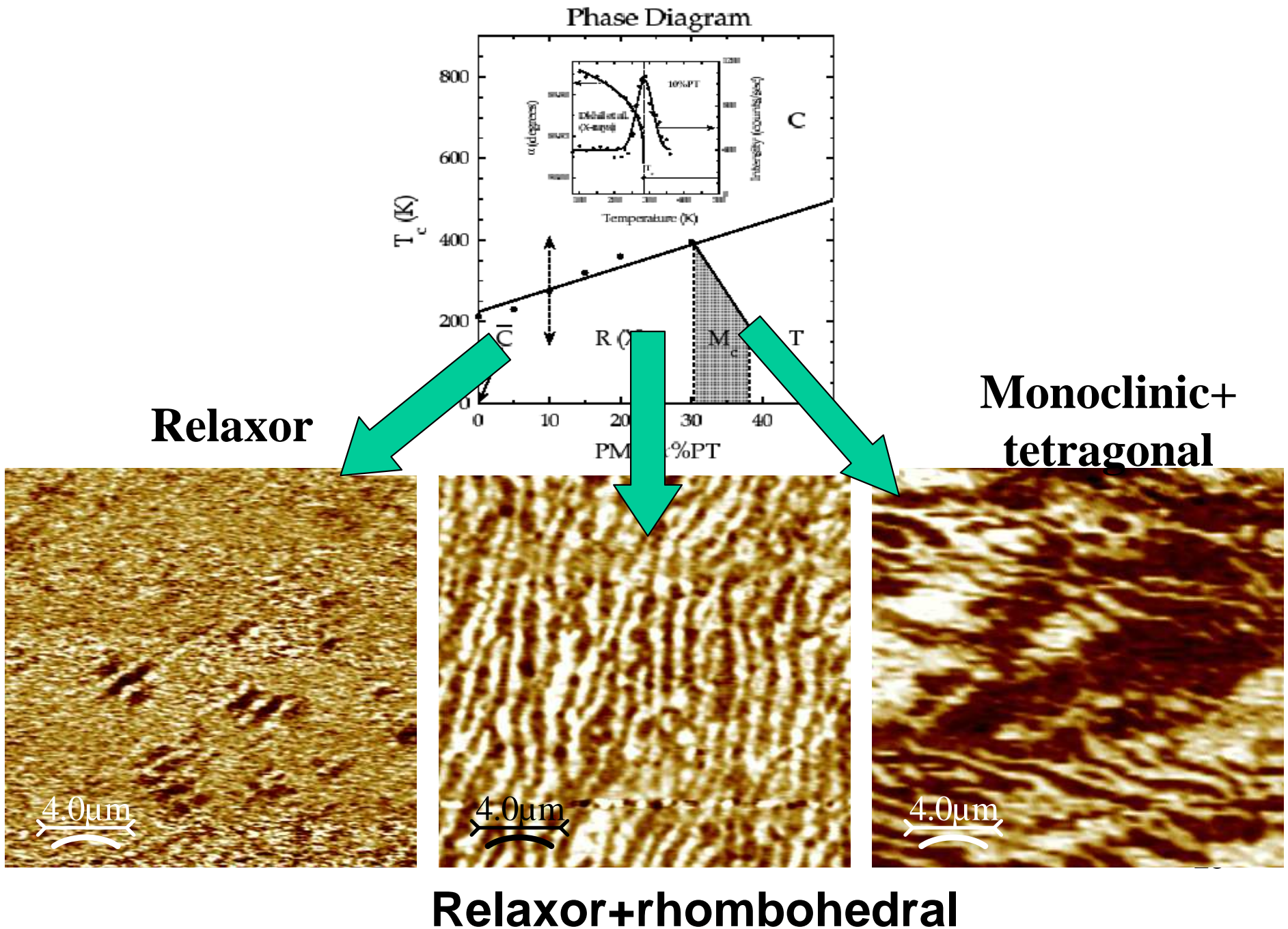


PMN-20%PT  
polar clusters +  
Rhombohedral domains

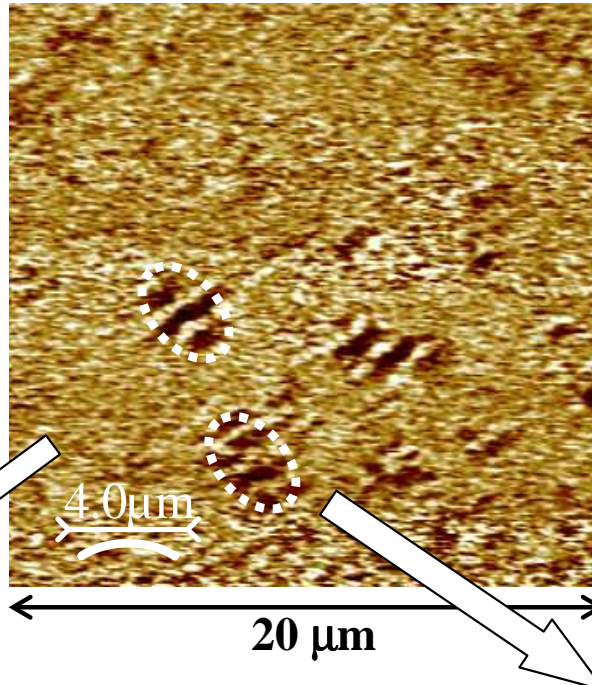
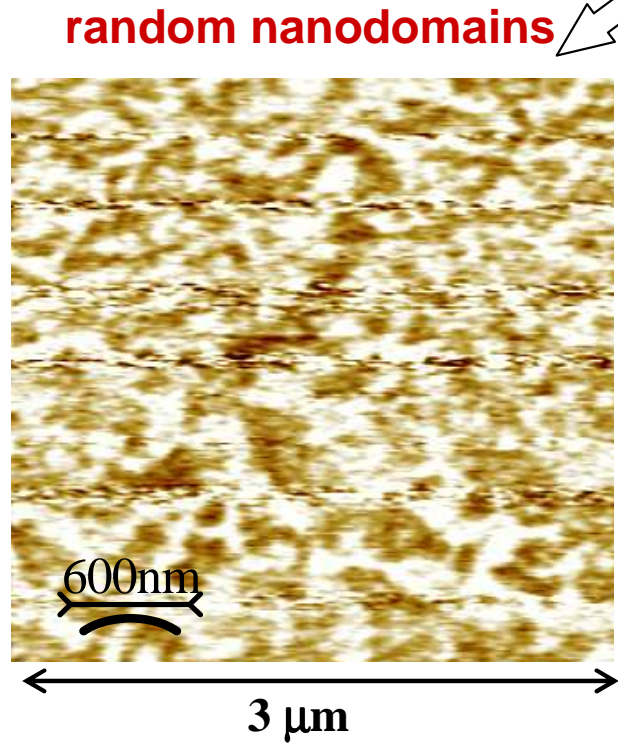


PMN-35%PT  
Tetragonal +  
Rhombohedral +  
Monoclinic (?) domains

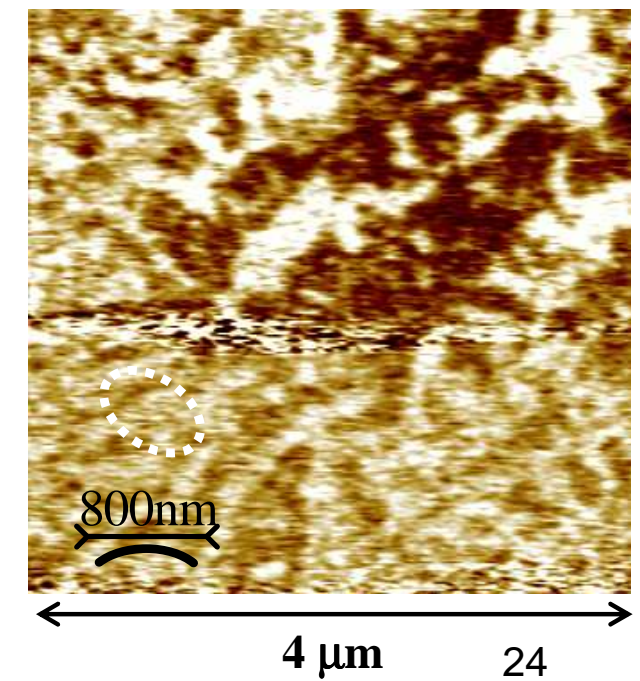
# Schematic of the results on PMN-PT single crystals

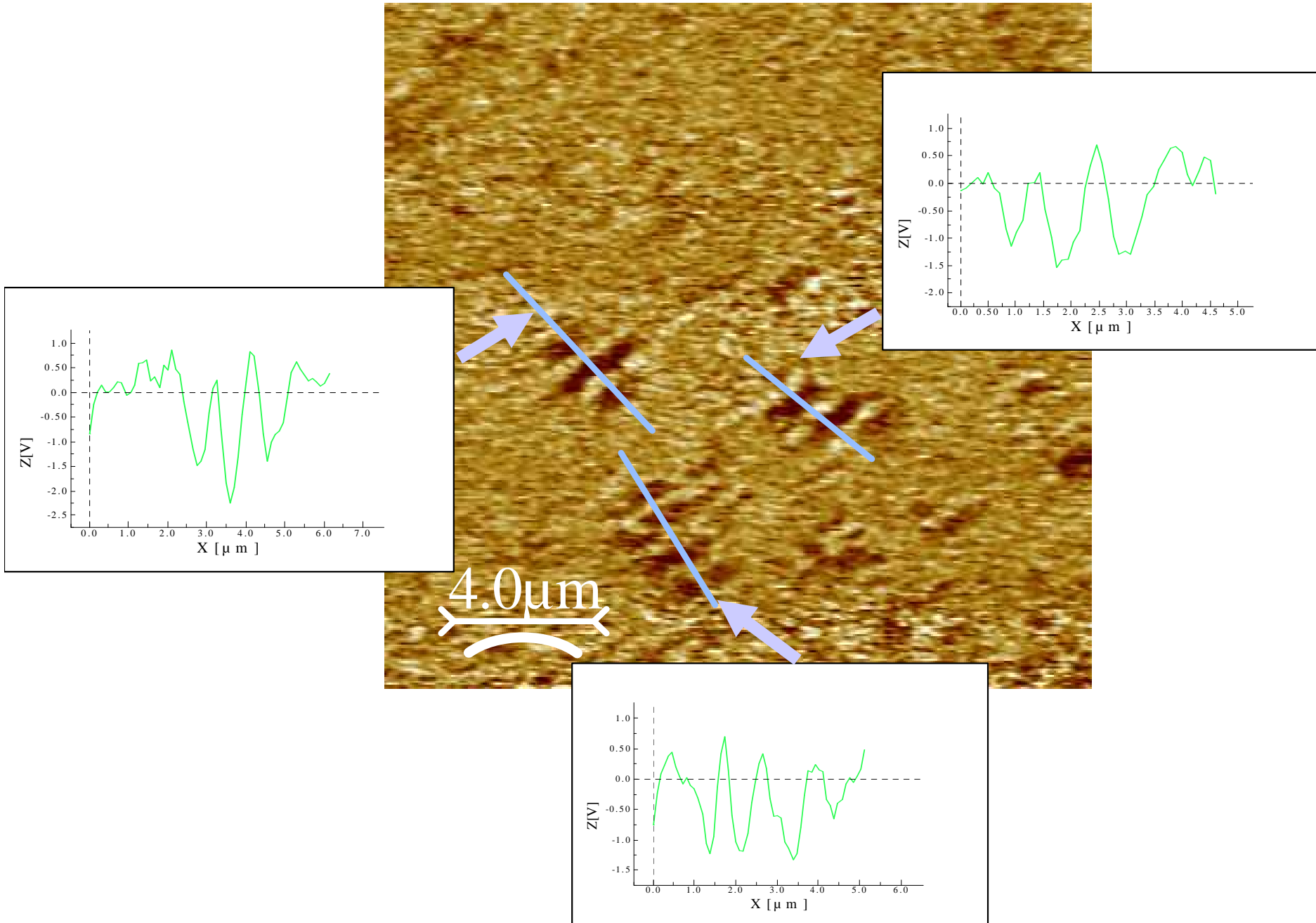


# $\text{Pb}(\text{Mg}_{1/3}\text{Nb}_{2/3})\text{O}_3$ -10% $\text{PbTiO}_3$



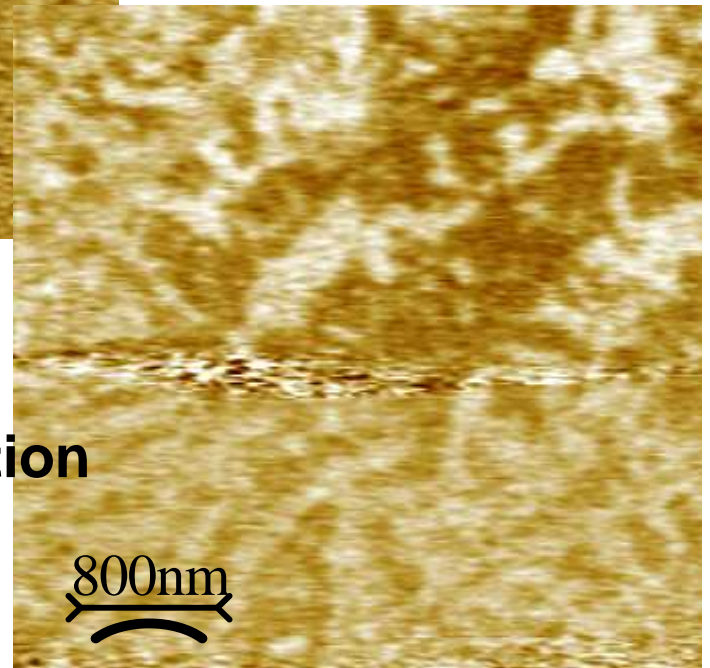
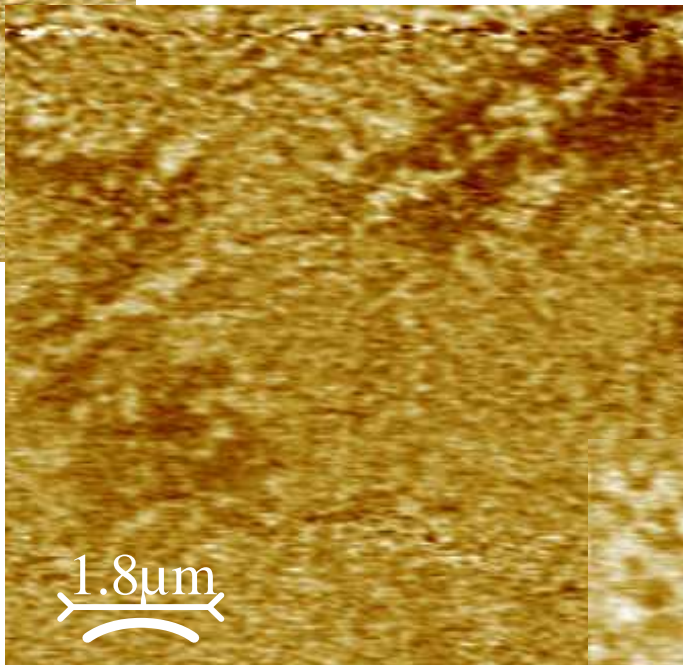
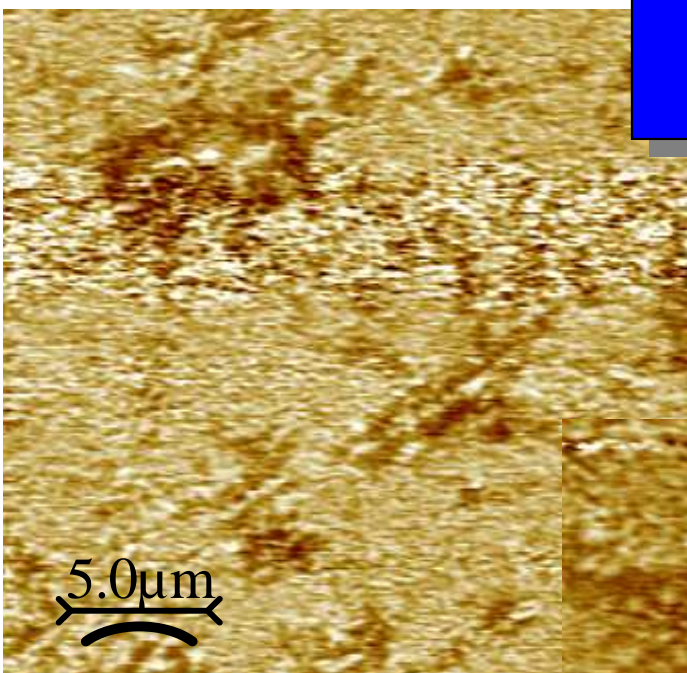
Concentration of  
“ferroelectric” islands  
is 15-20% of total  
area





■ Period of domain structure  $\sim 1 \mu m$ , size of ferroelectric islands  $1-5 \mu m$

## Domain patterns at different scales

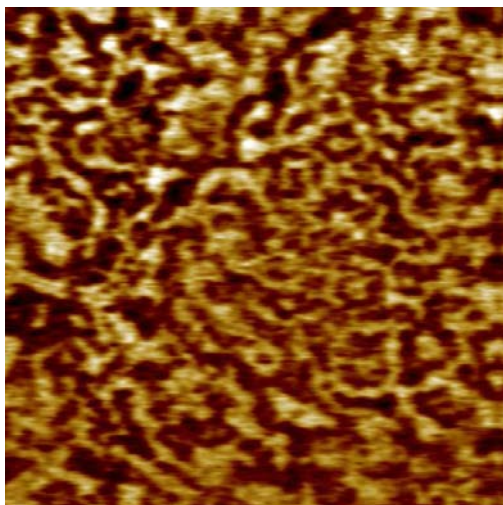


- Hierarchical structure and self-organization of domains at the nanoscale

# PMN-PT 90/10

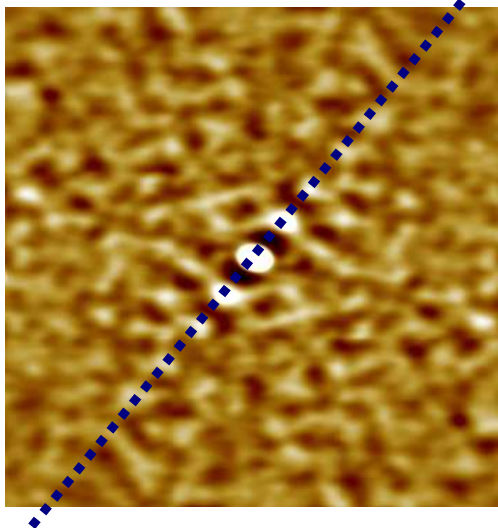
1 V  
-1 V

Piezoresponse, D



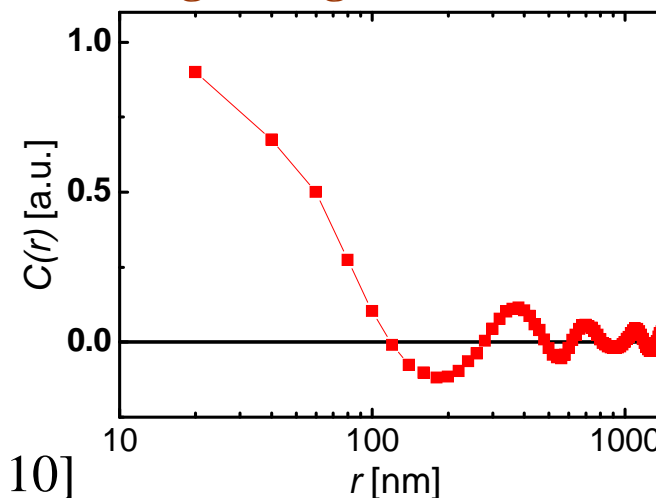
800 nm

Autocorrelation, C

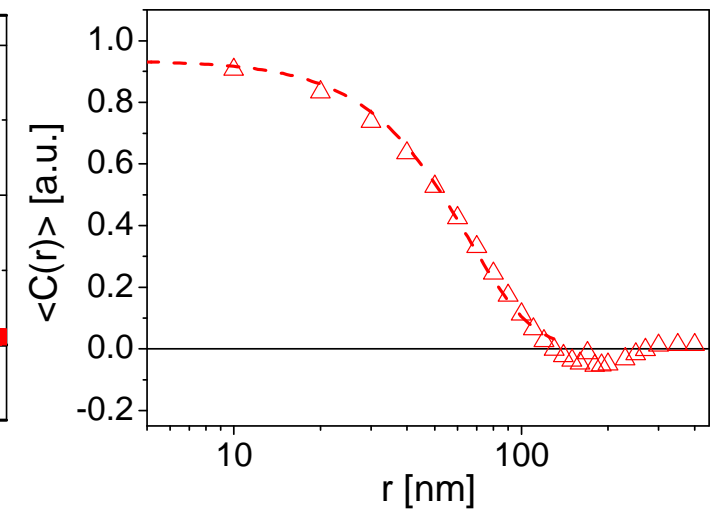


• [001]       $T_c = 280 \text{ K}$

Cross-section of the autocorrelation image along [110] direction



Averaged autocorrelation function



average correlation radius

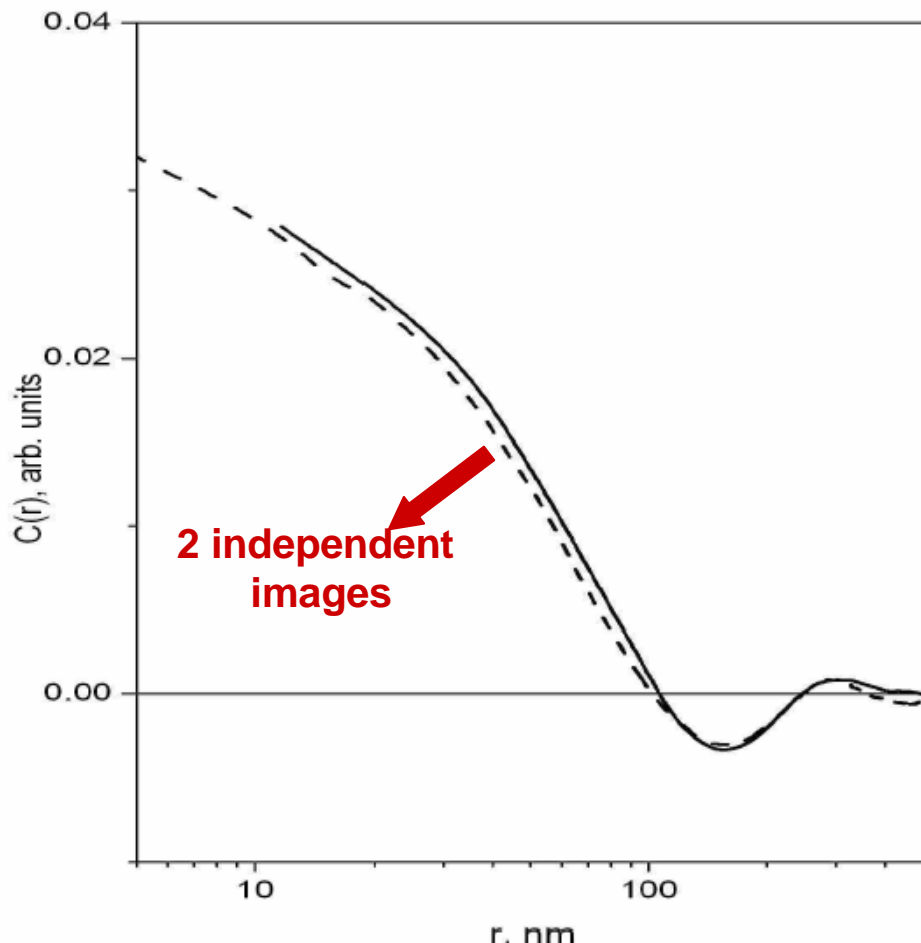
$\langle \xi \rangle \approx 70 \text{ nm} @ \text{RT}$

$$\langle C(r) \rangle = \sigma^2 \exp \left[ - \left( \frac{r}{\langle \xi \rangle} \right)^{2h} \right]$$

- Well defined static PNRs above  $T_c$
- Angular anisotropy of autocorrelation function - preferable orientation of PNR's boundaries

# Calculations of scattering cross-section

Average correlation function



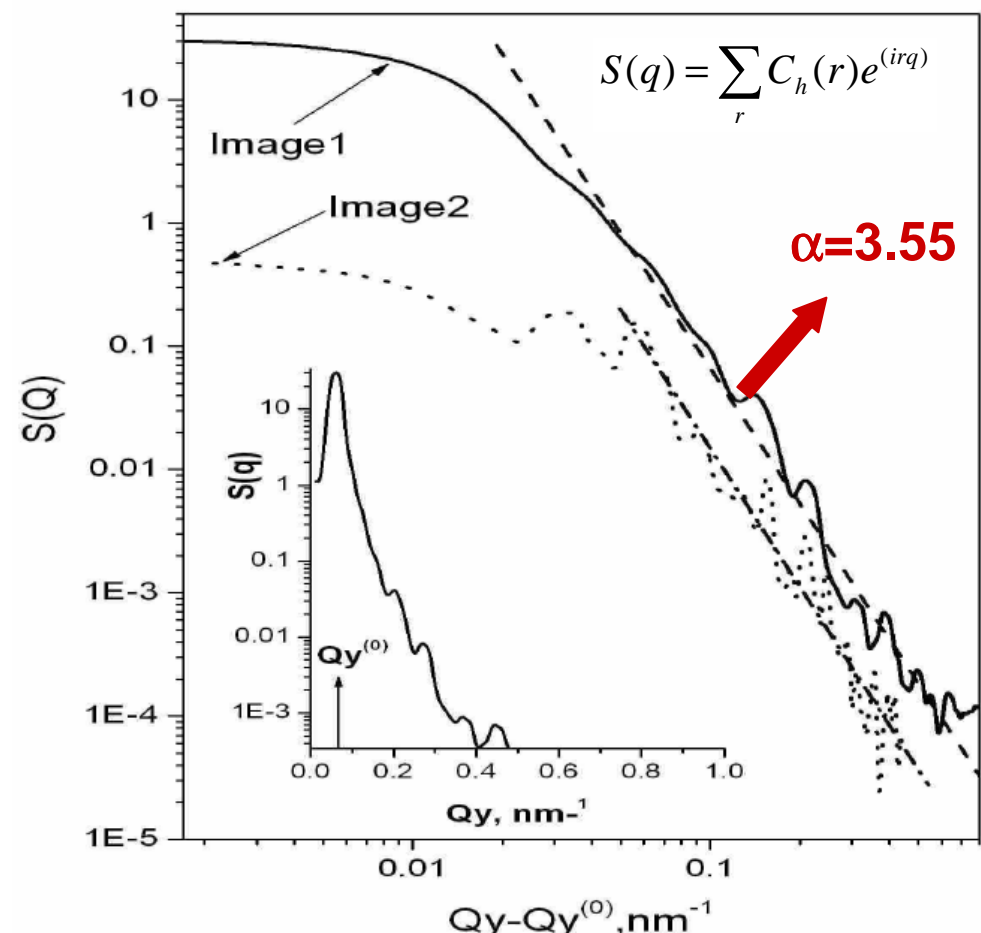
**Theory gives**  
(Prosandeev, 2003)

$$S(q) = \frac{1}{[(q - q_h)^2 + k]^2}$$

$k$  – inverse correlation length  
 $q_h$  - domain wall thickness

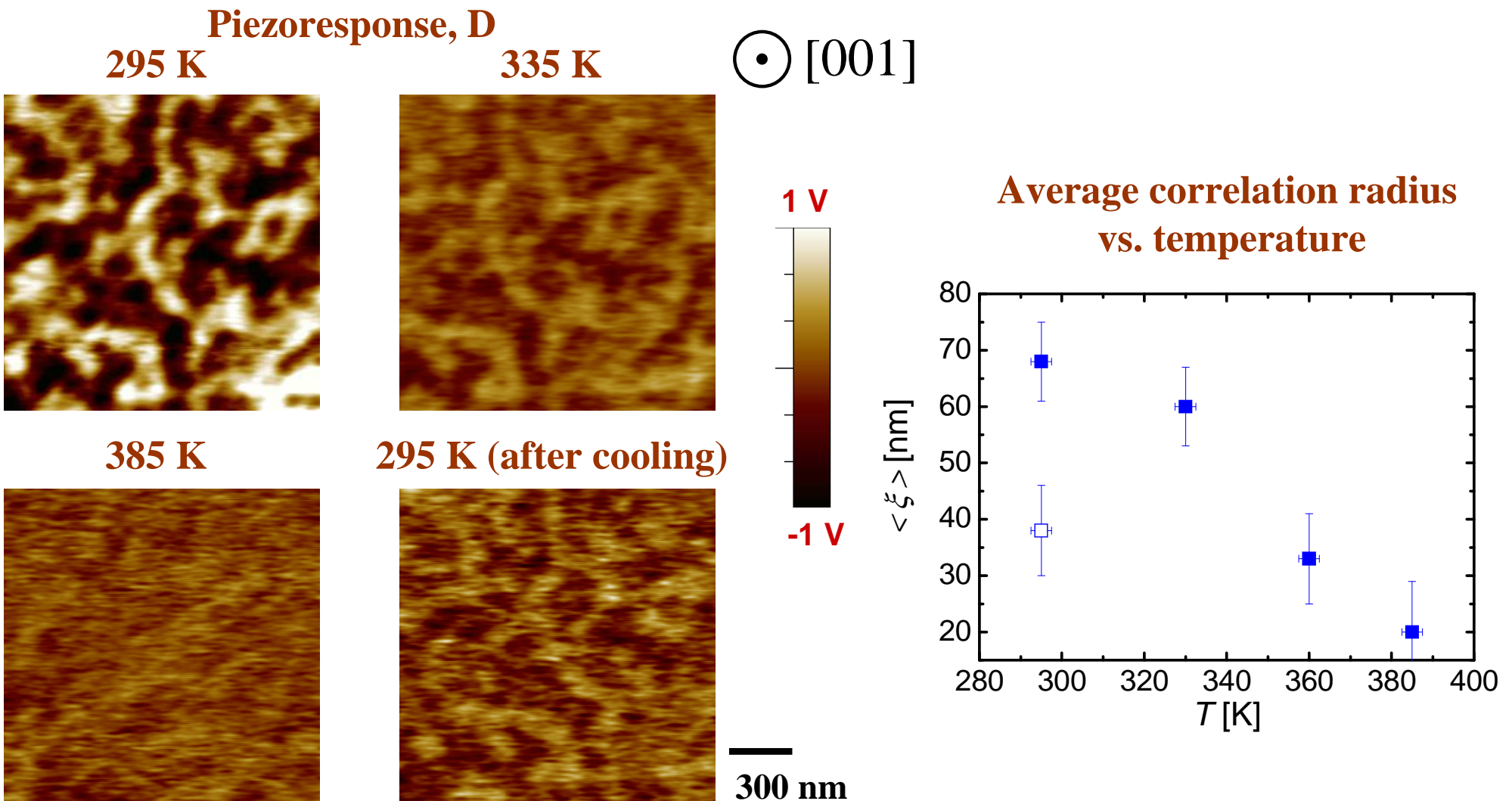
28

Scattering cross-section



# PMN-PT 90/10: temperature dependence

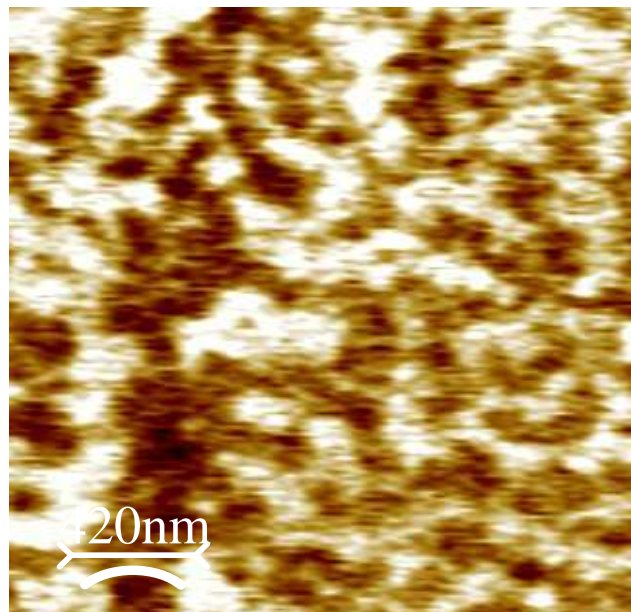
Shvartsman and Kholkin, J. Appl. Phys. 101, 064108 (2007)



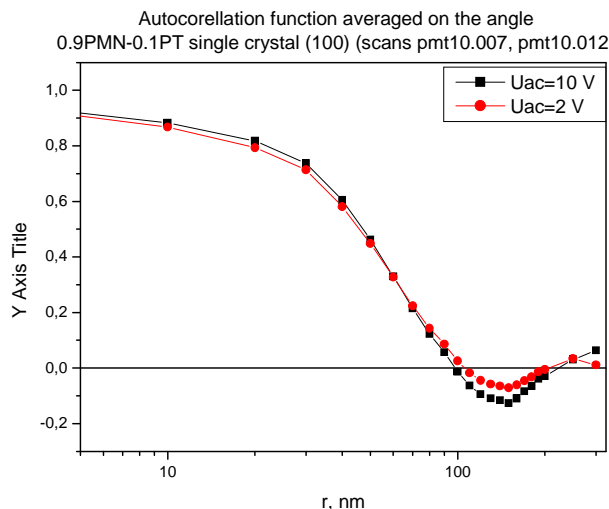
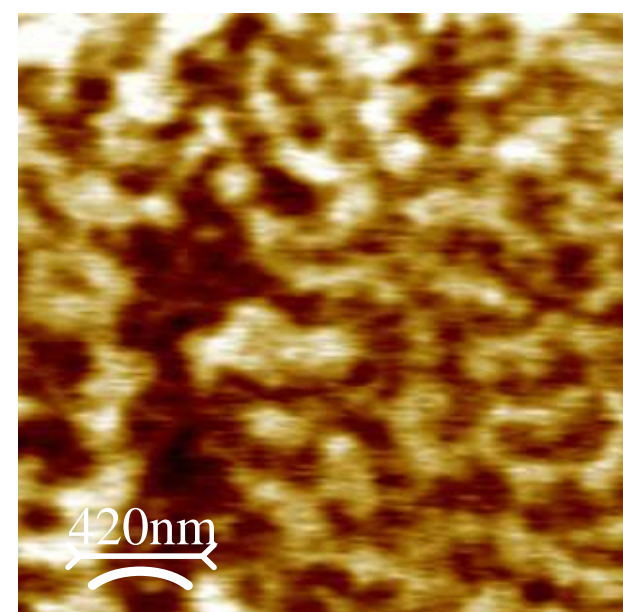
- Some static PNRs are observed at 100 K above  $T_c$
- Decrease of  $\xi$  - thermoactivated decay of „frozen“ PNRs
- Only partial reversibility after cooling back to RT

# Nanodomains vs. ac-field amplitude

$U_{ac}=2V$



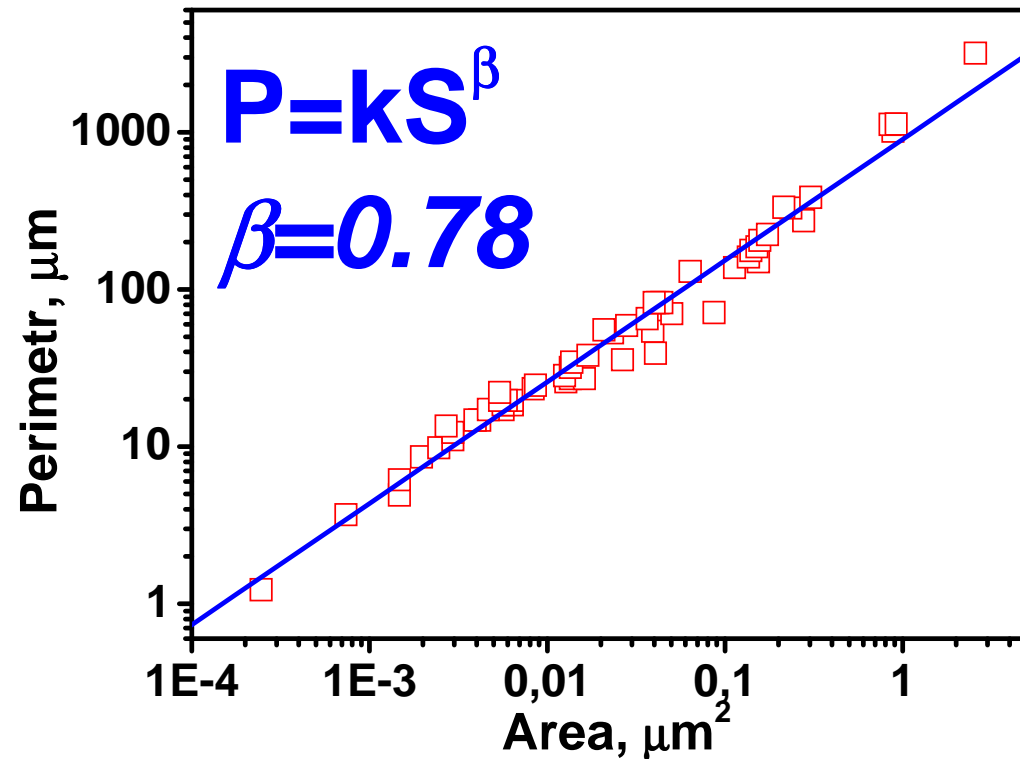
$U_{ac}=10V$



30

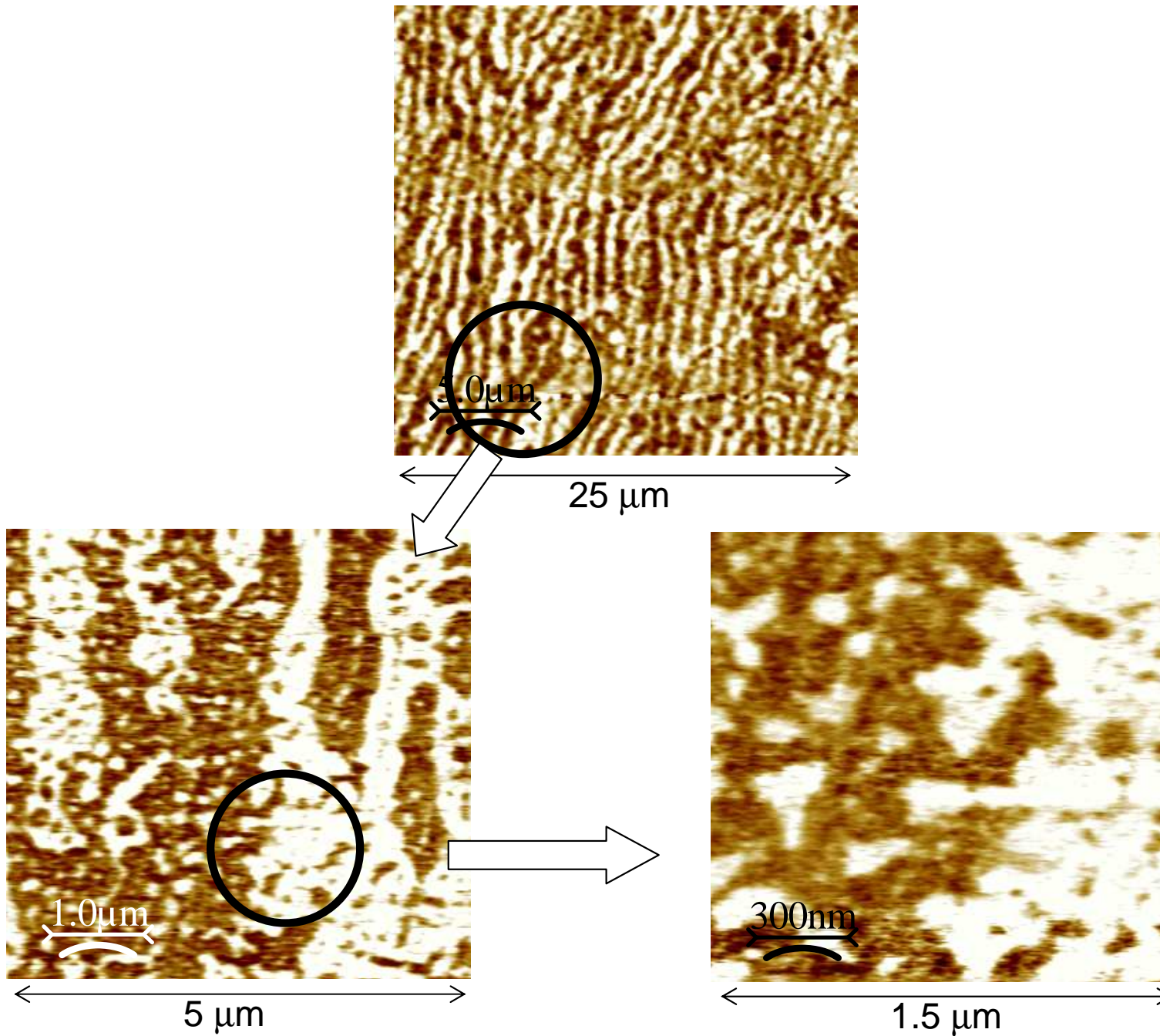
■ No changes with increasing ac-field amplitude

# Fractal analysis

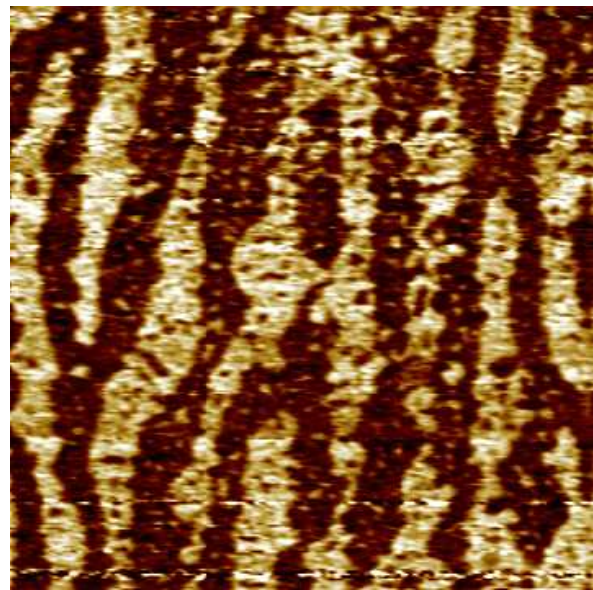


- Fractal dimension  $D=2\beta \approx 1.55$  is typical for random systems

# $\text{Pb}(\text{Mg}_{1/3}\text{Nb}_{2/3})\text{O}_3$ -20% $\text{PbTiO}_3$

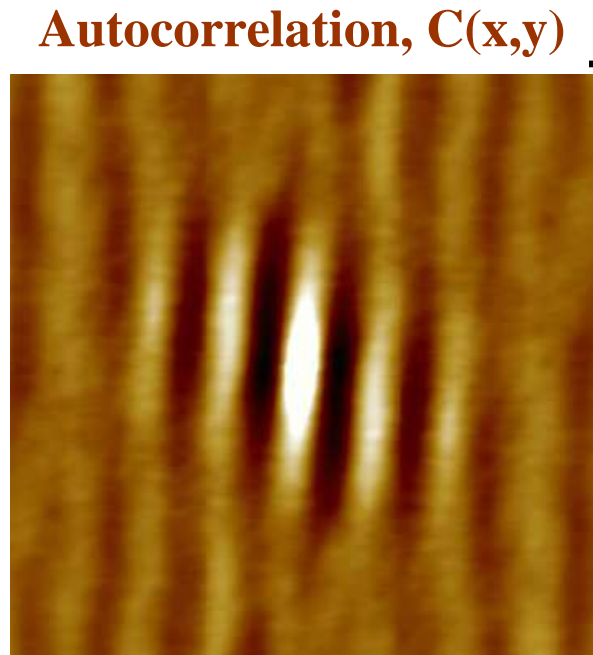


Piezoresponse, D



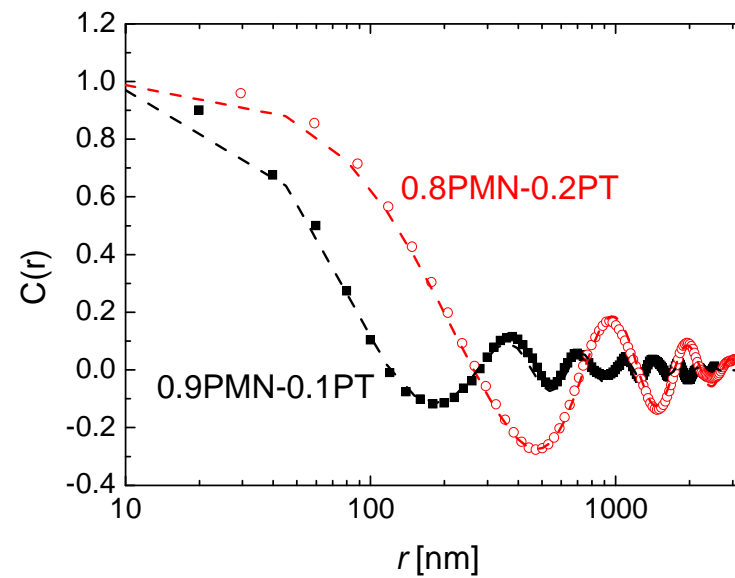
• [001]

Cross-section of autocorrelation images along  
[110] direction



1.5 μm

[110]



- Micron-sized domains forming a quasi-regular structure and embedded nanodomains.
- Correlation along  $\langle 110 \rangle$  direction is essentially stronger than in 0.9PMN-0.1PT

# PMN-PT 80/20: temperature dependence

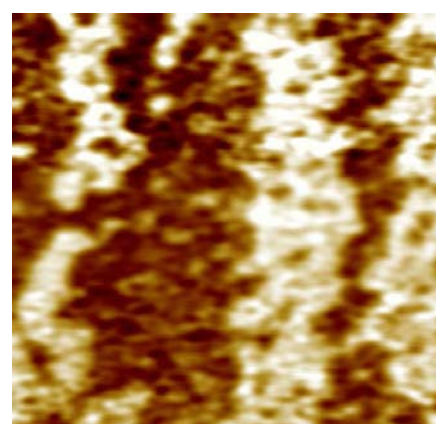
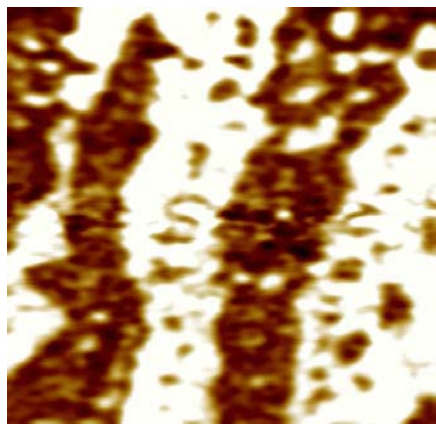
• [001]

Piezoresponse, D

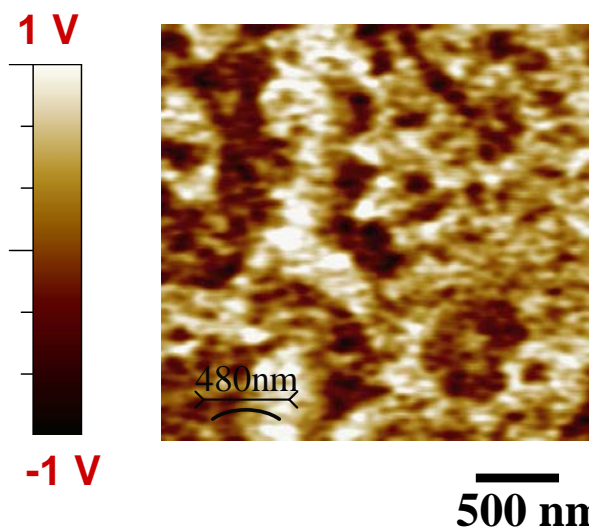
$T_c = 360 \text{ K}$

295 K

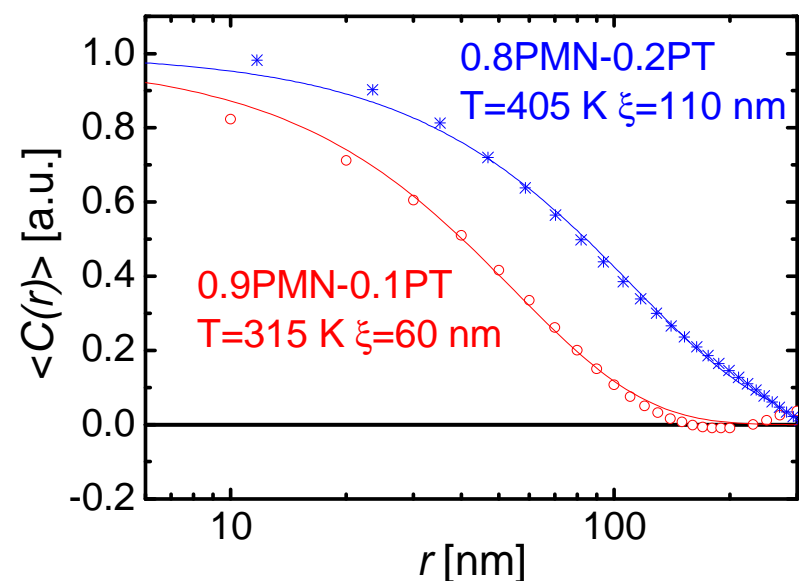
337 K



405 K

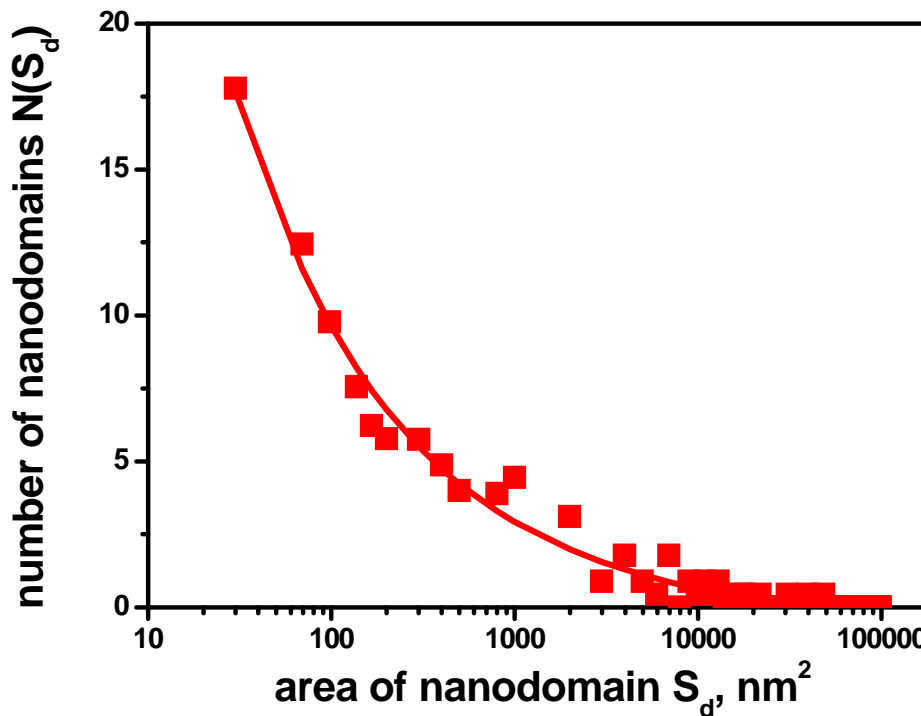


Averaged autocorrelation function vs. distance



- Decay of large domains around  $T_c$
- Nanodomains are observed at 50 K above  $T_c$ .
- Their size is about 2 times as compared to PMN-10%PT

# PMN-20%PT: nanodomain distribution



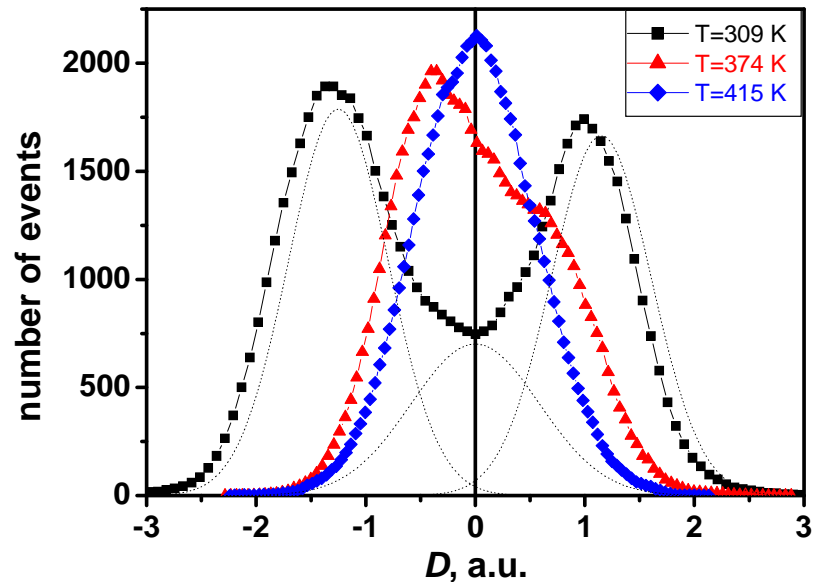
Random field Ising model:

$$N_d(S_d) \sim S_d^{-\delta} \exp\left(-\frac{S_d}{S_0}\right)$$

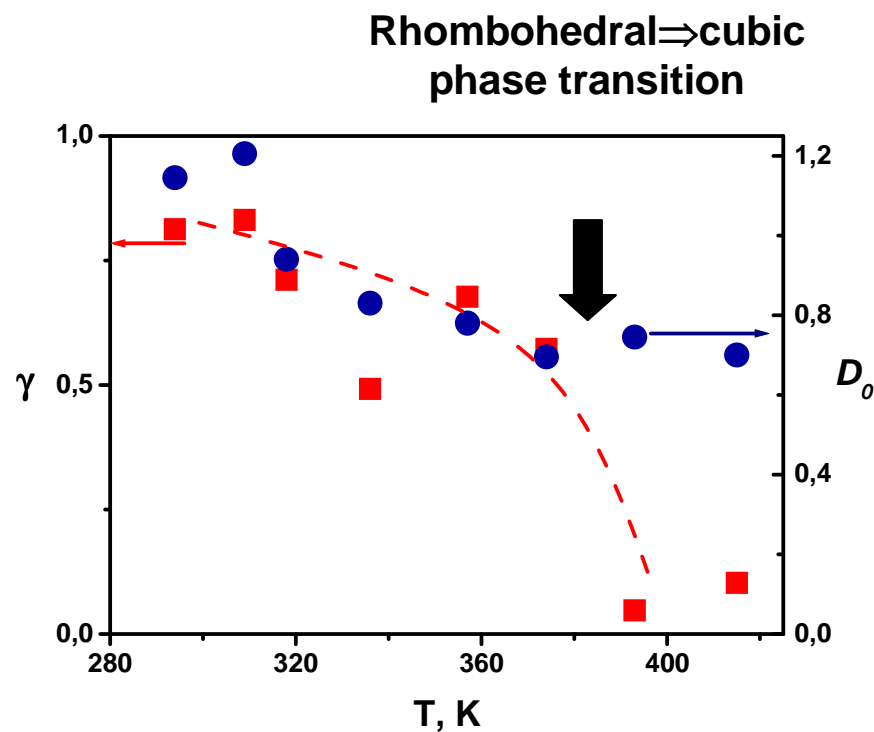
Fit gives  $\delta = 0.5 \pm 0.1$ ,  $S_0 \sim (2-3) \times 10^4 \text{ nm}^2$

In 2D RFIM  $\delta = 1.5 \pm 0.1$

# PMN-20%PT: temperature dependence



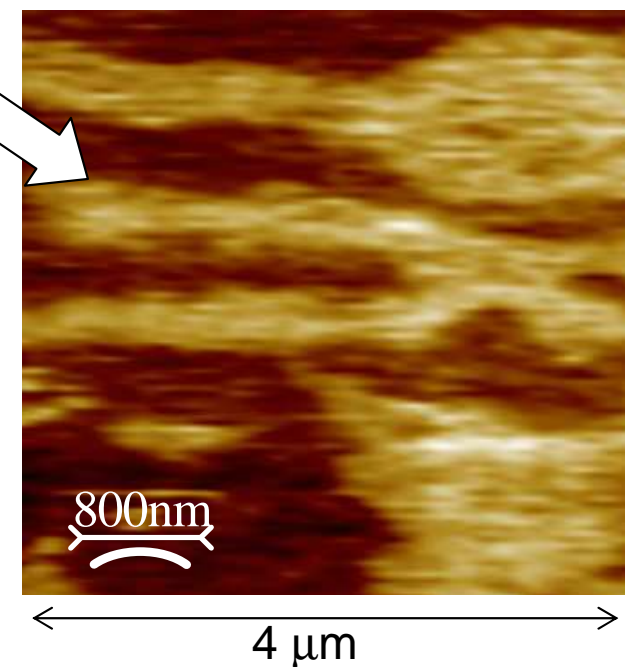
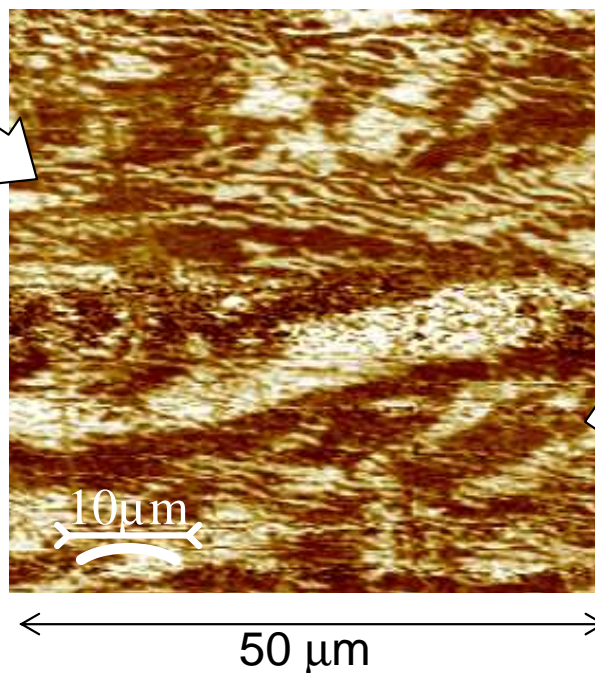
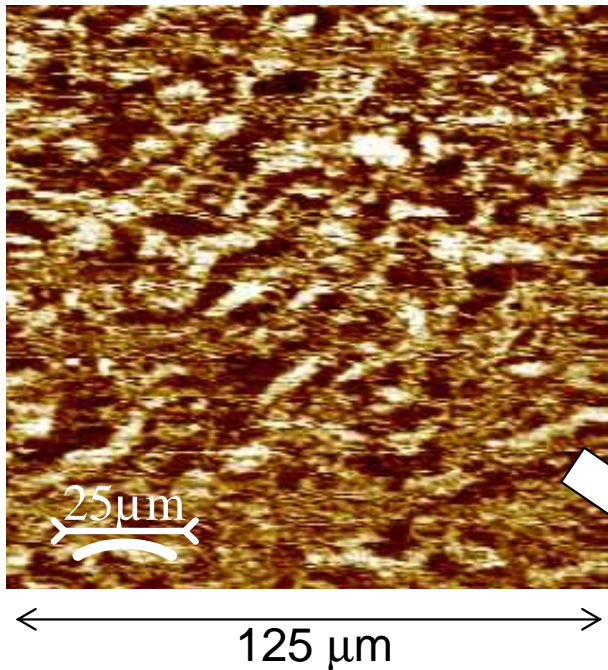
Domain histograms



Contrast vs. temperature

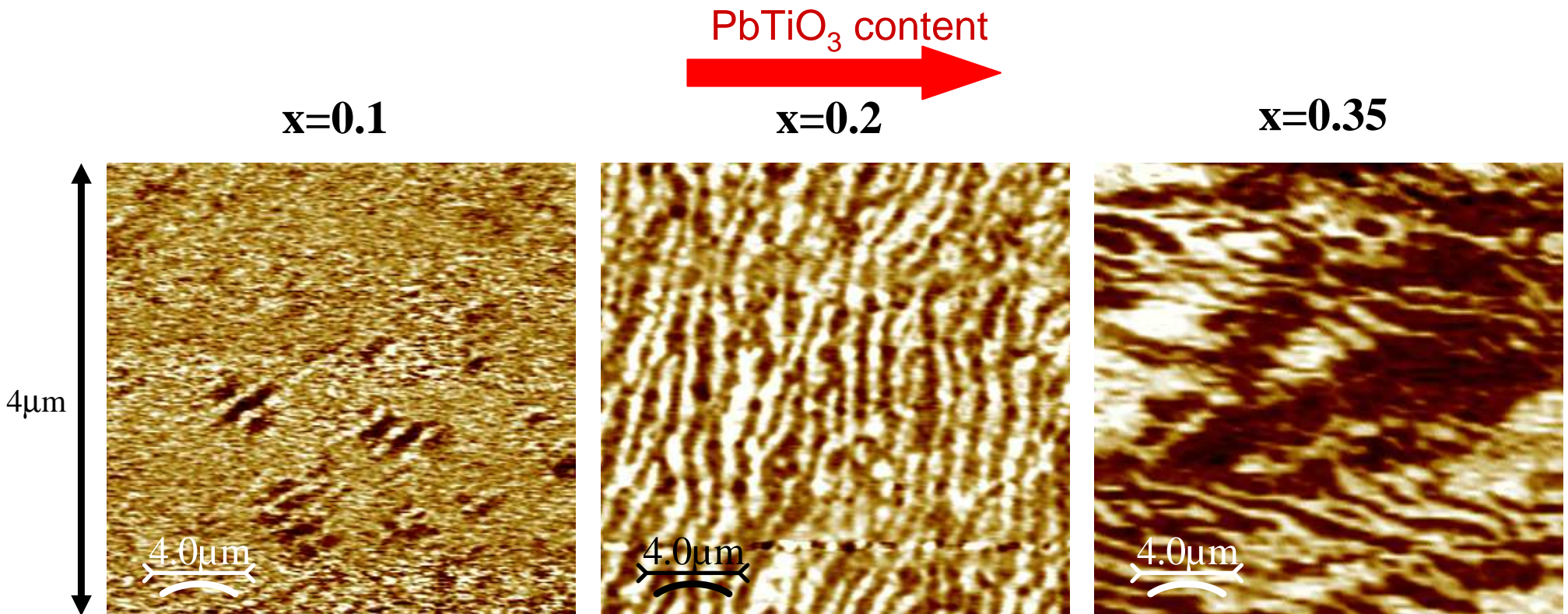
- Size of smallest domain is limited by the physical size of the tip (~8 nm)
- Nanodomains survive macroscopic phase transition but their number drops at  $T_c$ .

# $\text{Pb}(\text{Mg}_{1/3}\text{Nb}_{2/3})\text{O}_3$ -35% $\text{PbTiO}_3$



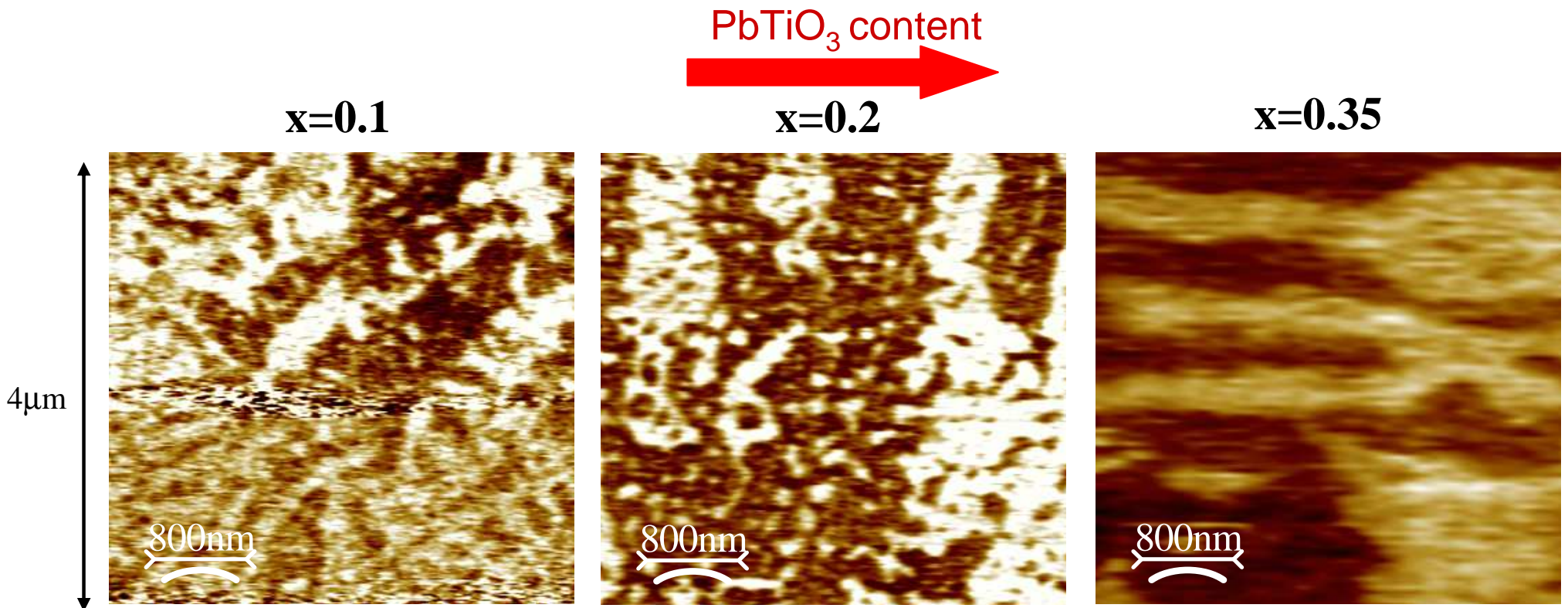
- No nanodomains
- Co-existence of rhombohedral/monoclinic and tetragonal domains

## Conclusion 1: macroscopic domains



- Area occupied by macroscopic domains increases with PT content
- Coexistence of nanodomains and micron-sized domains for  $x=0.2$
- Coexistence of rhombohedral and tetragonal domains for  $x=0.35$

## Conclusion 2: nanoscale domains

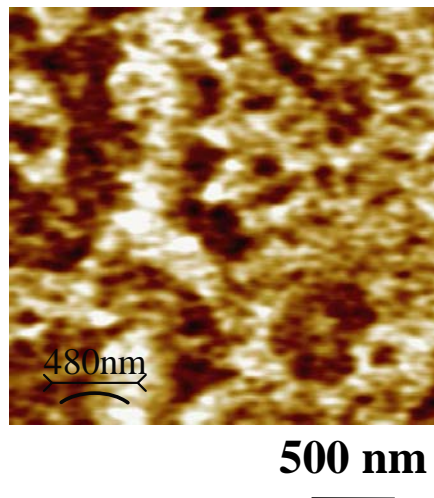


- Area occupied by nanoscale domains decreases with PT content
- Remains of nanodomains are still visible at  $x=0.2$

# Frozen PNRs above $T_c$

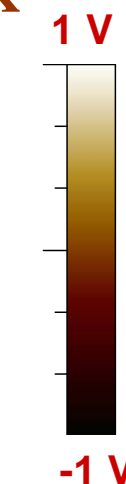
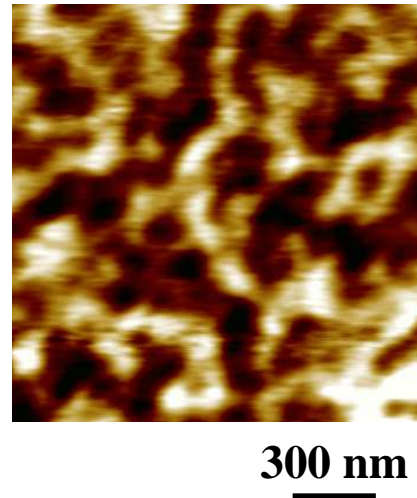
**PMN-PT 80/20**

$\xi \approx 110 \text{ nm} @ T_c + 45 \text{ K}$



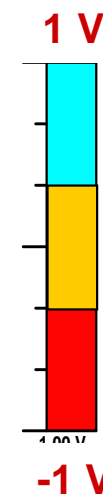
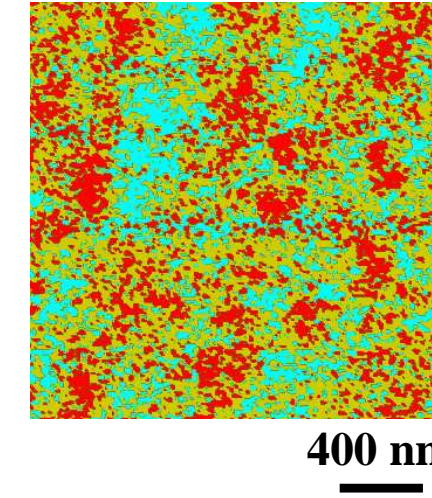
**PMN-PT 90/10**

$\xi \approx 70 \text{ nm} @ T_c + 15 \text{ K}$



**SBN61**

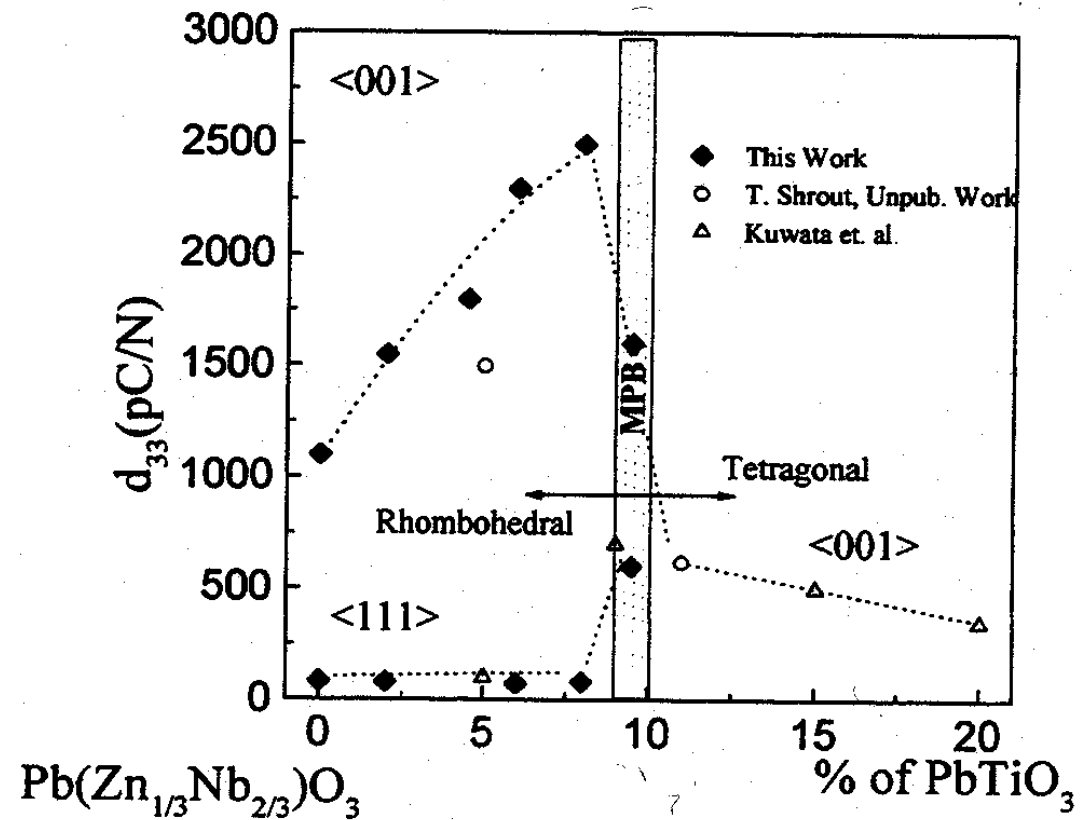
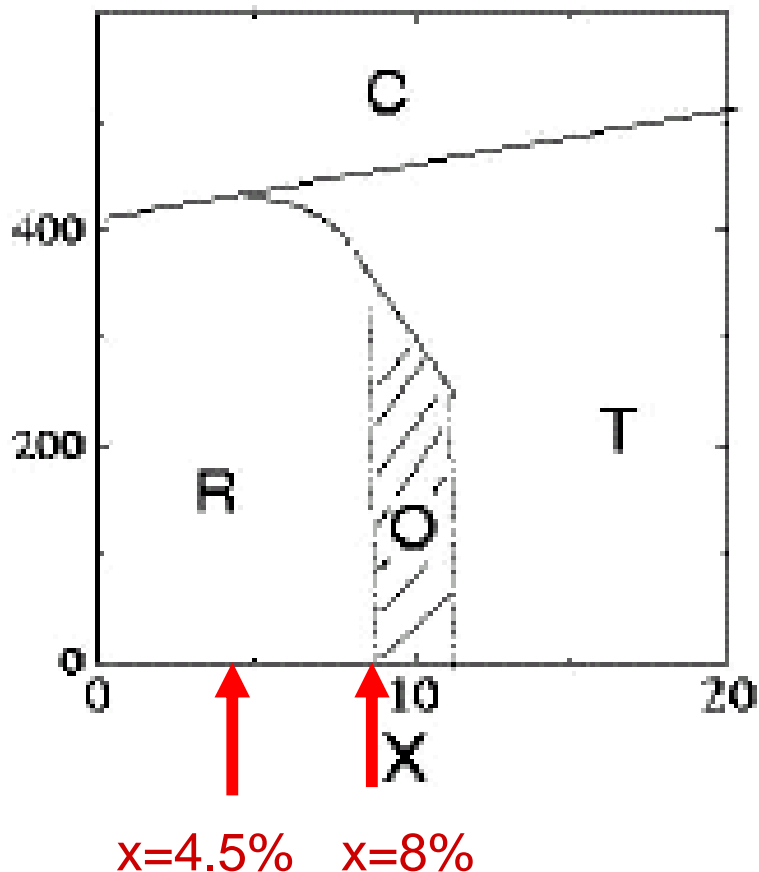
$\xi \approx 45 \text{ nm} @ T_c + 10 \text{ K}$



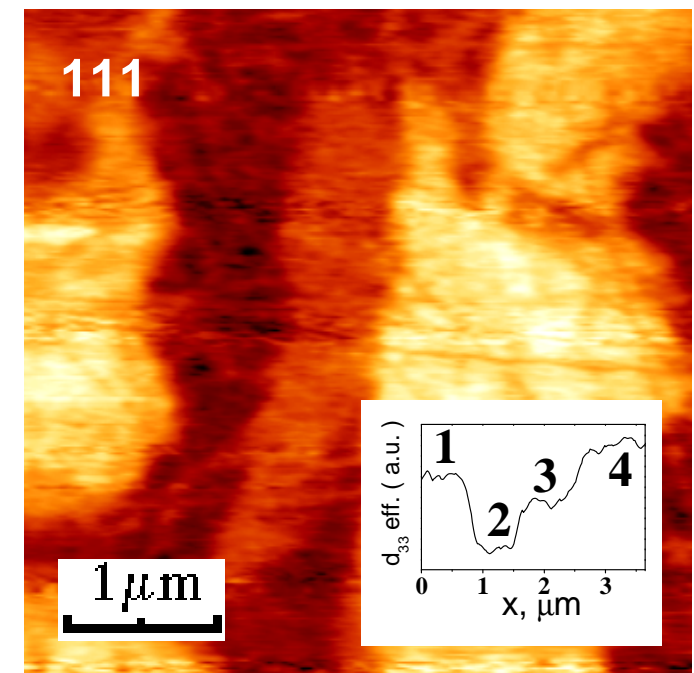
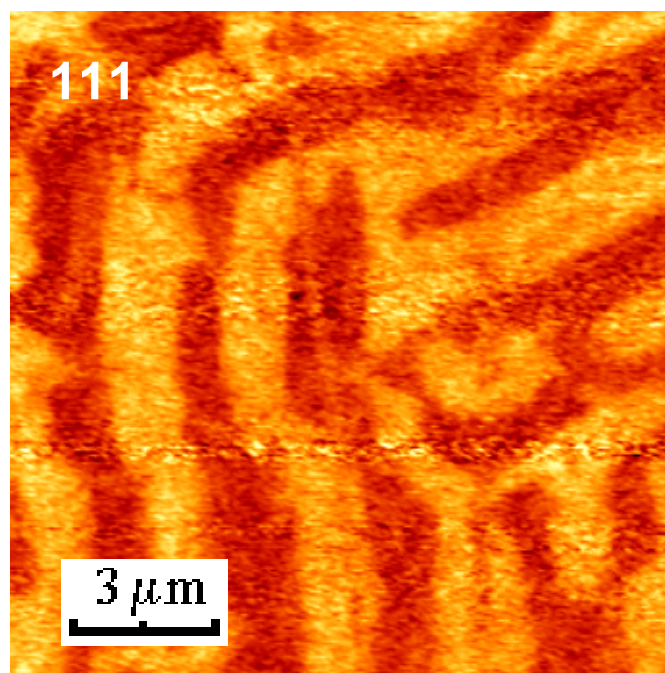
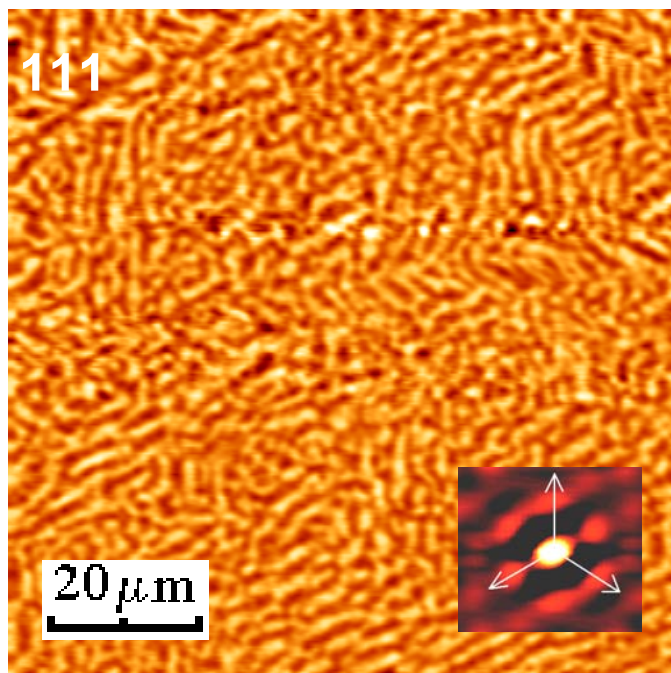
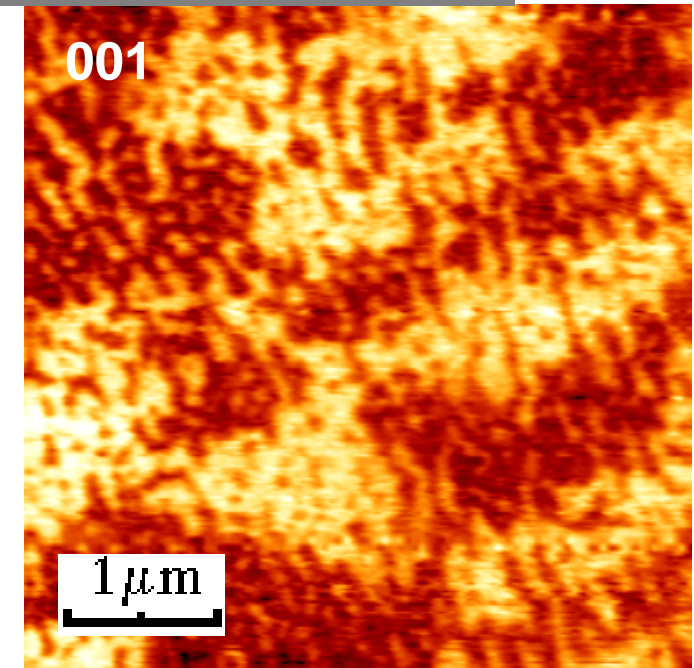
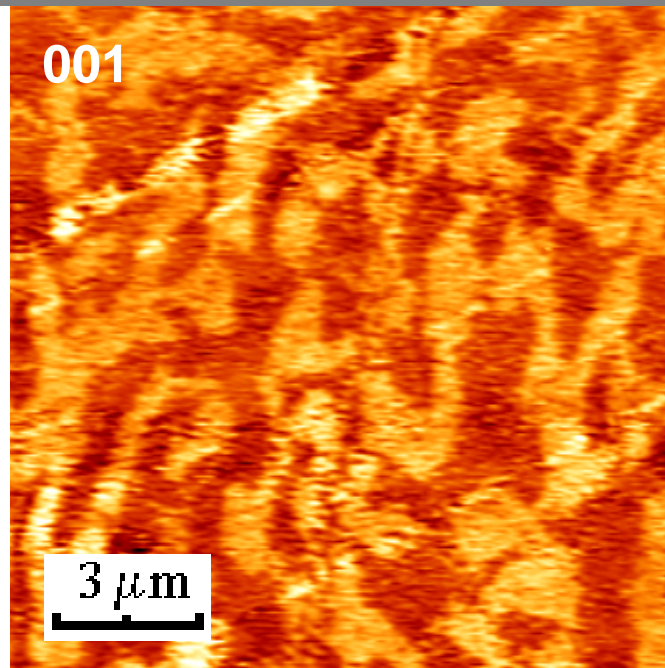
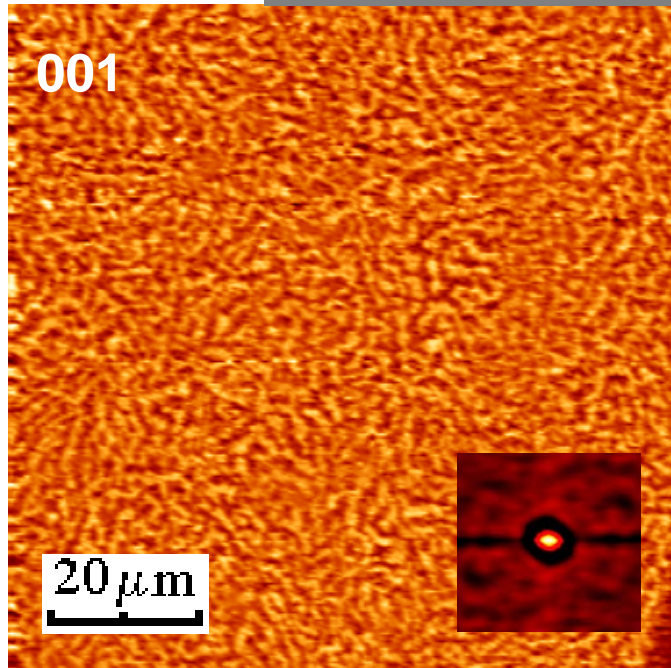
- No sharp transition from ergodic relaxor state into long-range ordered ferroelectric state. Coexistence of large quasi-static PNRs (nanodomains) and dynamic PNRs in a certain temperature range.
- Static PNRs are larger in cubic relaxors and exist in a broader temperature range above  $T_c$  than in uniaxial SBN.
  - Stronger ferroelectric correlation
  - Self-organization of smaller PNRs in larger entities (nandomains) to accommodate mechanical strain

# PbZn<sub>1/3</sub>Nb<sub>2/3</sub>O<sub>3</sub>-PbTiO<sub>3</sub> system

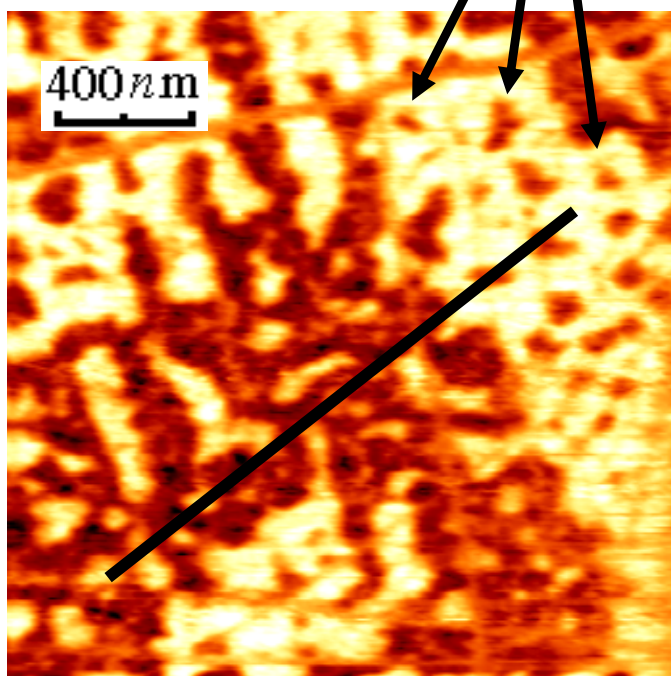
PZN-PT



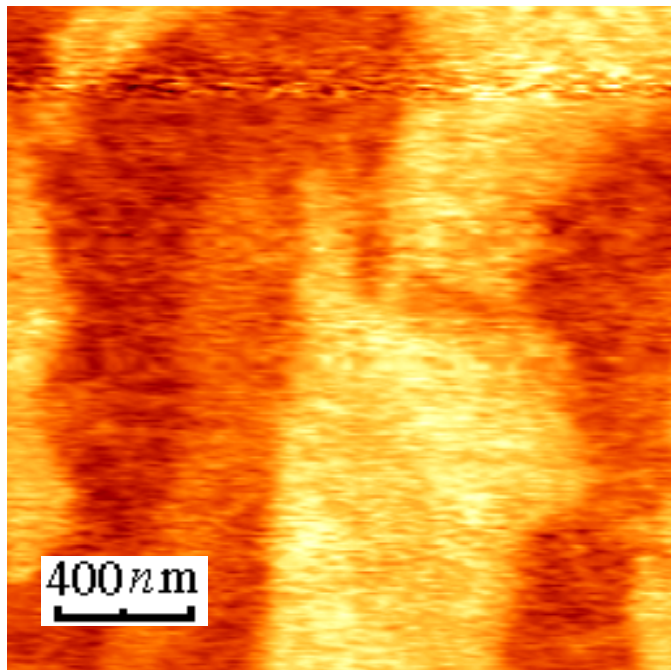
# As-grown domains on (001) and (111) surfaces



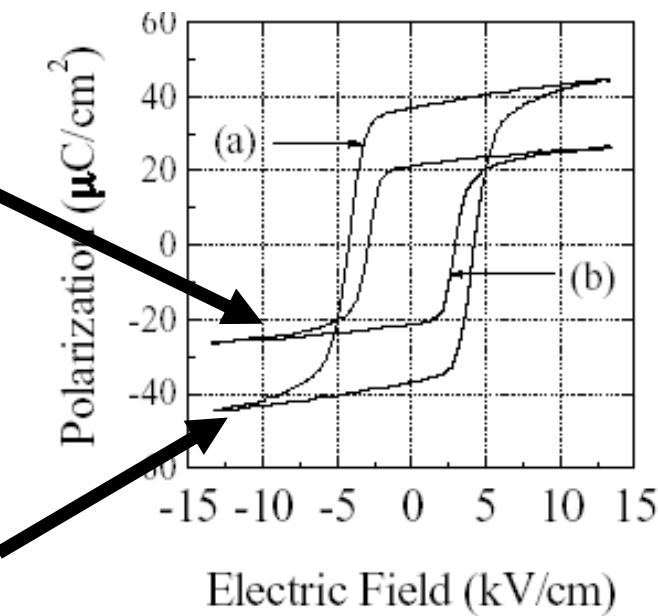
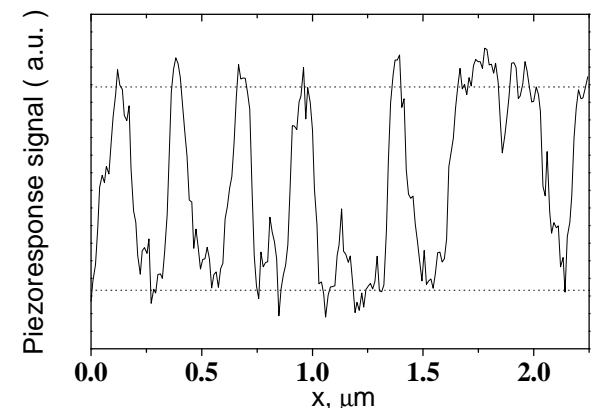
(001)



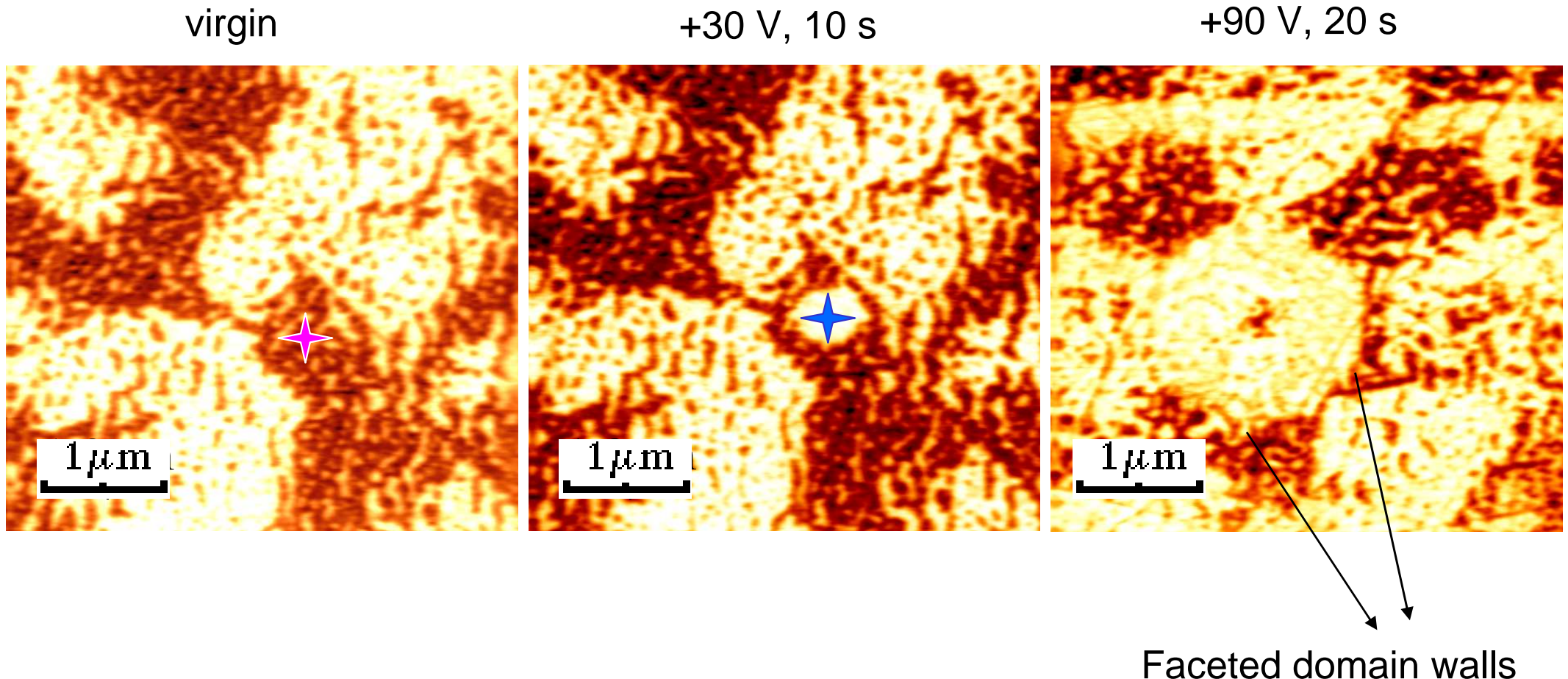
(111)



### Polar nanodomains

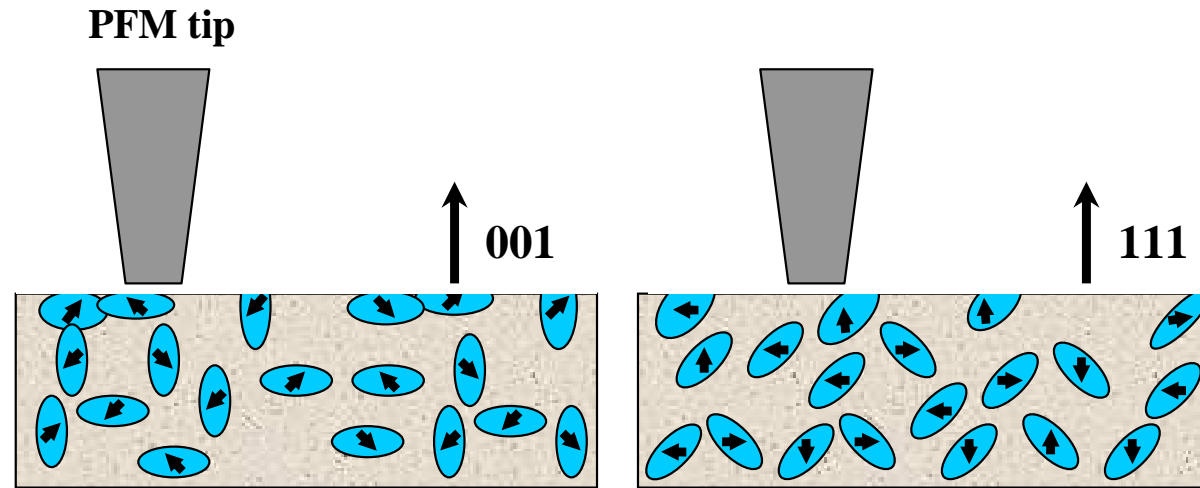


## Poling with the PFM tip



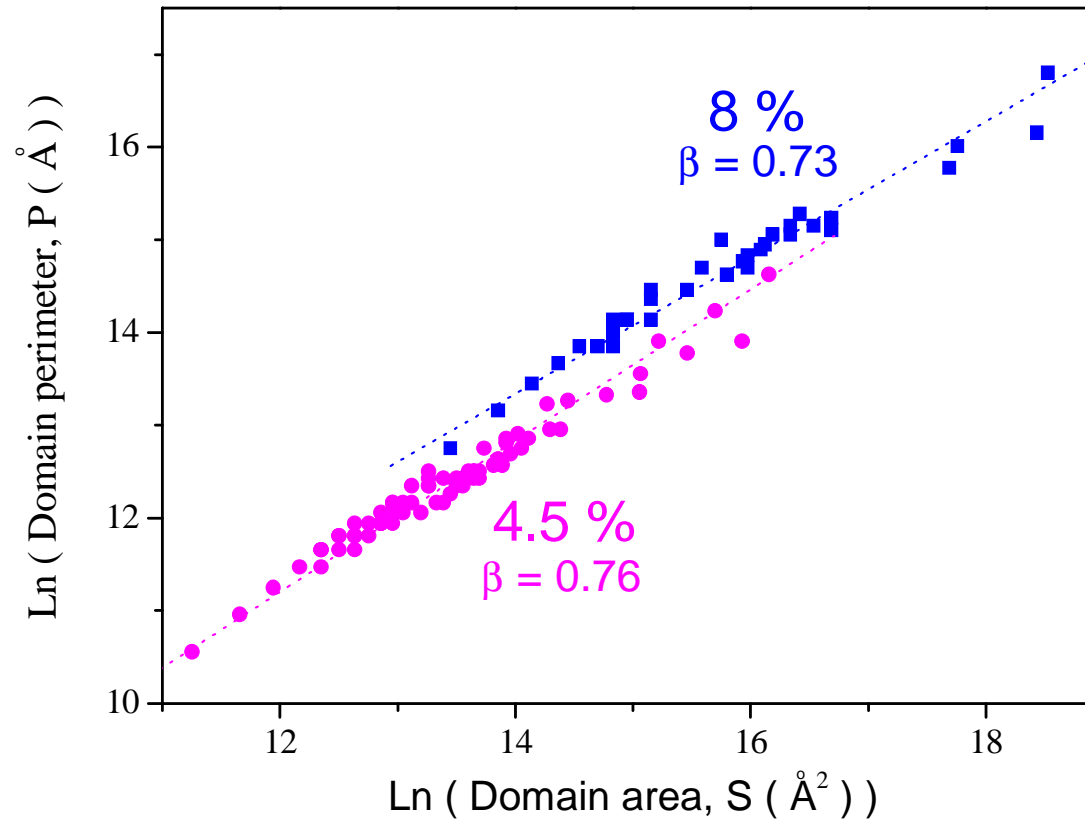
- Poling does not remove nanodomains
- “Normal” micron-sized domains can be written

# Explanation of orientation dependence



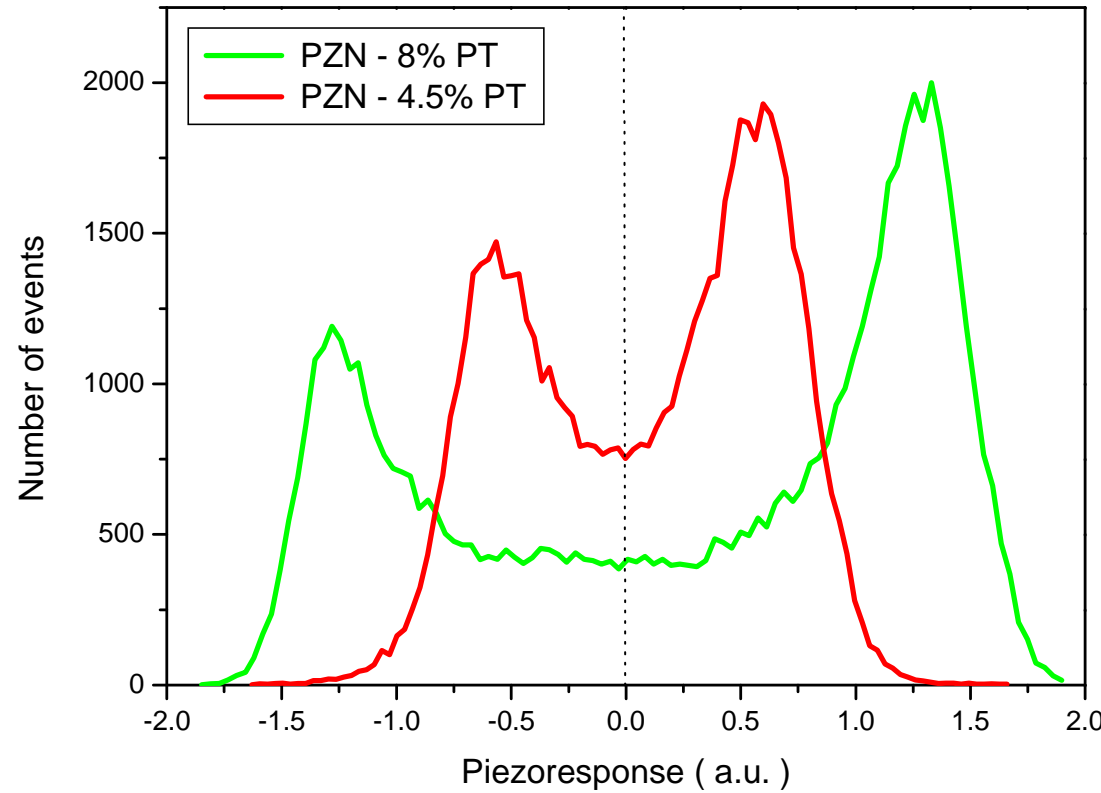
- Polarization is directed along  $<111>$  but longer correlation length along  $<001>$ !
- Size of nanodomains is larger on (100) oriented surfaces, therefore they can be detected by PFM tip

## Fractal analysis of PZN-4.5% and PZN-8%



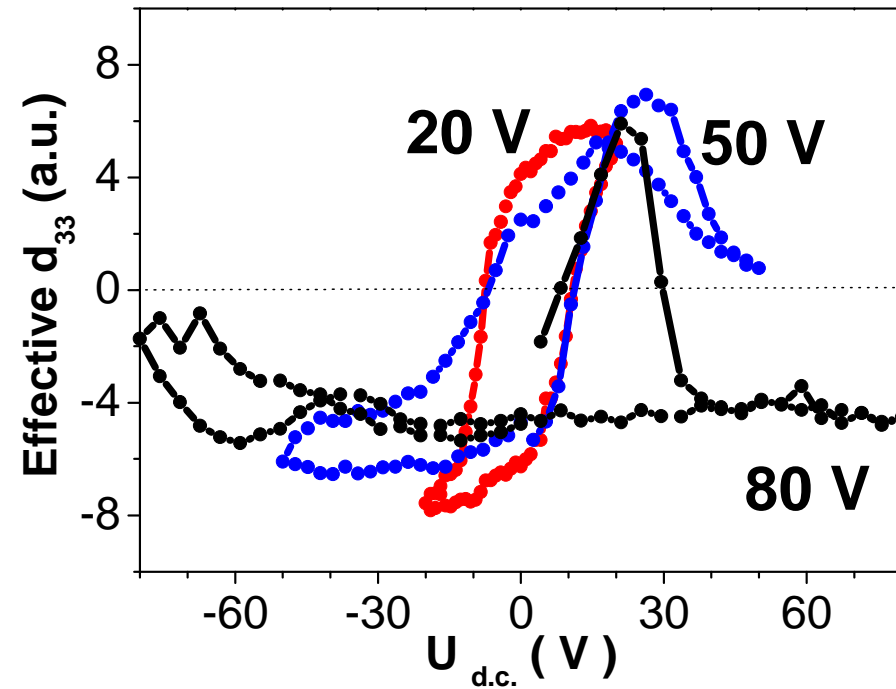
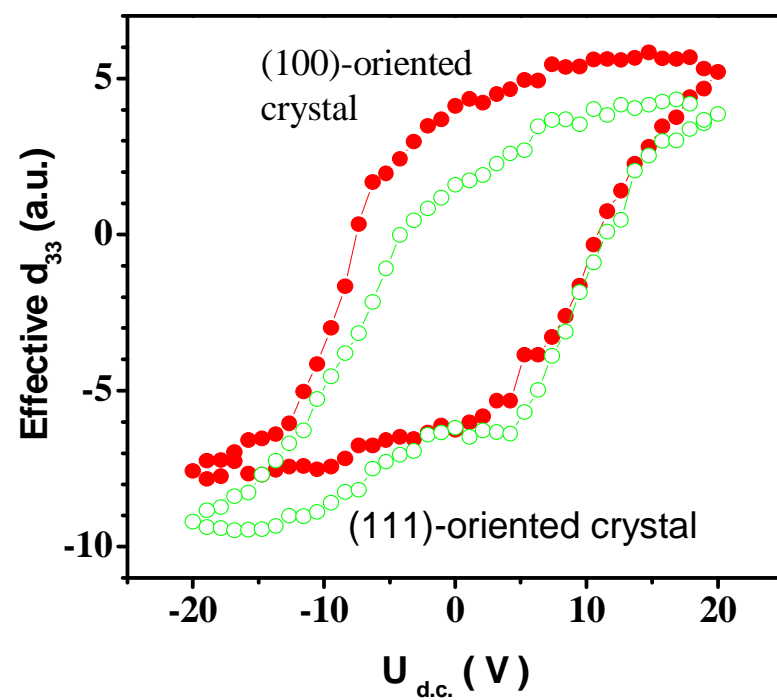
- Fractal dimension is independent on PT content (same as in PMN-PT case)

# Comparison of domain histograms in PZN-4.5% and PZN-8%PT



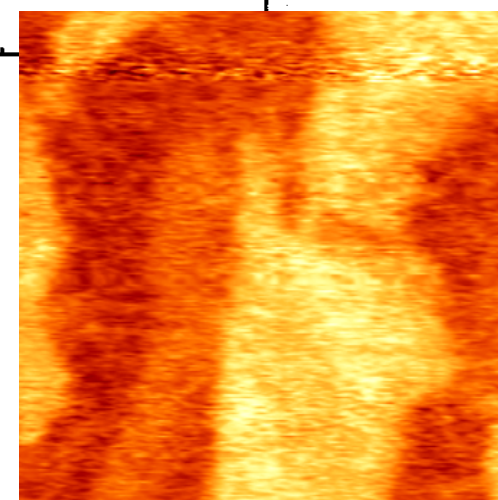
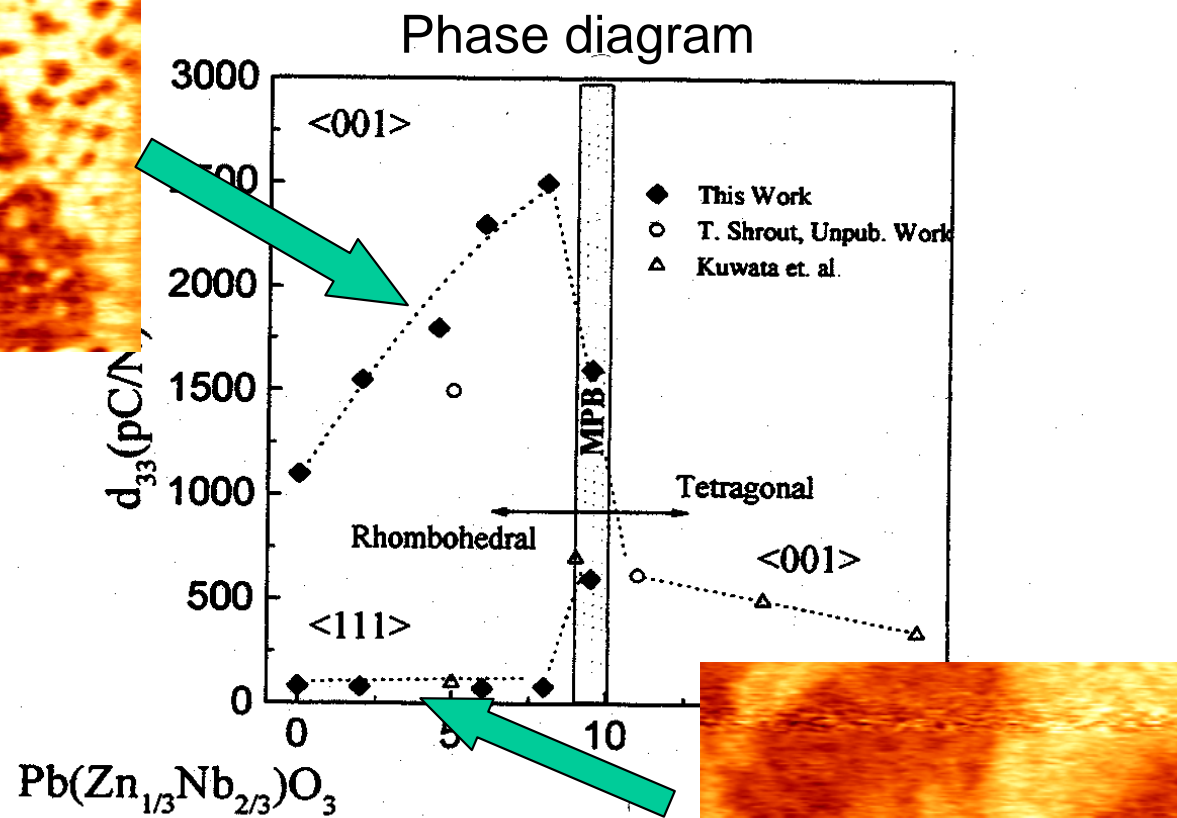
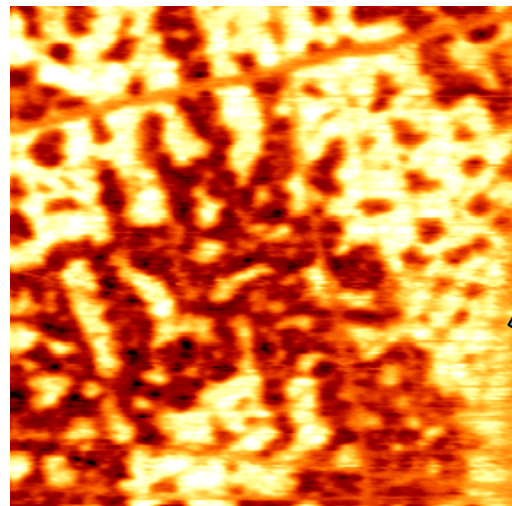
- Large increase of area corresponding to nanodomains
- “Ferroelectric” piezoresponse is 2 times higher in PZN-8%PT

# Local hysteresis at the nanoscale



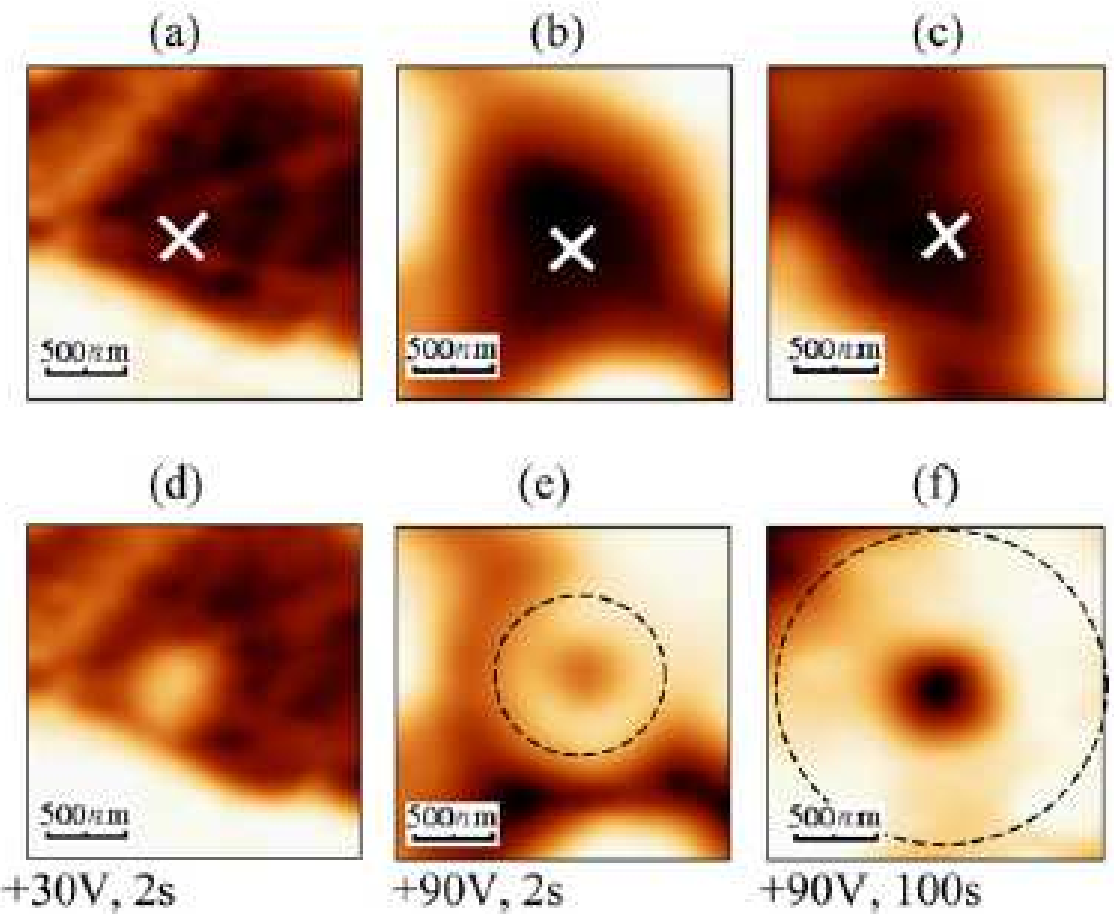
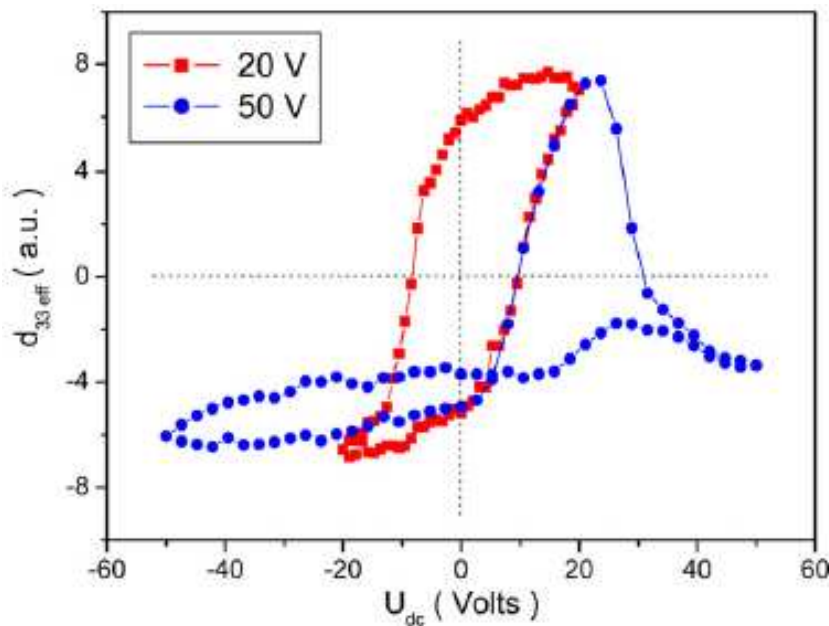
- No evidence of electric field induced phase transition
- Higher voltage induces only sign reversal of local  $d_{33}$

# Origin of giant piezoelectric response



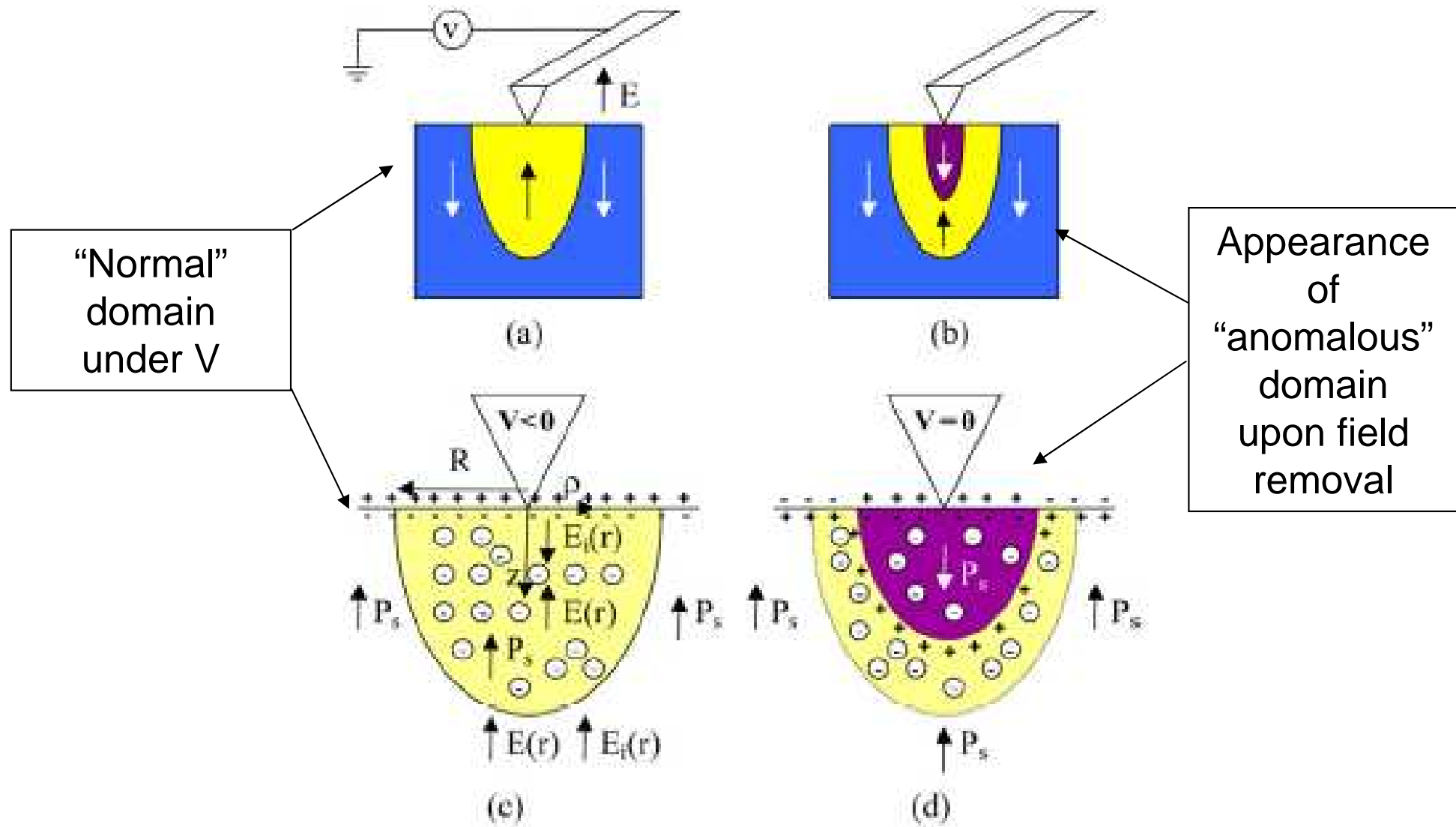
# Anomalous polarization inversion

## Local hysteresis

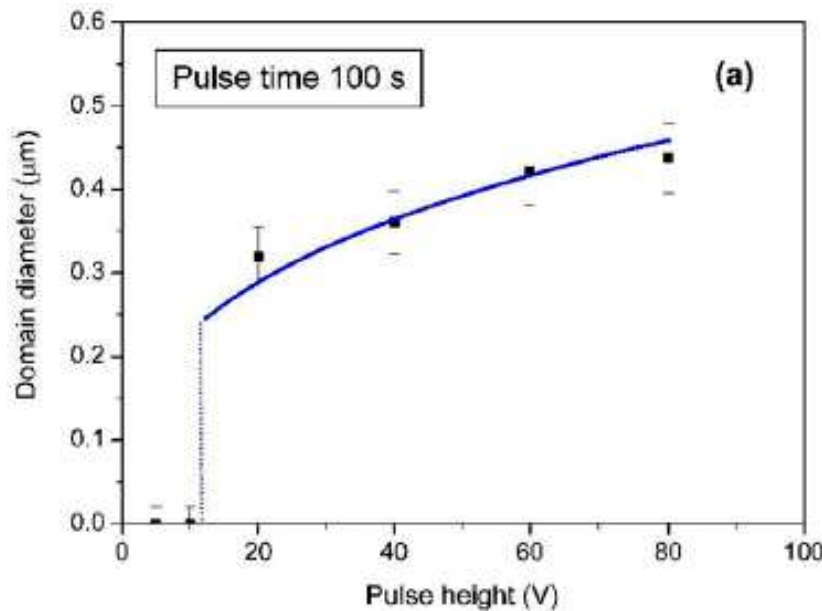


## Switching by the tip

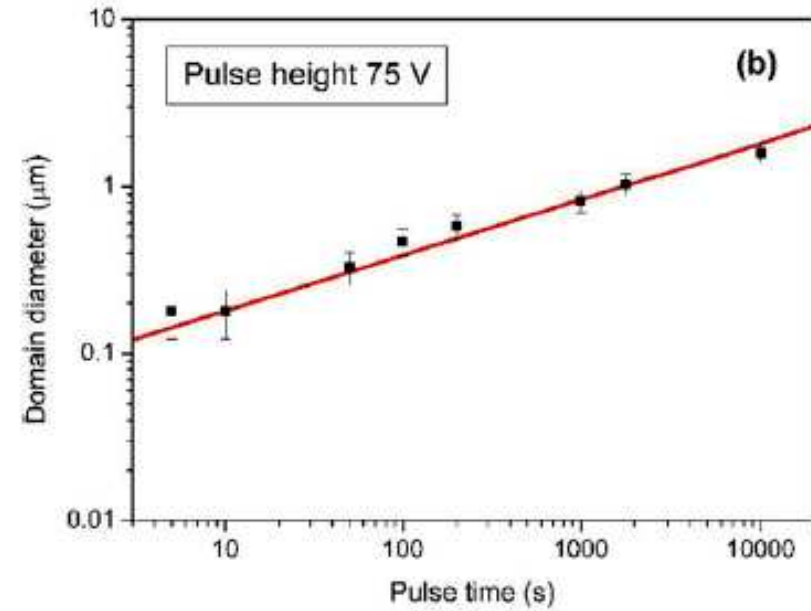
# Schematic of $E$ -field and $P$ distribution



# Voltage and time dependencies



Voltage dependence



Time dependence

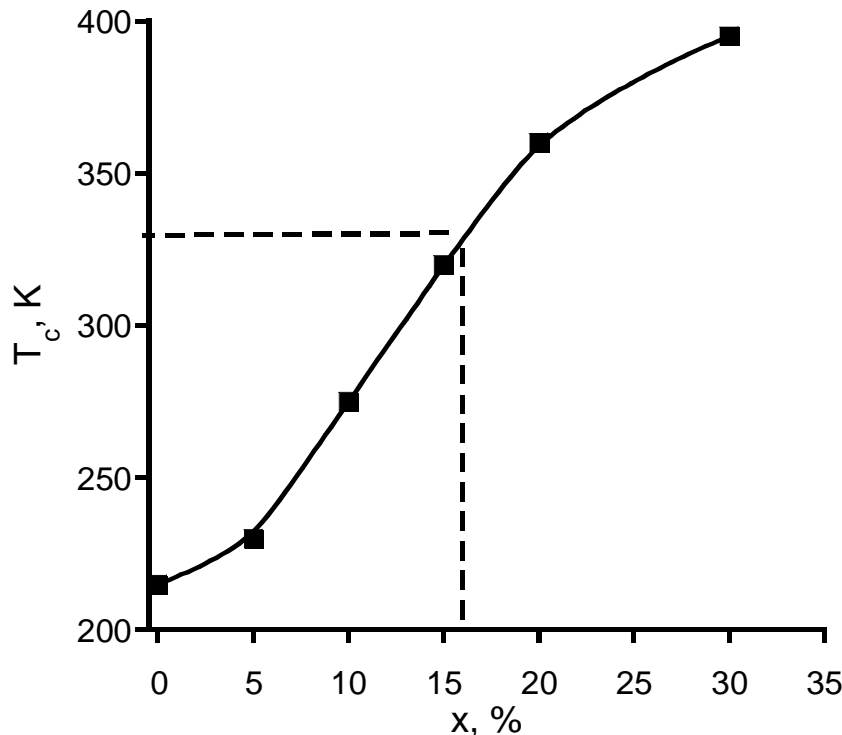
Diameter of inverse  
domain

$$D(V, \tau) \approx 2\eta \left( \frac{3C\mu_{\text{eff}}}{2\pi\epsilon_0\sqrt{\epsilon_{\perp}\epsilon_{\parallel}}} V \tau \right)^{1/3}$$

# ***Consequences for domain writing***

- Wrong bit can be created (bit error)
- New method for local mobility measurements
- Local control of Fermi level in ferroelectrics via charge injection
- Very stable small domains imprinted due to charge on deep traps

# Relaxor ceramics: PMN-16%PT



Ye et al., Phys. Rev B (2003)

**0.84PbMg<sub>1/3</sub>Nb<sub>2/3</sub>O<sub>3</sub>-0.16PbTiO<sub>3</sub>:**  
composition intermediate between pure  
relaxor (PMN) and piezoelectric (PMN-  
0.35PT).

## Ferroelectric features:

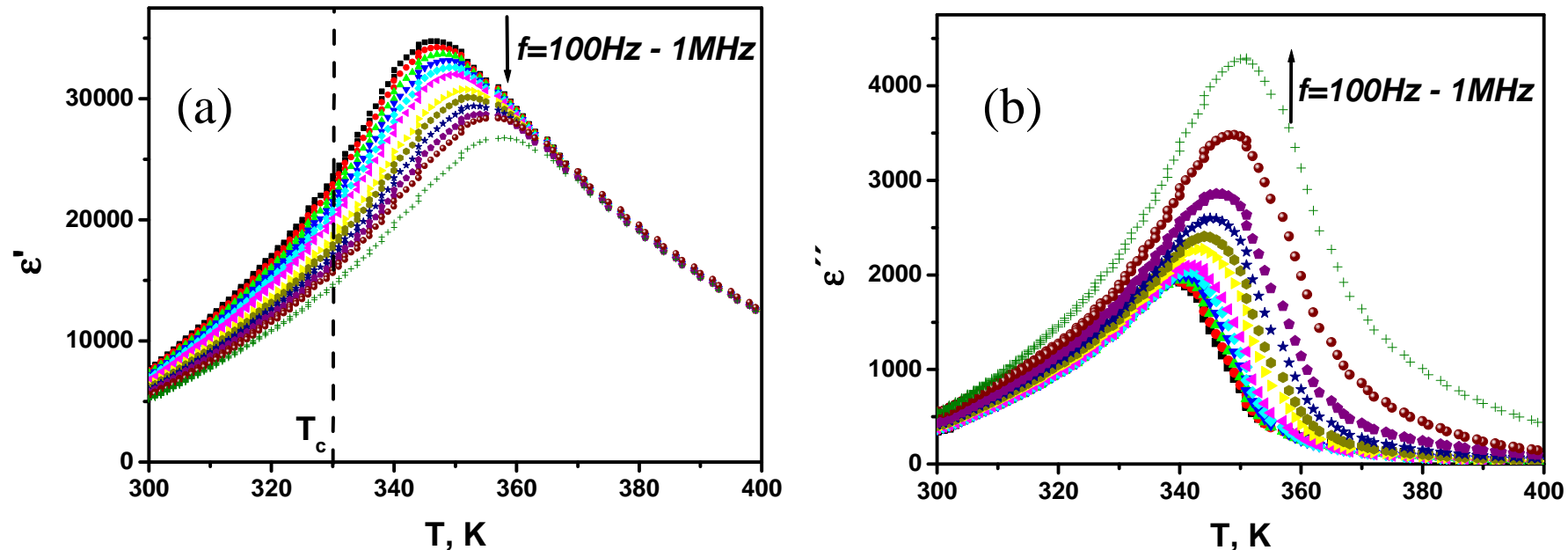
- ✓ spontaneous transition to macroscopic ferroelectric phase with rhombohedral symmetry – XRD
- ✓ ferroelectricity induced by dc field

## Relaxor features:

- ✓ remains macroscopically cubic - neutron scattering
- ✓ relaxor-like behavior of dielectric permittivity

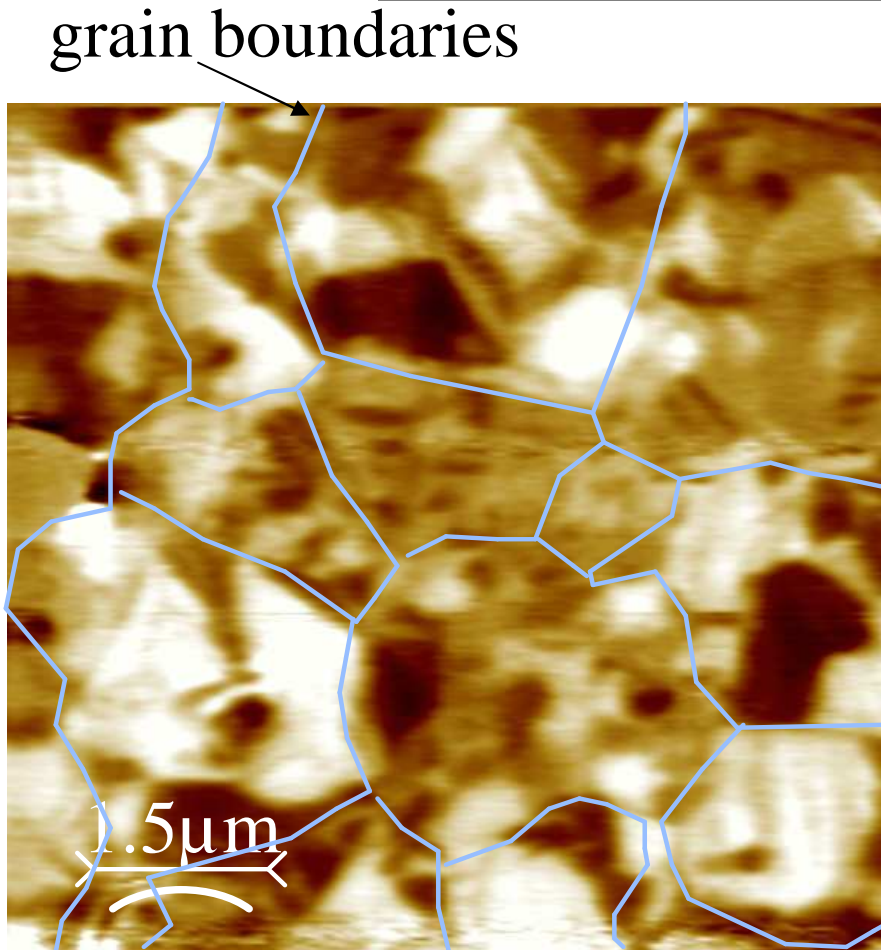
# Dispersion of dielectric permittivity

Temperature dependencies of real (a) and imaginary (b) part of dielectric permittivity.



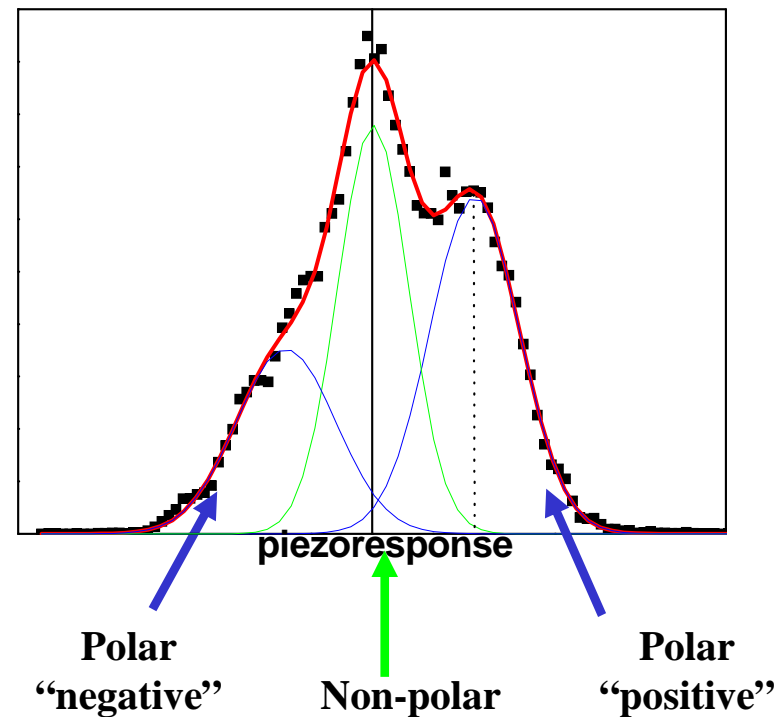
- Dielectric permittivity exhibit diffuse phase transition with maximum at **345-360 K**
- Observed frequency dispersion is typical for relaxor materials
- Deviation from Curie-Weiss law starting at **T~460 K**

## Room-temperature domains ( $T < T_c$ )



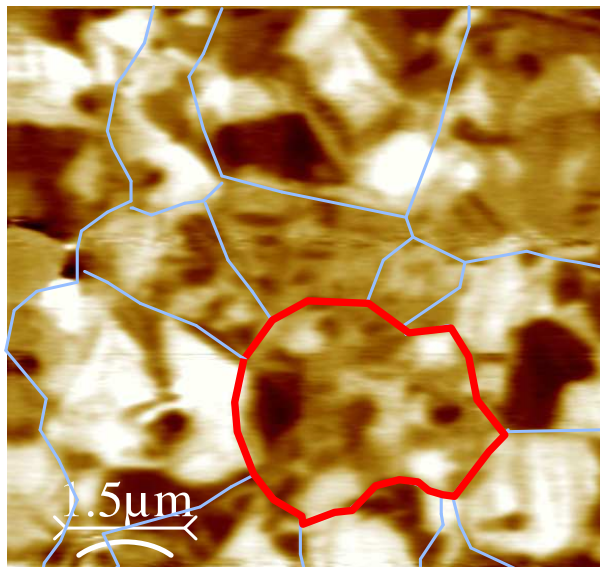
Typical piezoresponse image  
at the room temperature

Piezoresponse histogram

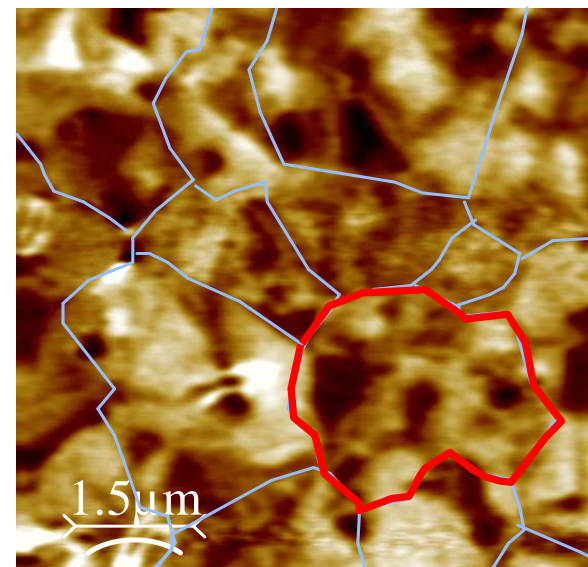


- Piezoelectric histograms can be deconvoluted into simple Gaussian peaks corresponding to polar and non-polar phases

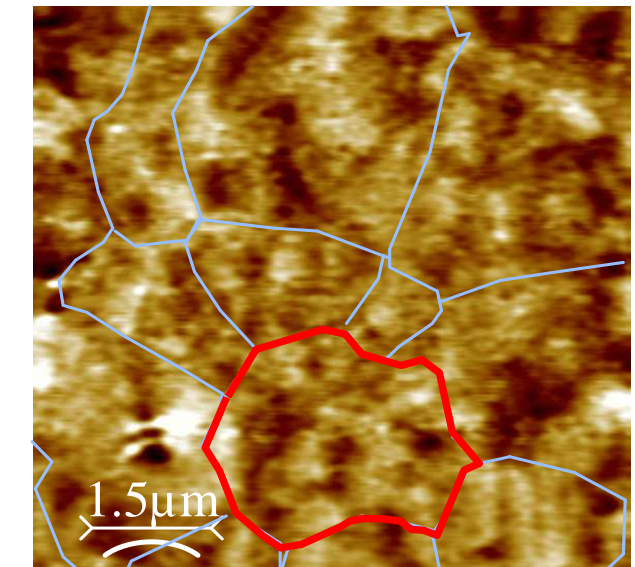
## As-grown domains vs. heating (ZFH)



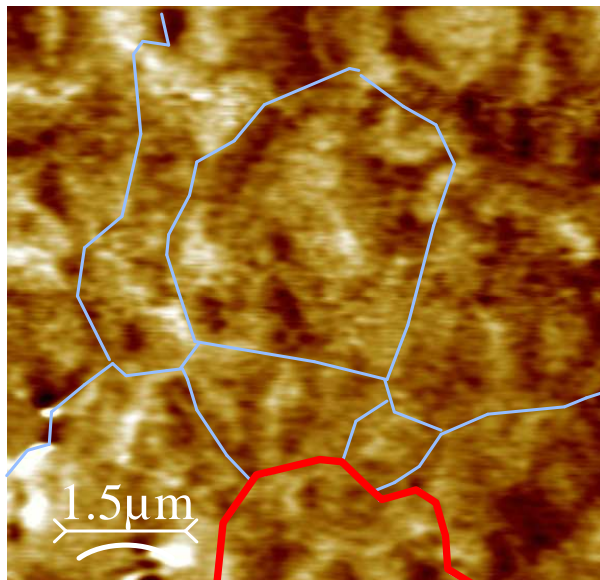
310K



$T < T_c$



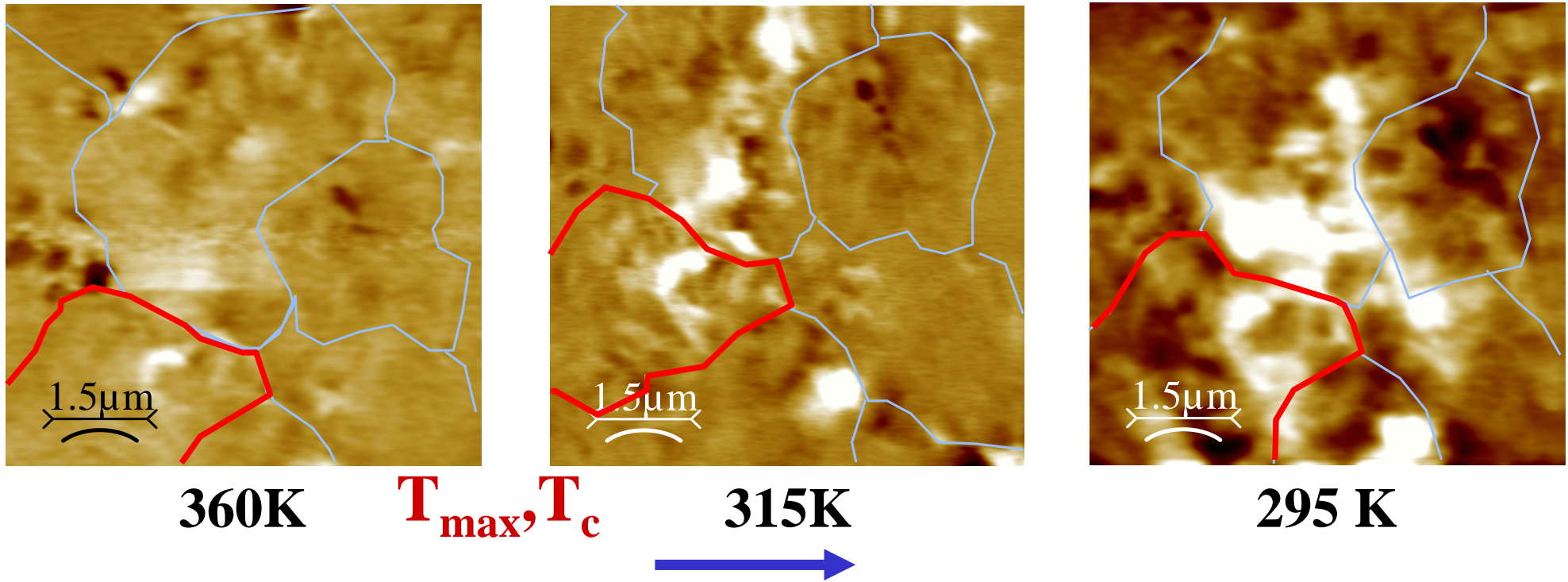
$350K \approx T_{max}$



360K no dispersion

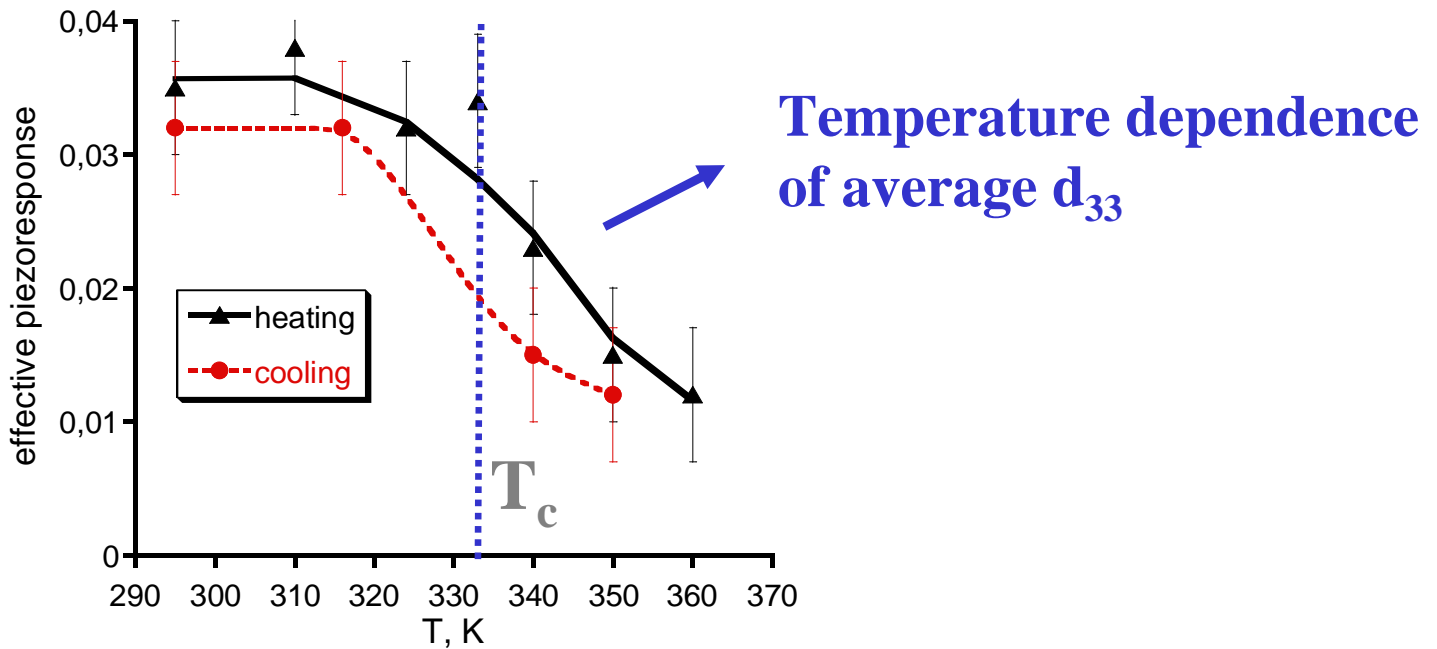
- ✓ Domains persist above  $T_c$  and above  $T_{max}$  (352 K)
- ✓ Ferroelastic domains survive bulk phase transition
- ✓ Polar domains gradually shrink with temperature

## As-grown domains vs. cooling (ZFC)

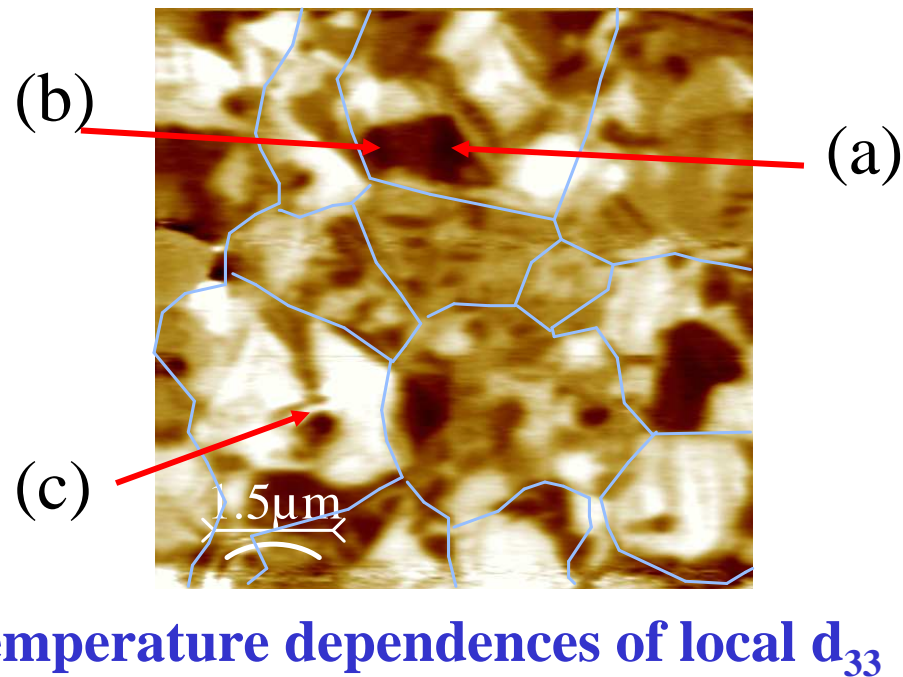


- ✓ Sample was annealed to 410 K *in situ*
- ✓ Small domains of size of several hundred nm appeared above T<sub>c</sub> and T<sub>max</sub>
- ✓ On cooling nanoscale domains grow and new domains nucleate
- ✓ Preferencial nucleation on a grain boundary

# Temperature dependence vs. position

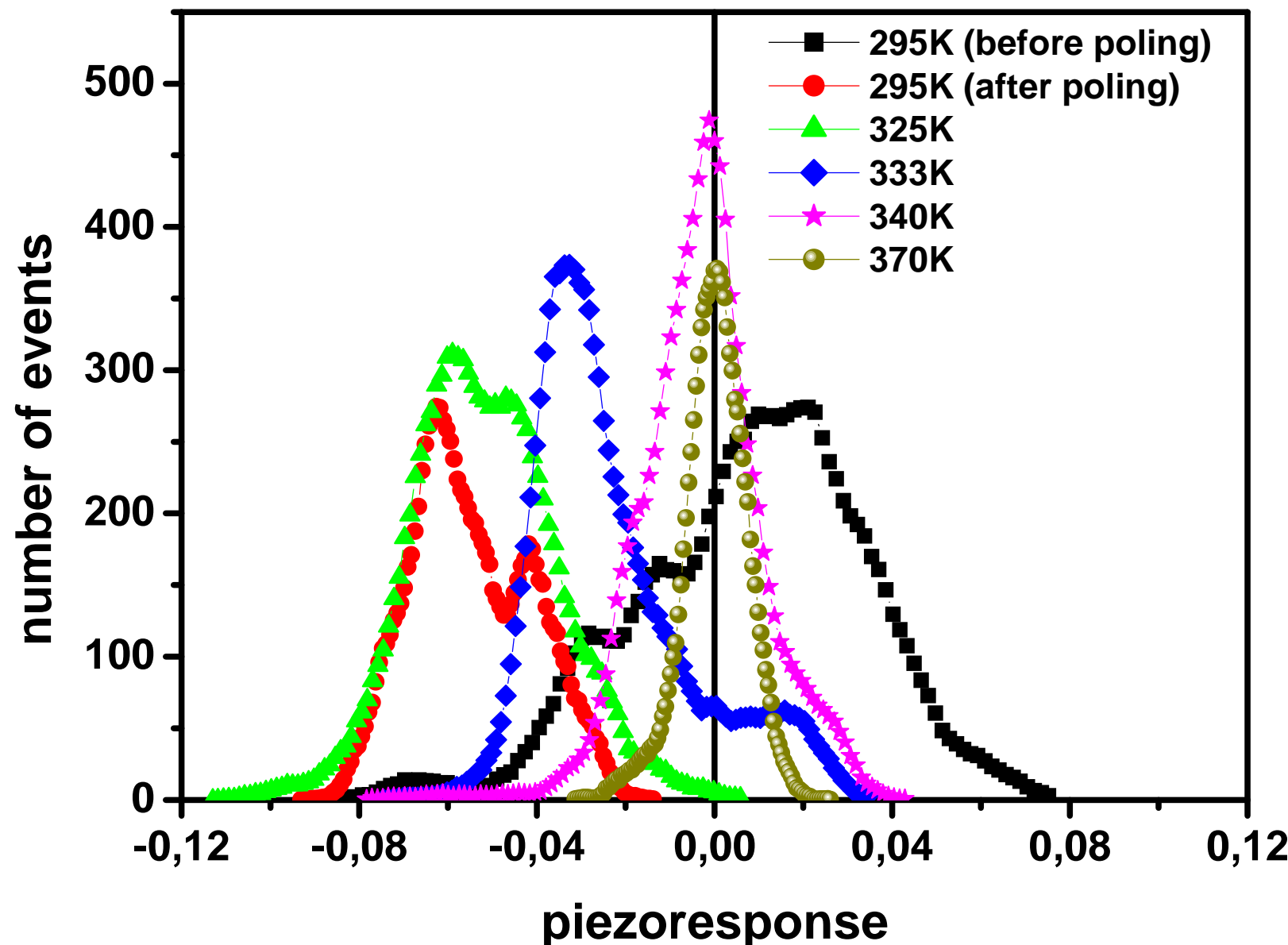


Temperature dependence  
of average  $d_{33}$

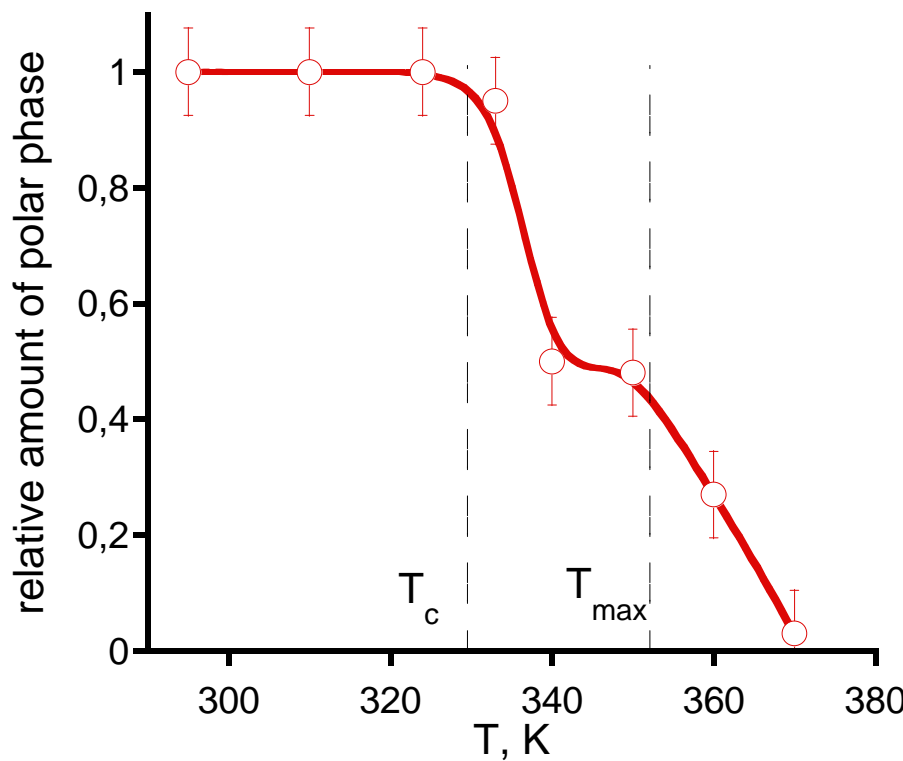


Temperature dependences of local  $d_{33}$

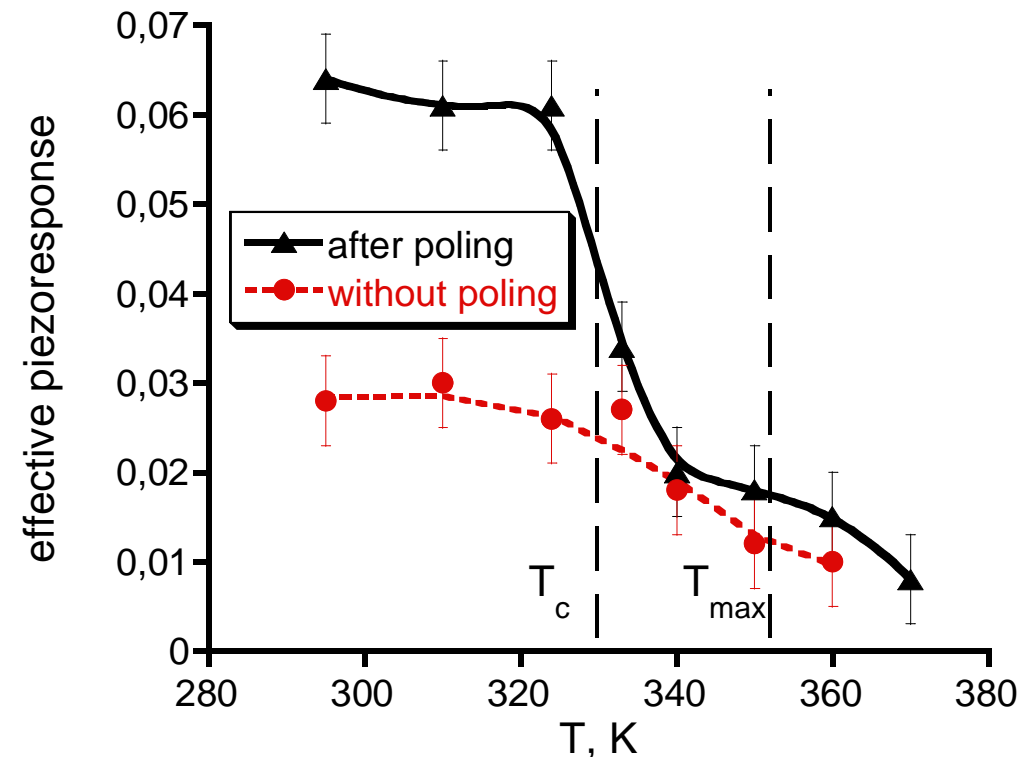
# Evolution of piezohistograms with T



# Temperature evolution of histogram parameters



Temperature dependence of polar phase concentration inside the poled area

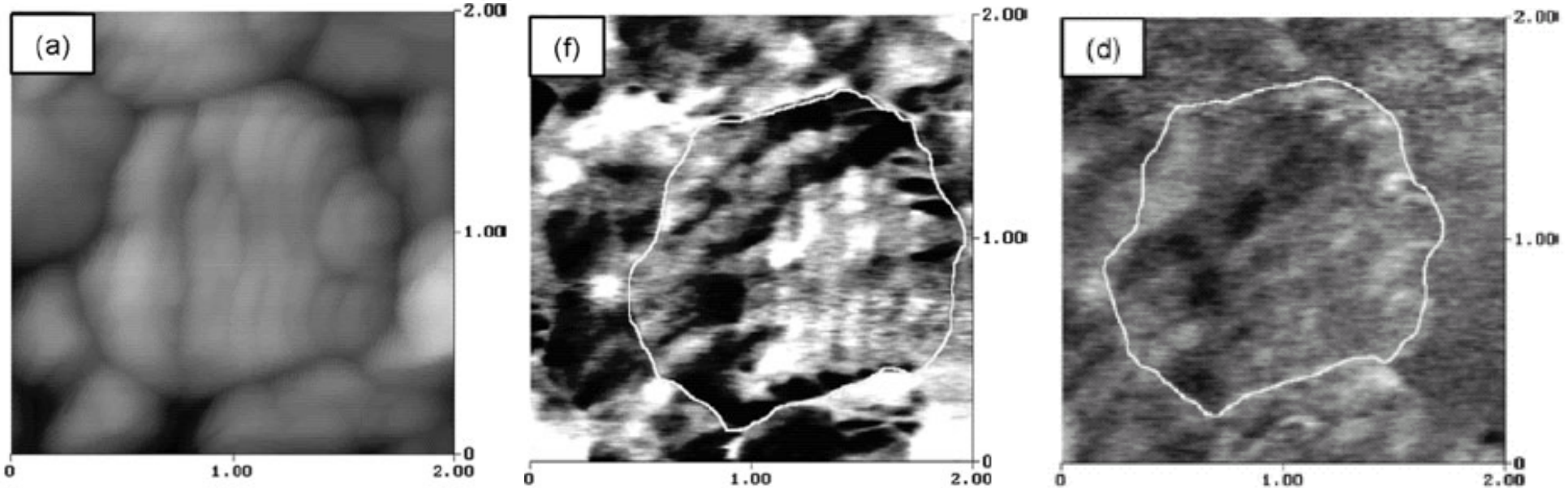
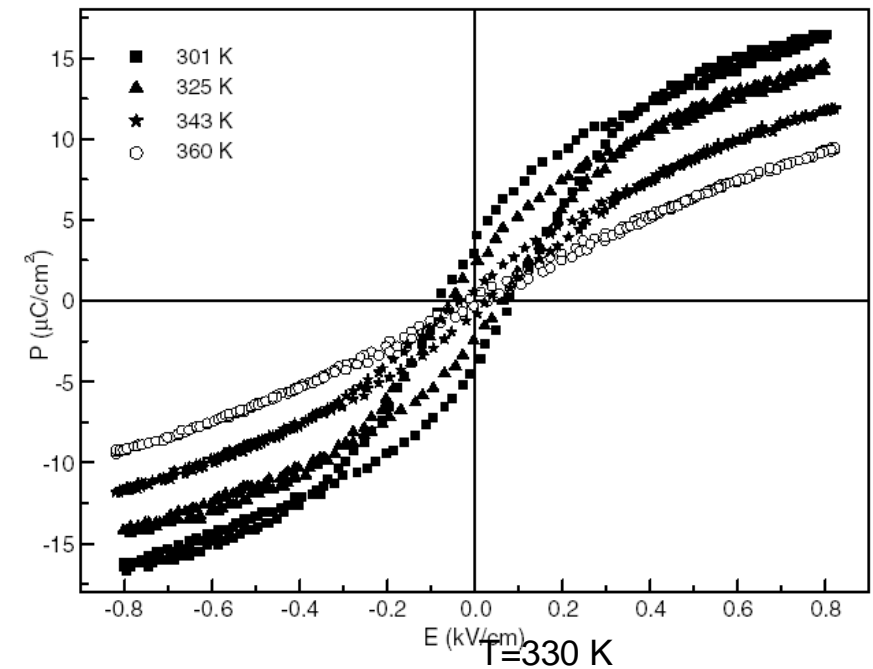
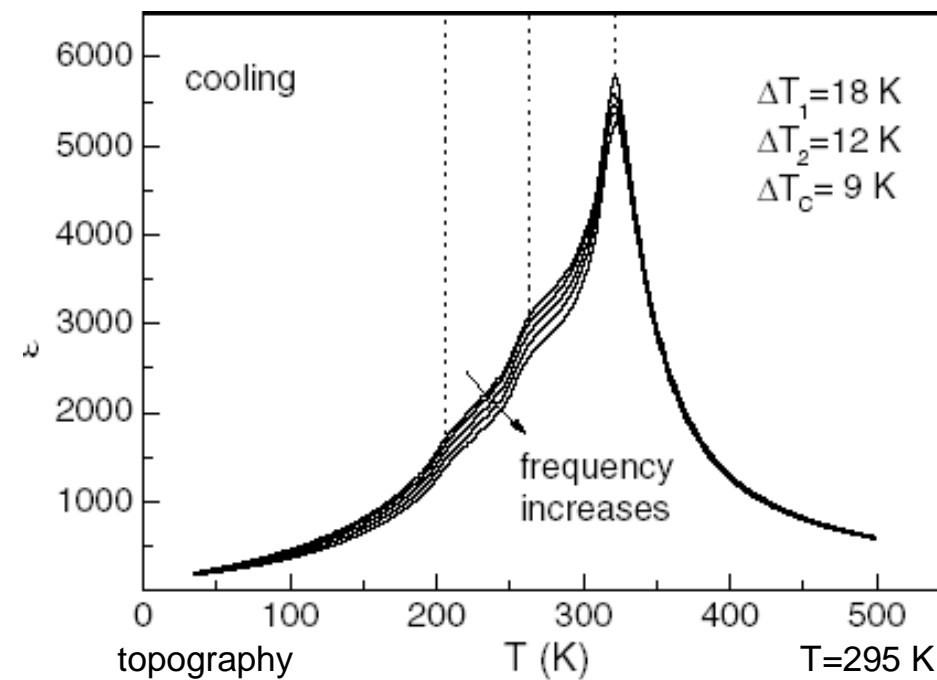


Temperature dependencies of effective piezoresponse in poled and non-poled areas

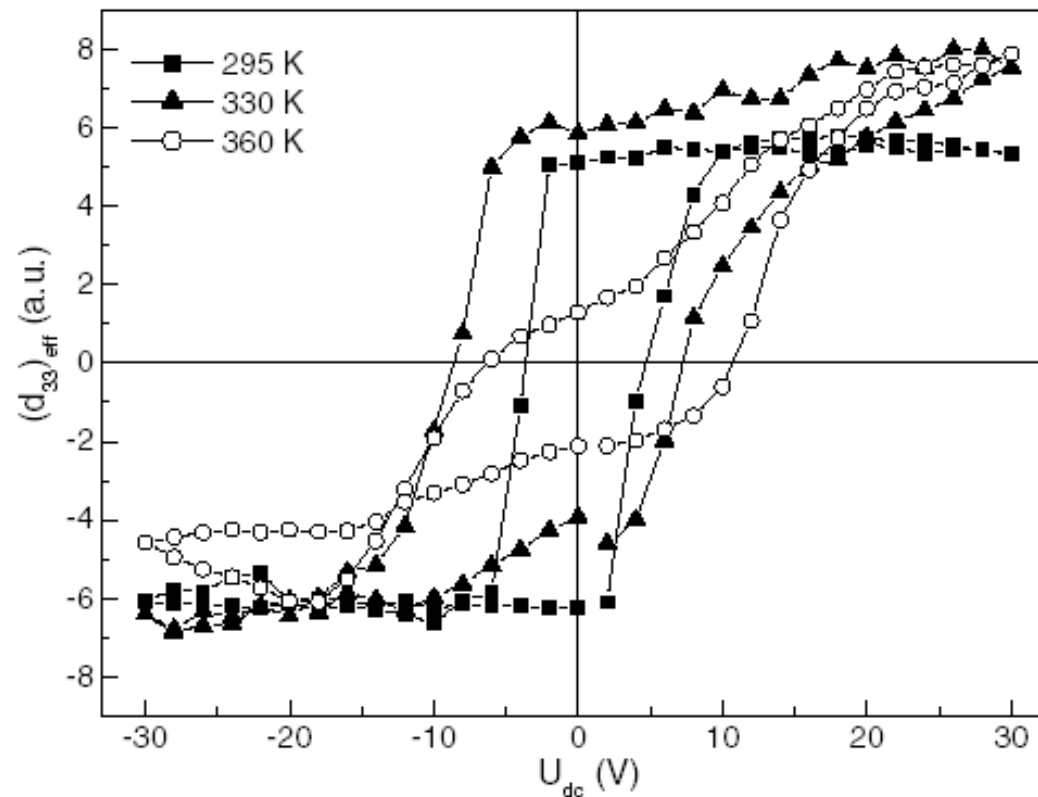
- Temperature of disappearance of artificial domain (depolarization temperature) is close to Curie temperature determined from XRD
- Further decay of effective piezoresponse is analogous to that observed in non-poled regions

# BaTiO<sub>3</sub>-based relaxor ceramics

BaTiO<sub>3</sub>-2.5%La(Mg<sub>1/2</sub>Ta<sub>1/2</sub>)O<sub>3</sub>



# Hysteresis at the nanoscale



- “Normal” ferroelectric hysteresis below  $T_c$
- “Double” hysteresis loops at  $T > T_c$ : electric field-induced transition into ferroelectric phase

# $Pb_{1-y}La_y(Zr_xTi_{1-x})_{1-y/4}O_3$ ceramics (PLZT x/65/35)



Properties of ferroelectric/relaxor PLZT:

- ❖ high optical transparency
- ❖ tunable electrooptic properties
- ❖ fast response
- ❖ wide viewing angle
- ❖ multicolor capability
- ❖ solid state nature and simplicity of construction

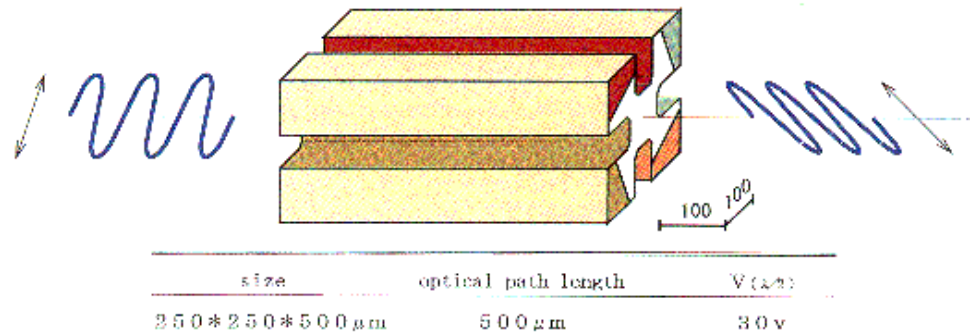
Applications of PLZT ceramics:

- ❖ segmented displays
- ❖ light shutters
- ❖ coherent modulators
- ❖ color filters
- ❖ linear gate arrays
- ❖ image storage devices

# Commercial and military applications of PLZT electrooptic ceramics



**PLZT Optical Shutter MOS-30V**



B1-B Cockpit Viewing Port



EEU-2P Flyers Goggles

# Phase diagram and non-stoichiometry

## Chemical formula

$Pb_{1-x}La_x(Zr_yTi_{1-y})_{1-0.25x}V^B_{0.25}O_3$ ,  $V^B$ : B site lattice vacancy

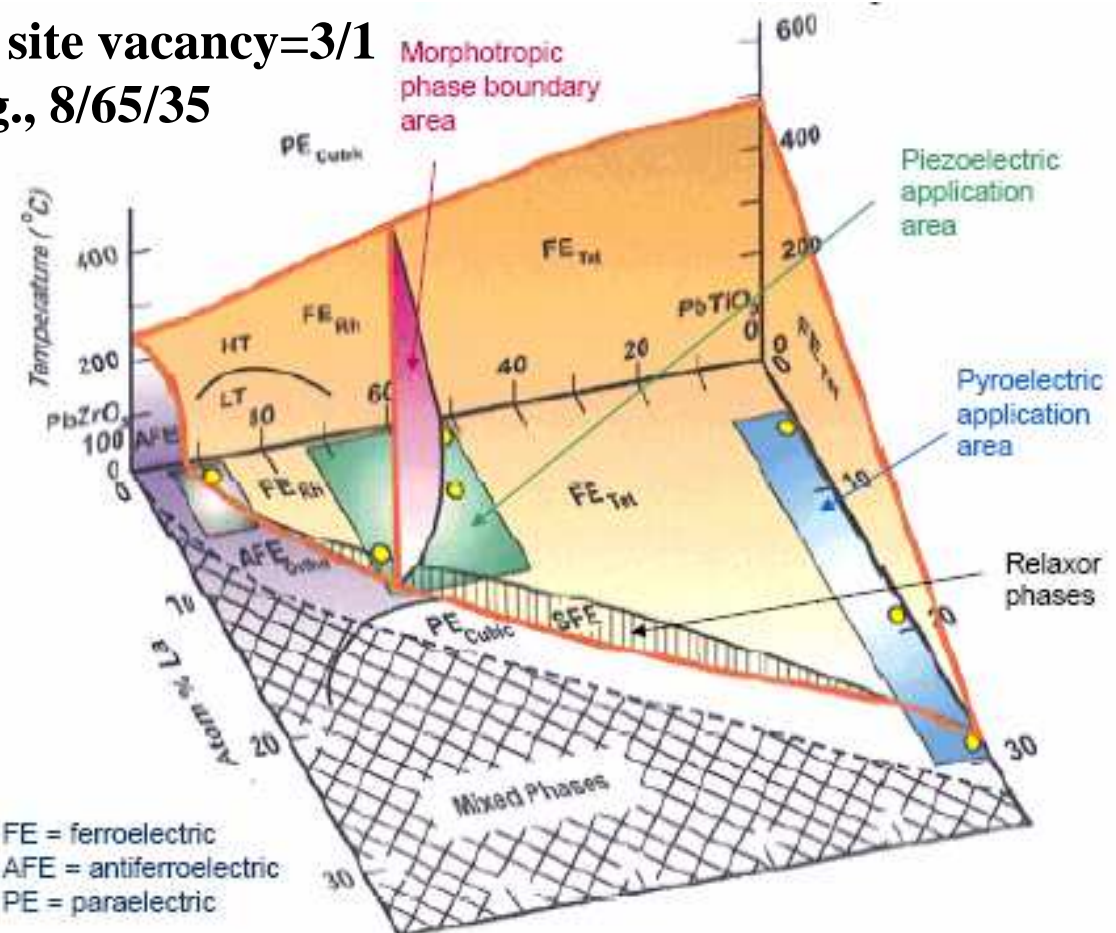
High  $PbZrO_3$ : A site vacancies majority

High  $PbTiO_3$ : B site vacancies majority

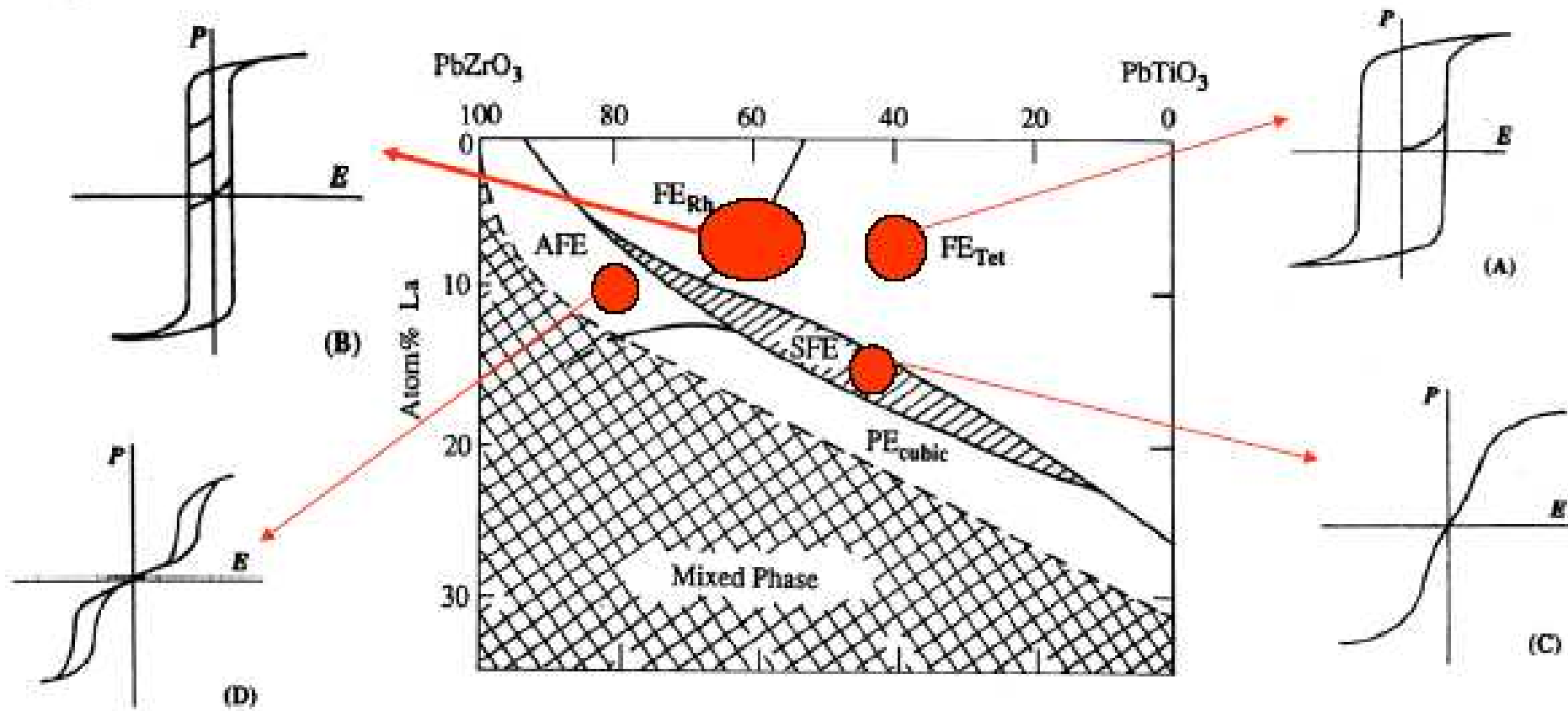
$PbZrO_3/PbTiO_3=65/35$  : A site vacancy/B site vacancy=3/1

PLZT composition :  $x/y/(1-y)$  notation, e.g., 8/65/35

for  $Pb_{0.92}La_{0.08}(Zr_{0.65}Ti_{0.35})_{0.98}O_3$



# The phase diagram of PLZT system at room temperature



**PE<sub>Tet</sub>:** ferroelectric tetragonal phase

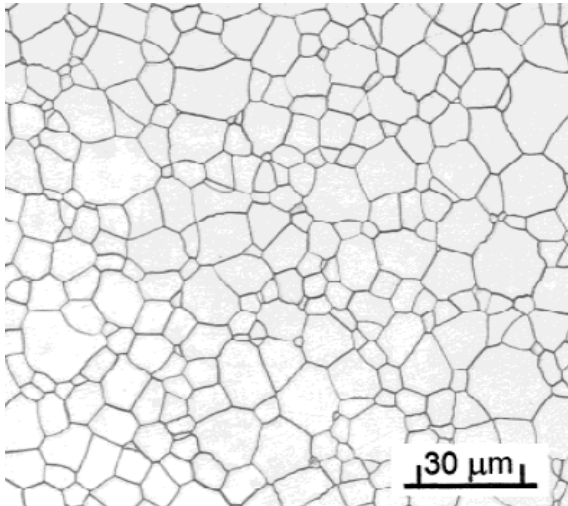
**FE<sub>Rh</sub>:** ferroelectric rhombohedral phase

**AFE :** antiferroelectric

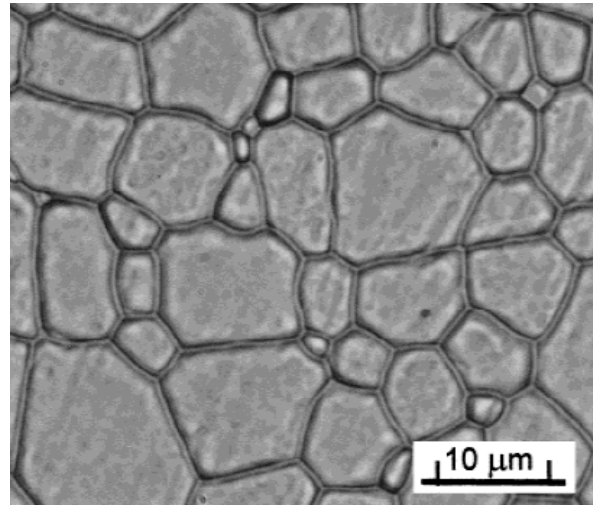
**PE<sub>cubic</sub>:** paraelectric cubic phase

**SFE :** relaxor phases

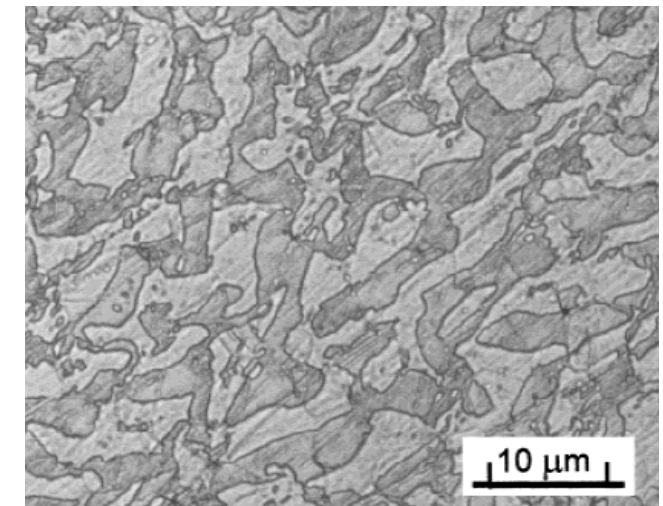
# Processing & Microstructure



**Hot-pressed electrooptic  
PLZT 9/65/35**

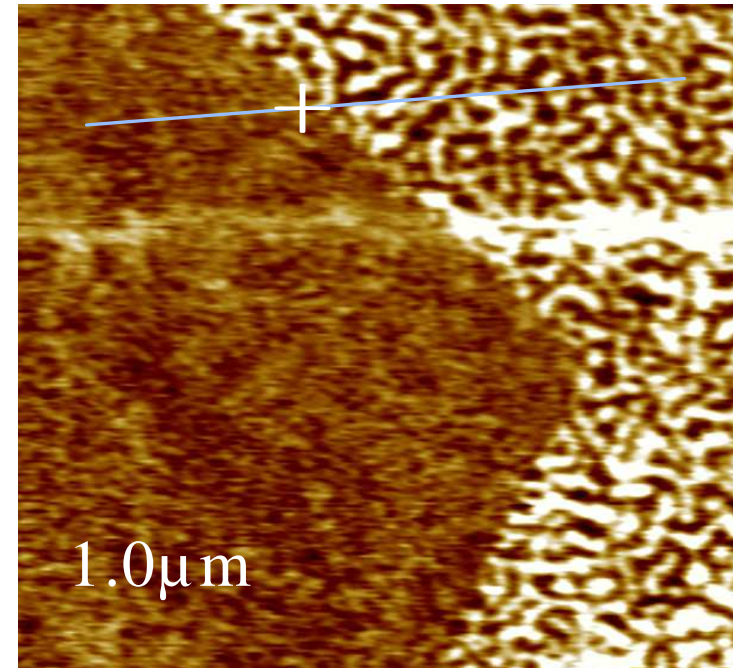
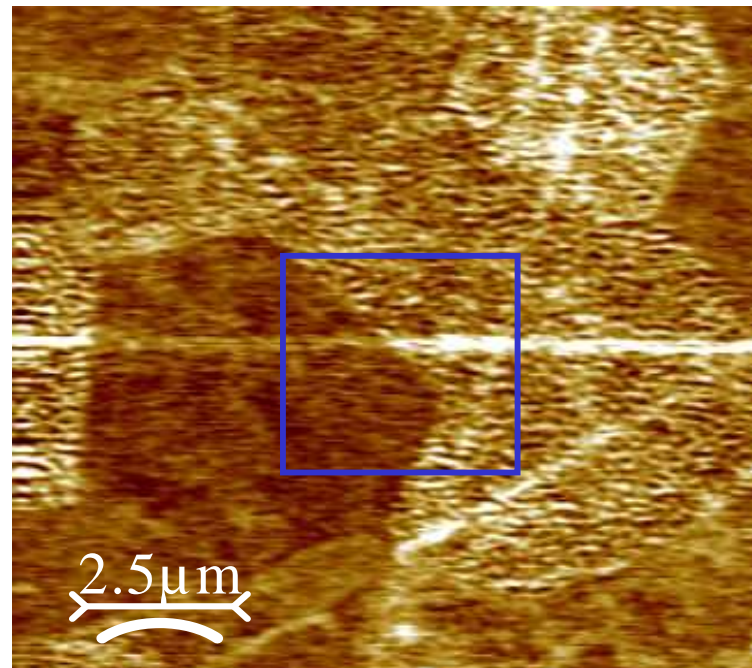


**hot-pressed electrooptic  
PLZT 9/65/35  
at higher magnification**

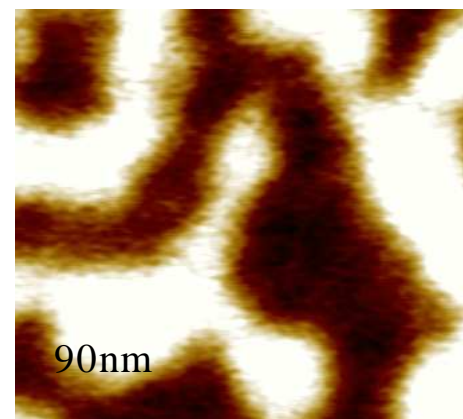


**chemically etched PLZT 7/65/35  
in reflected light.**

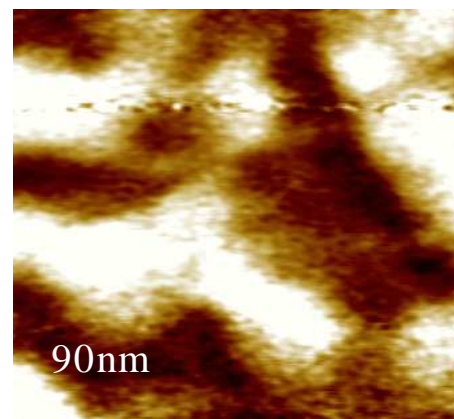
# *As-grown domains in PLZT 9.75/65/35*



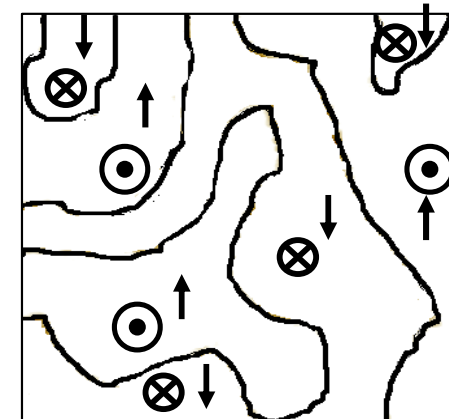
vertical piezoresponse



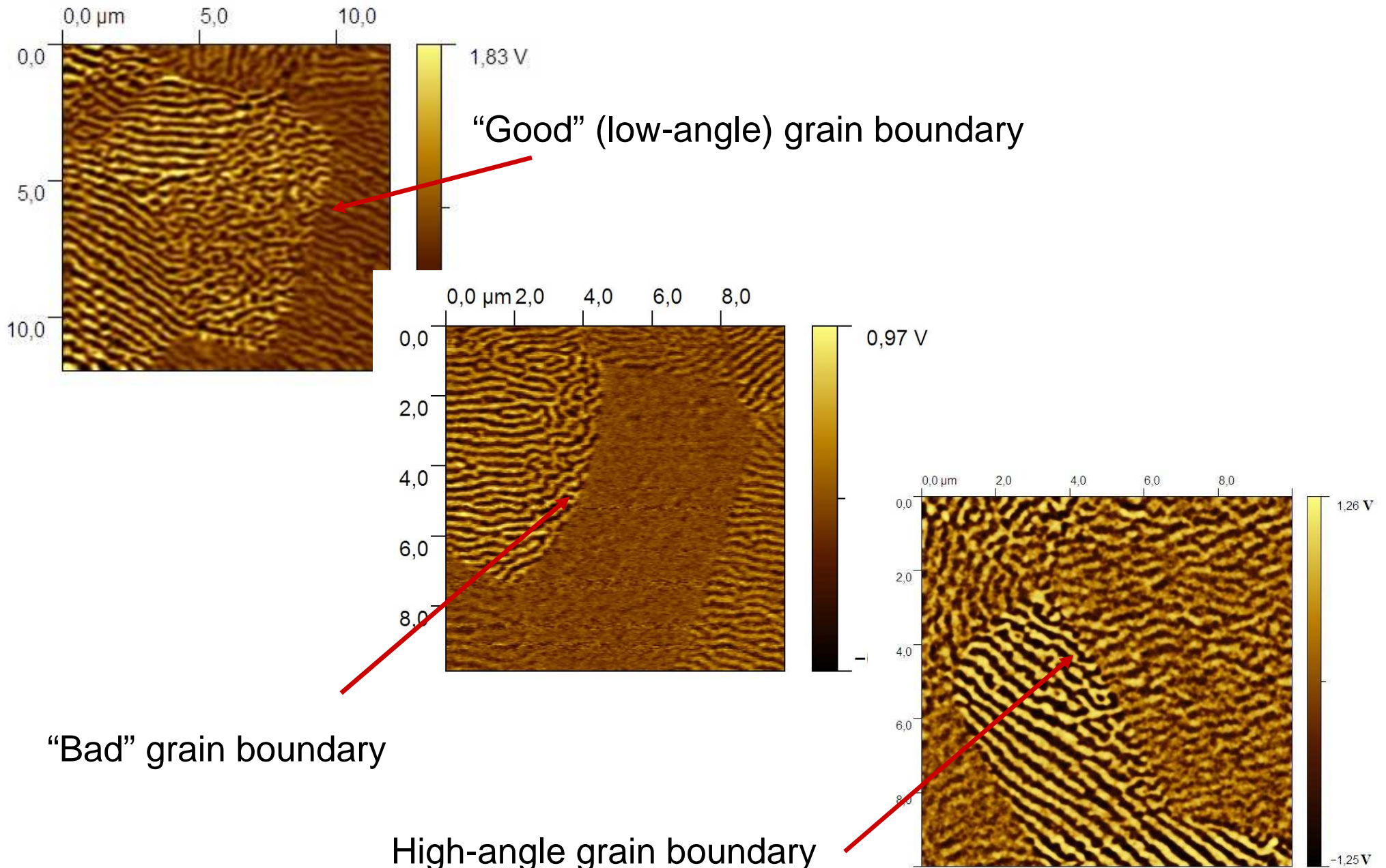
lateral piezoresponse



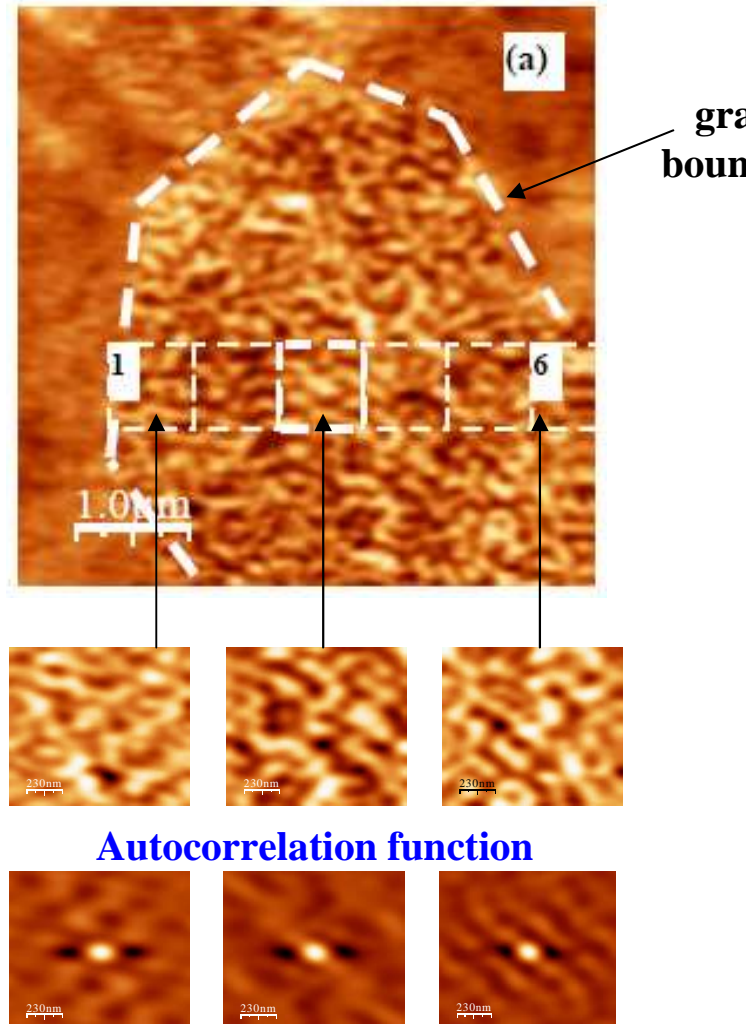
reconstructed domains



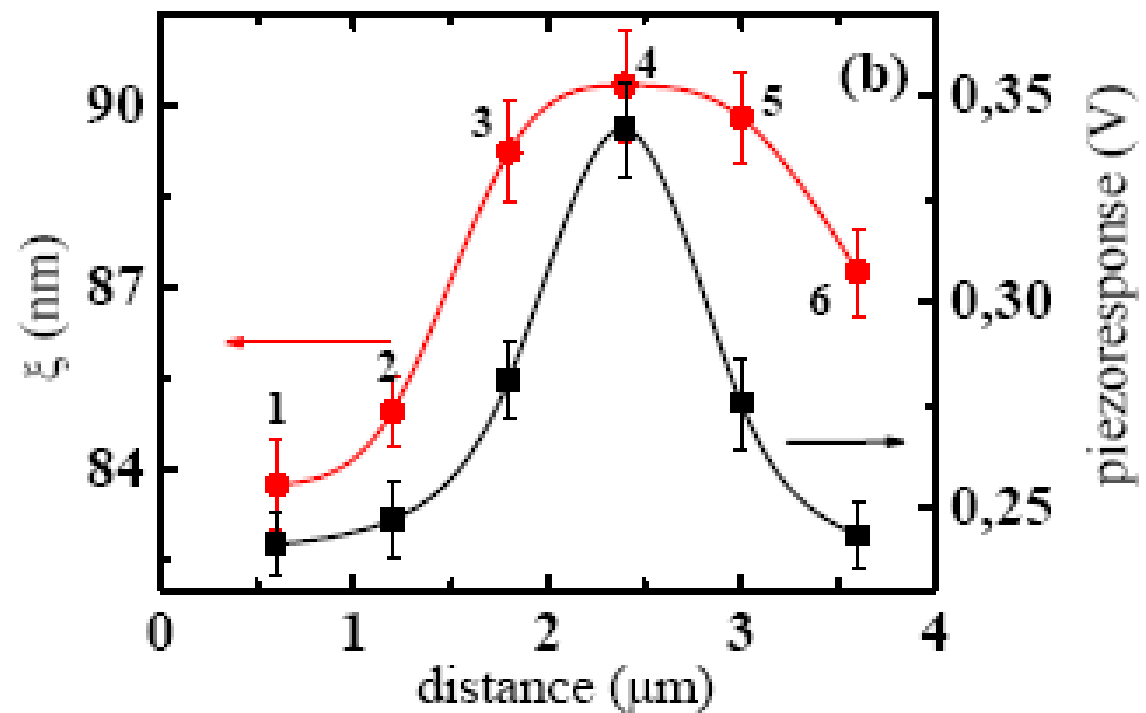
# Effect of grain boundaries in PLZT 9.5/65/35



# Mesoscale variations of correlation length

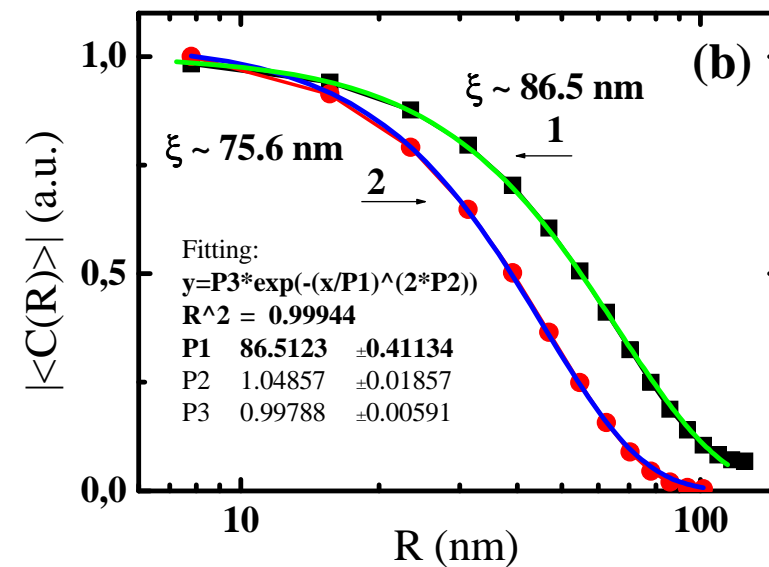
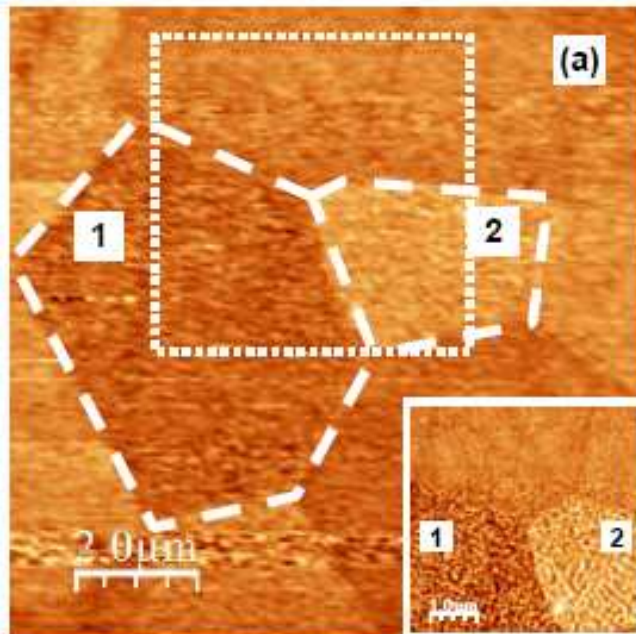


$$\langle C(r) \rangle = \sigma^2 \exp \left[ - \left( \frac{r}{\langle \xi \rangle} \right)^{2h} \right]$$

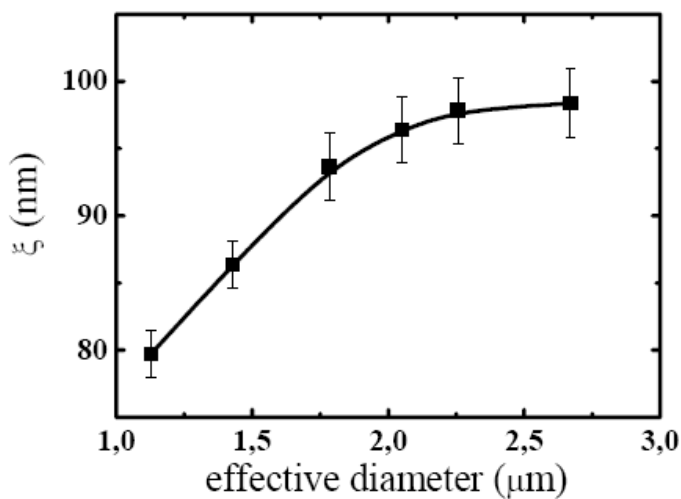


2D image of  $C(r)$  represents areas with correlated (parallel) polarization (bright contrast) and areas with antiparallel polarization (dark contrast)

# Grain size effect in PLZT

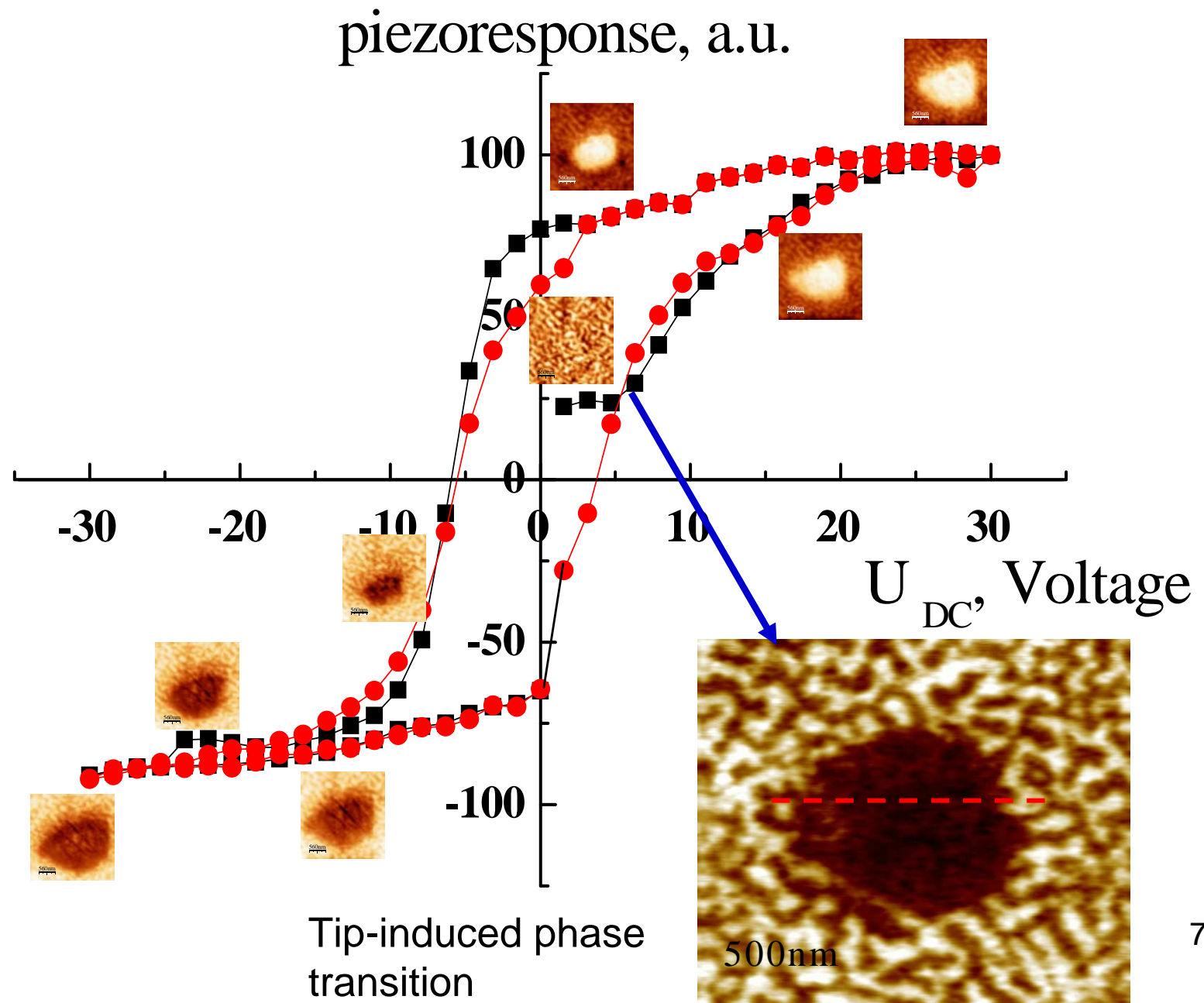


Piezoresponse images of two neighboring grains (a) and the corresponding autocorrelation functions (b) showing difference of the correlation lengths in grains of different dimensions.

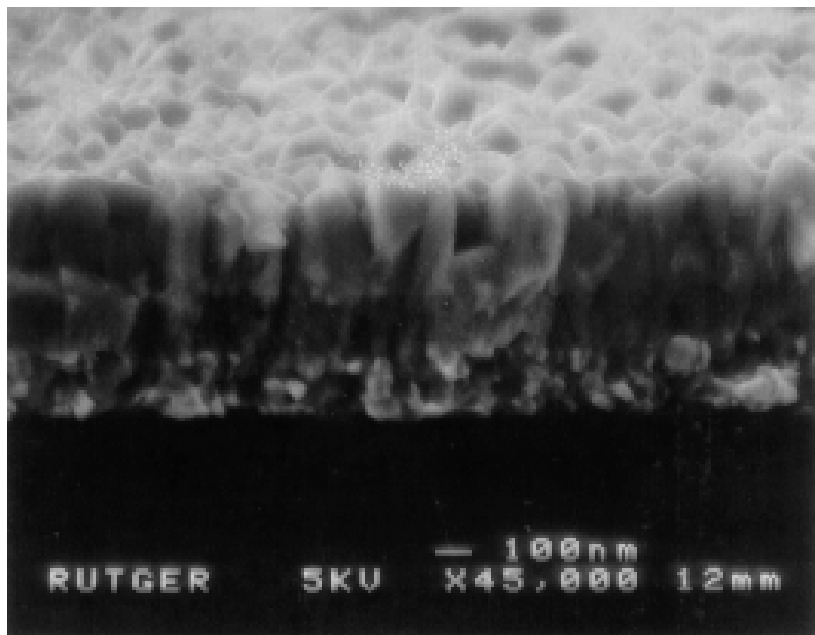


Average correlation length in PLZT ceramics taken over entire grain as a function of its effective diameter.

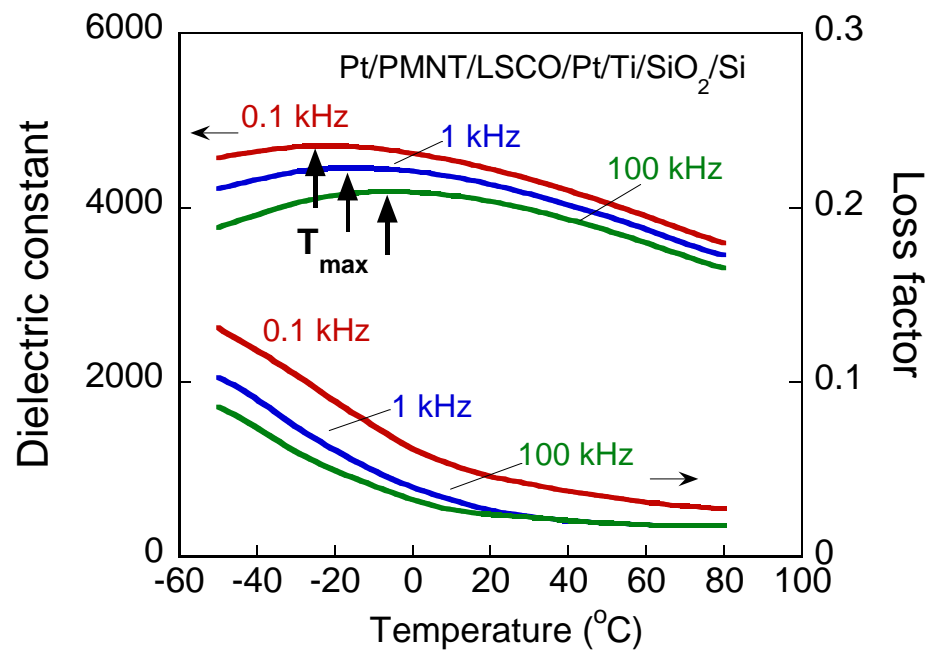
## Hysteresis in relaxor PLZT 9.75/65/35



## Relaxor PMN-10%PT films by PLD



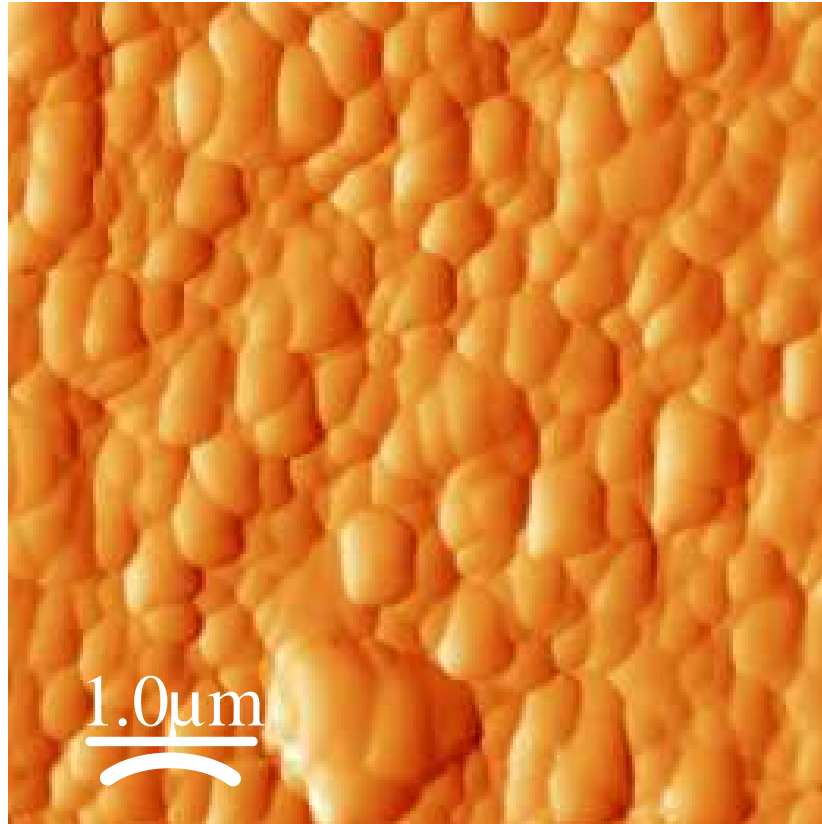
SEM cross-section



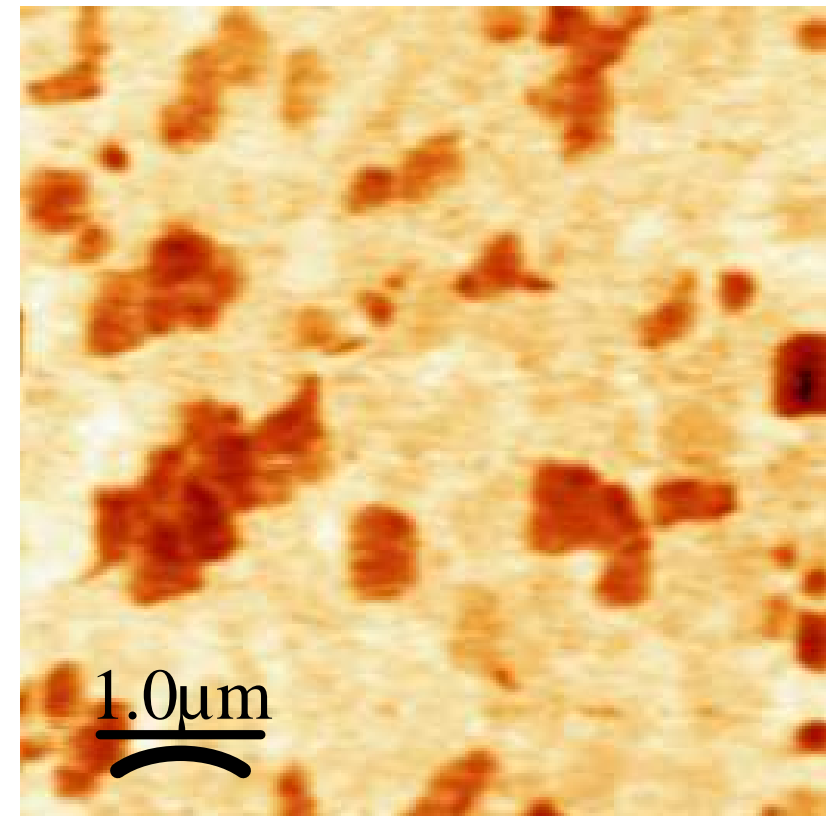
Dielectric properties

# Piezoresponse in PMN-10%PT films

Topography

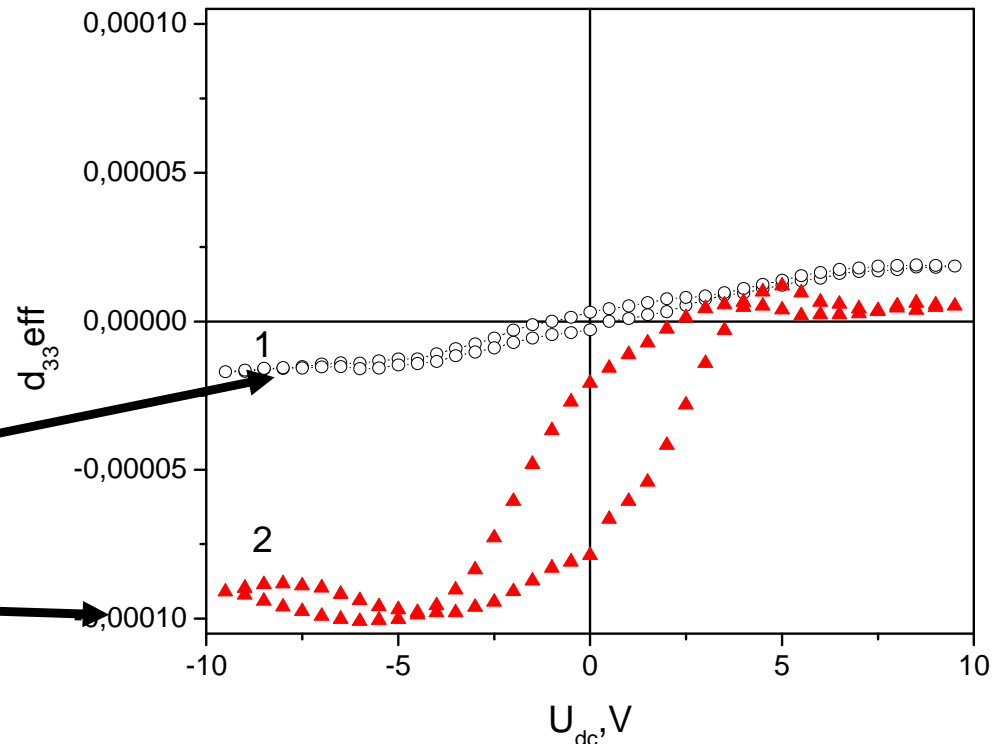
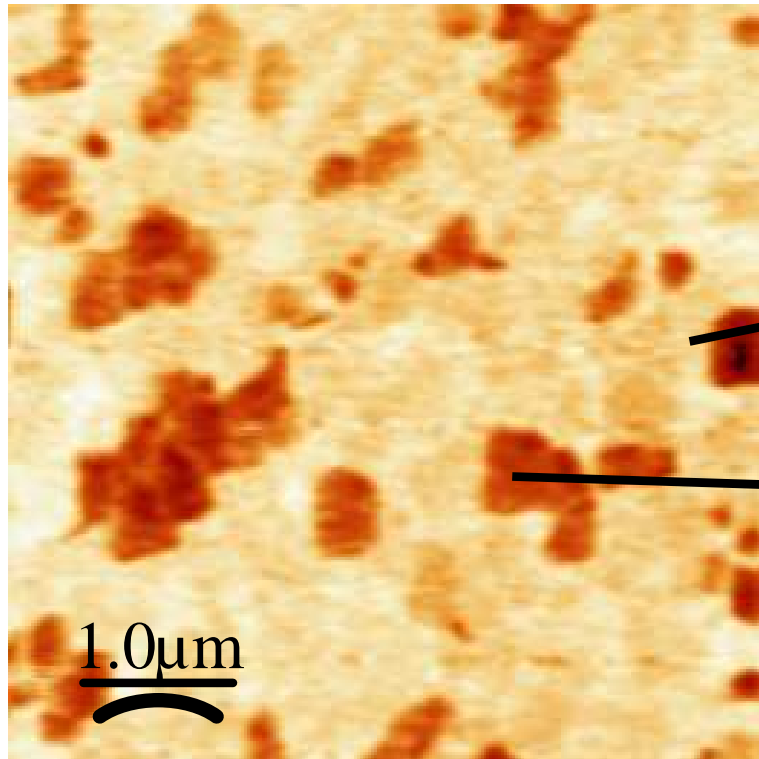


Piezoresponse



- Strong piezoelectric contrast inside some grains
- No nanodomains observed due to small grain size

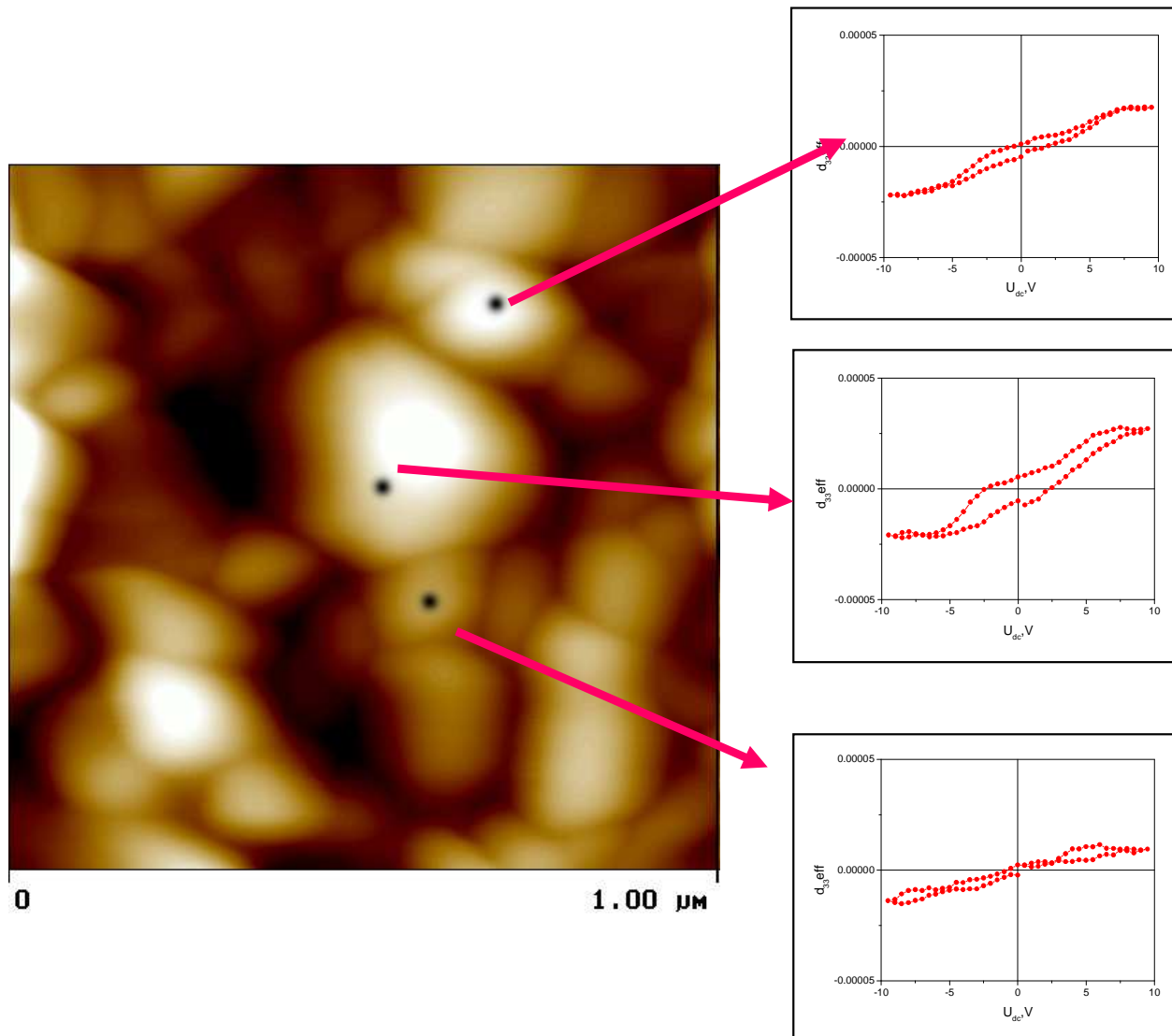
# Nanoscale hysteresis in PMN-10%PT films



- ~ 20% of the grains are in ferroelectric state (ferroelectric hysteresis)
- ~ 80% of the grains are in relaxor state (slim hysteresis loops)

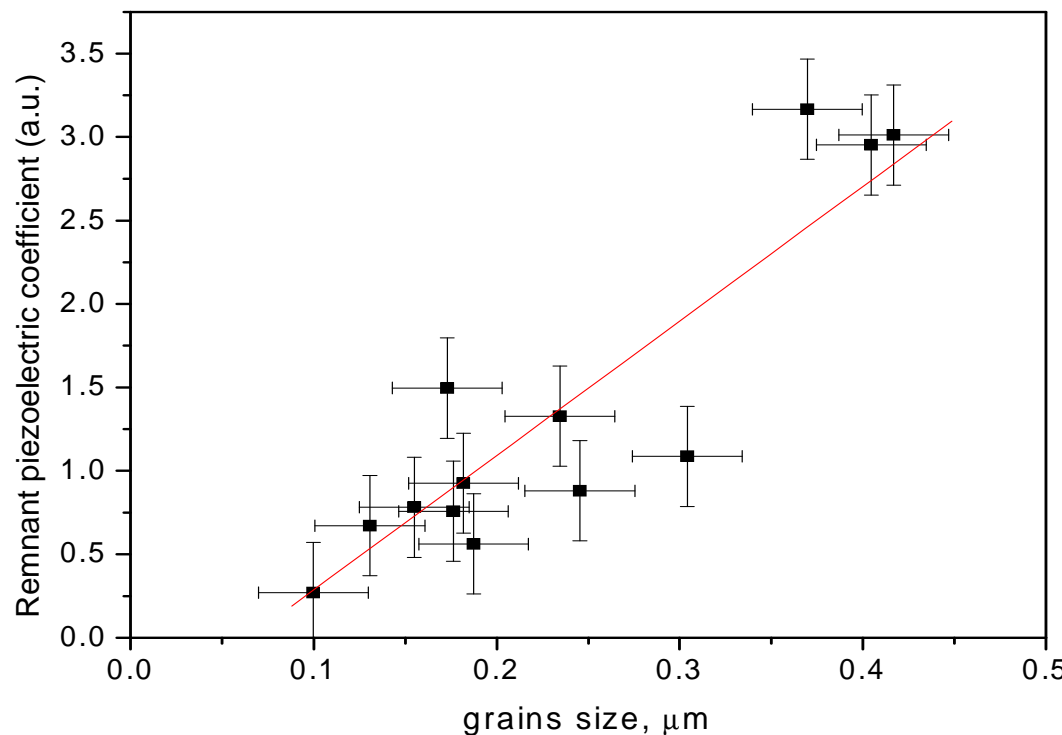
76

# Hysteresis vs. grain size in PMN-10%PT



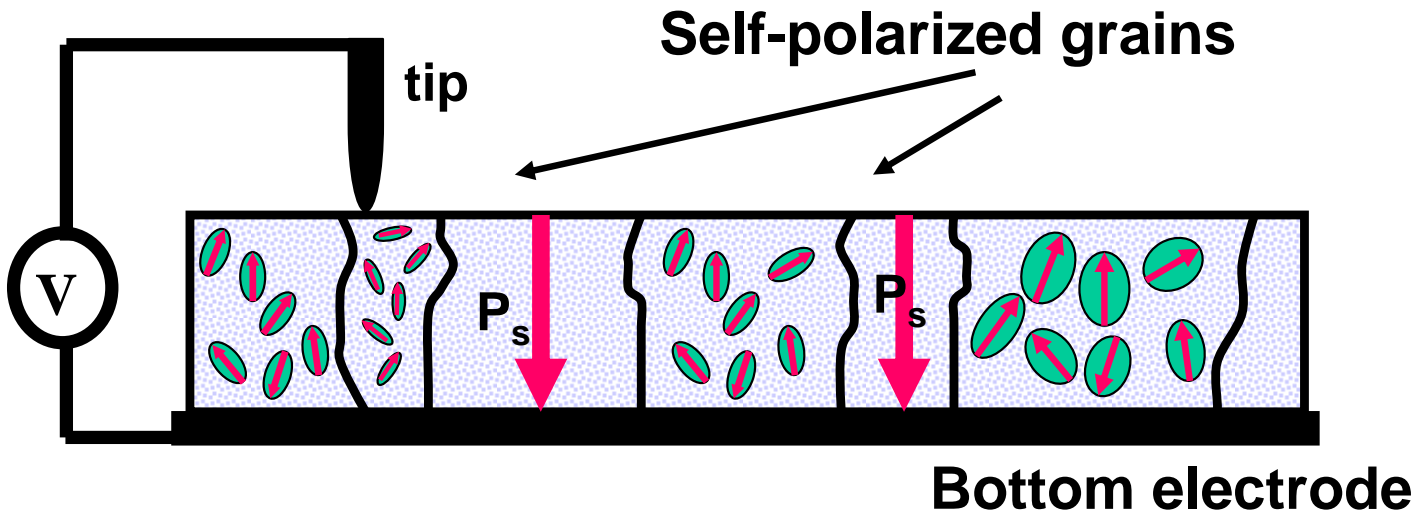
- Distinct grain size effect in relaxor grains

# Grain size effect in PMN-10%PT films



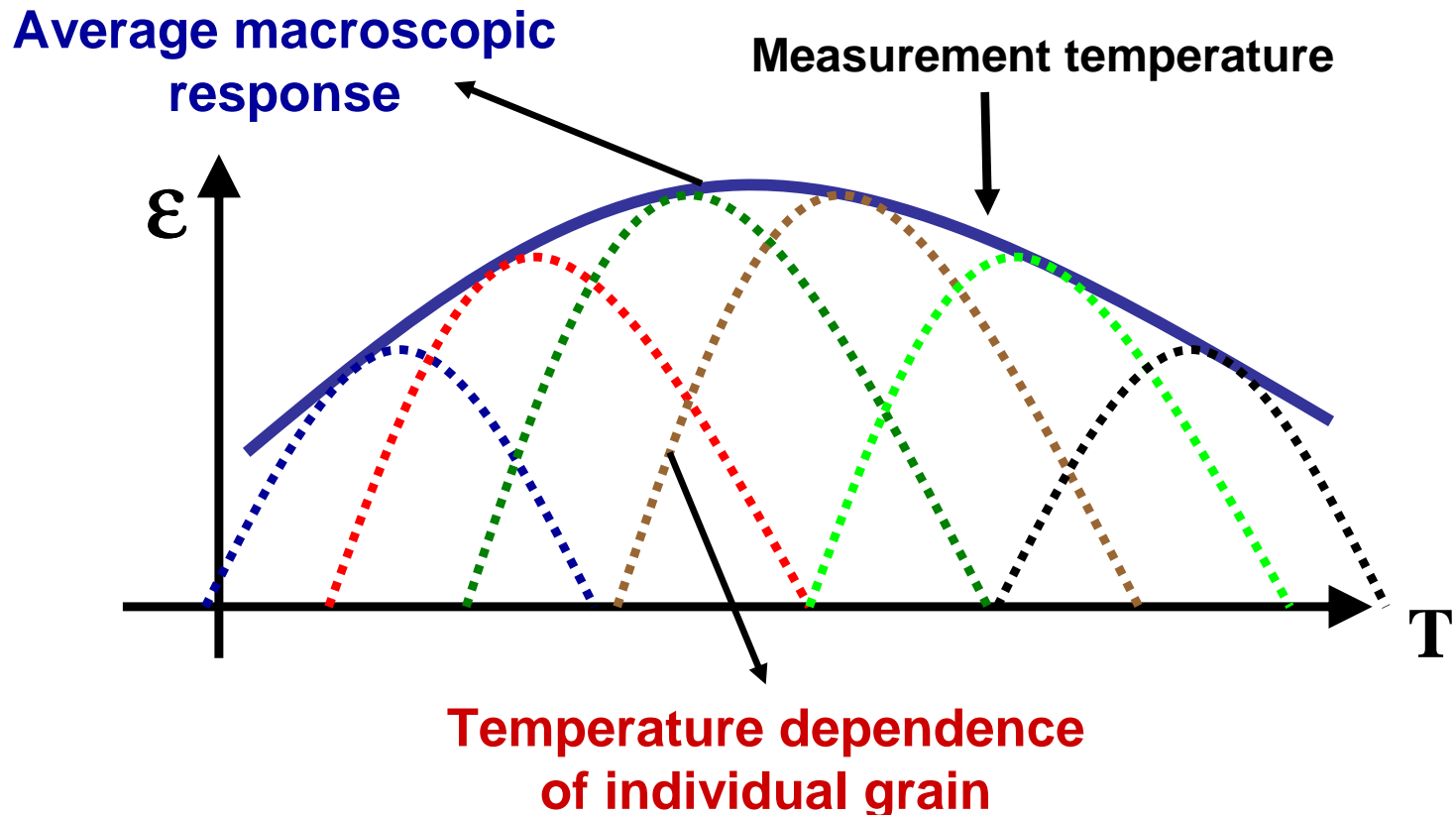
- Mechanical clamping by adjacent grains  
**larger grains are less stressed**
- Inhomogeneous distribution of  $\text{PbTiO}_3$   
**Smolensky model at mesoscopic scale**
- Influence of orientation

# Schematic of PNRs in PMN-PT films



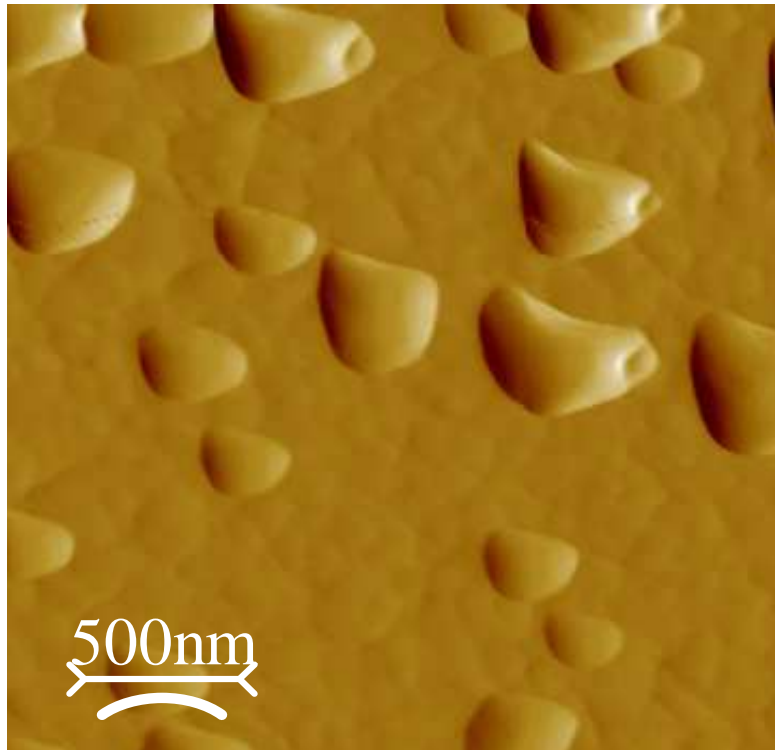
- Macroscopic properties are determined by the average response of the individual grains and can be probed by PFM
- Local variation of the dielectric response determines diffuseness of the phase transition.

# Origin of broad temperature peak in relaxor films

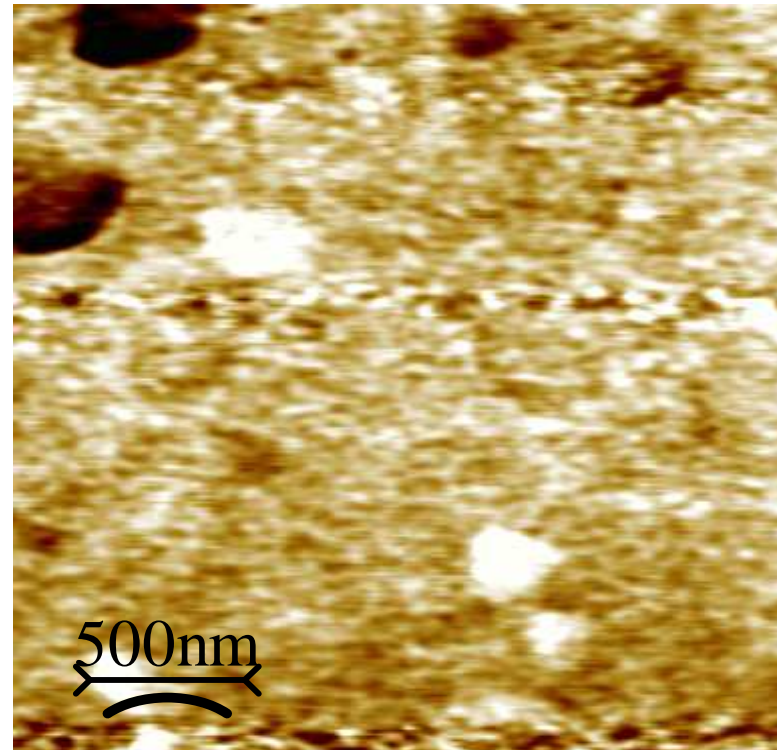


# Piezoresponse of as-grown PMN films

Topography

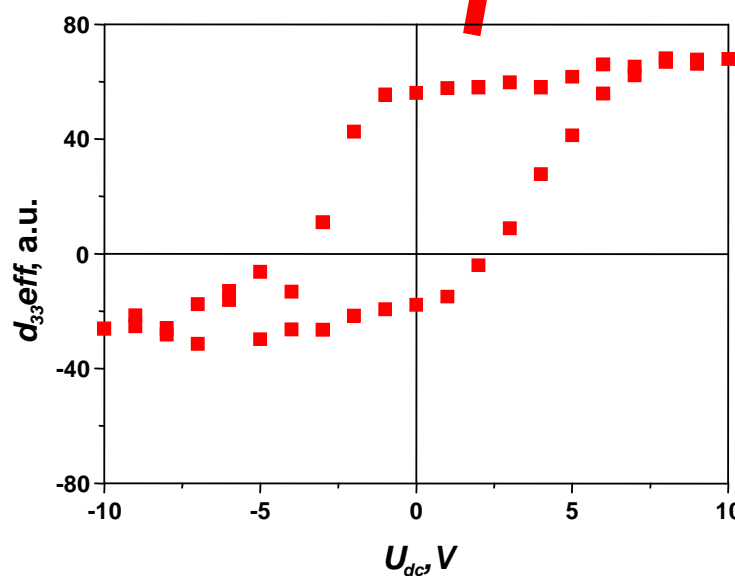
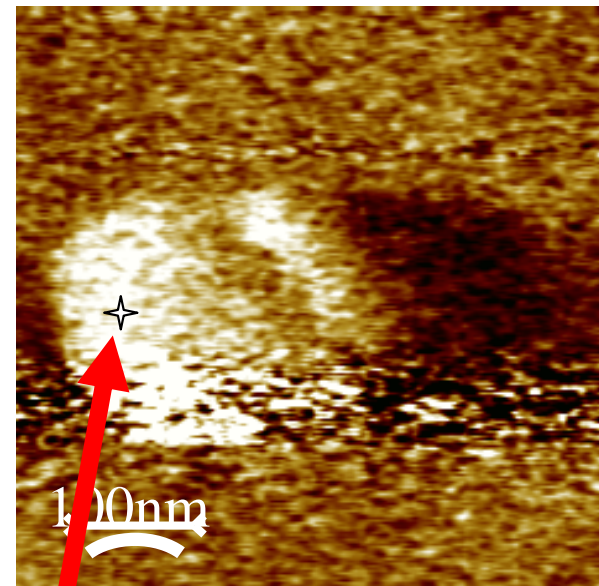
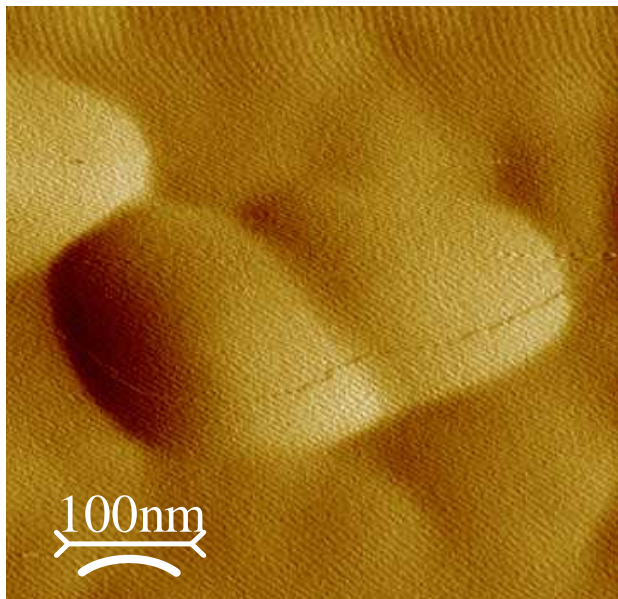


Piezoresponse



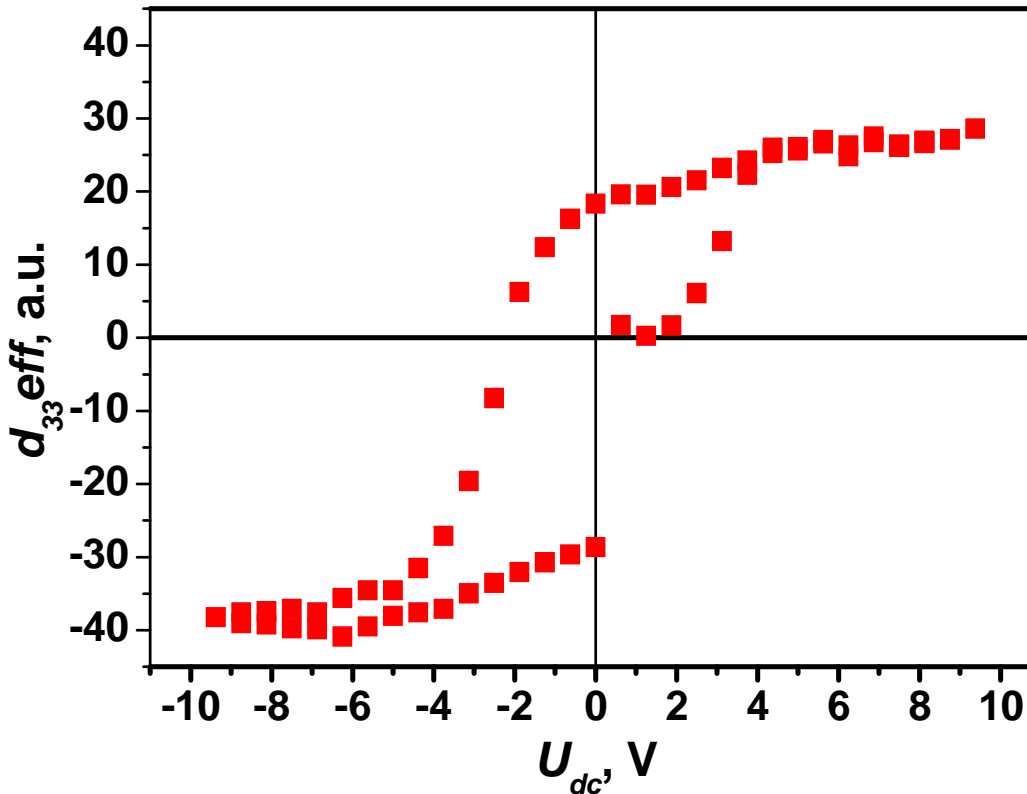
- Single crystalline grains with in-plane orientation of facets
- Protruding outgrowths are self-polarized with both black and white contrast (phase difference  $\sim 180^\circ$ )

# Hysteresis in “ferroelectric” grains



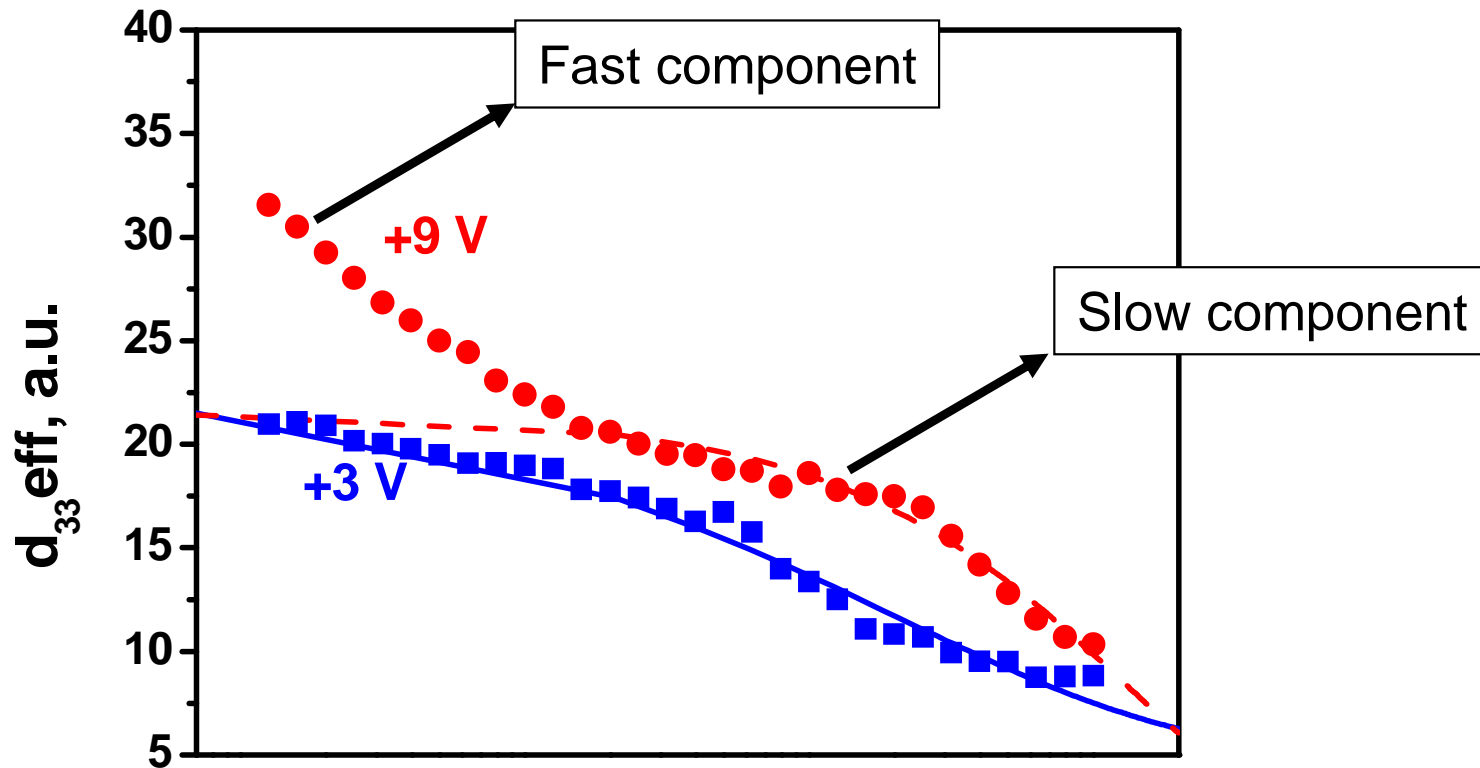
- “Normal” ferroelectric hysteresis with notable offset

# Hysteresis measured on “relaxor” surface



- Switching into ferroelectric state at  $V_c \approx 2$  V
- Polar state is unstable and slowly decays at room temperature

# Relaxation kinetics of locally induced polarization



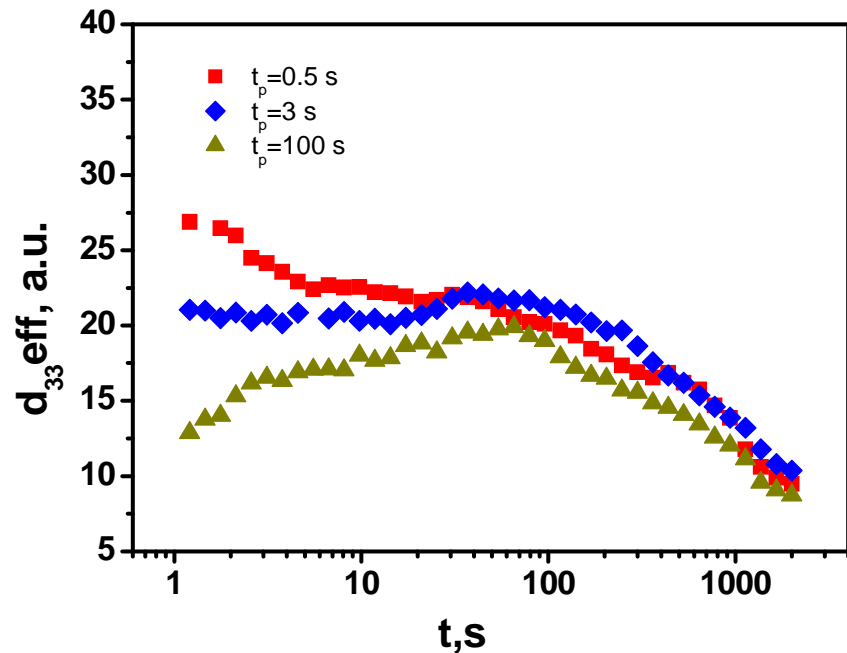
Kohlrausch-type dependence of slow component:  $d_{33}^{eff} \propto \exp\left[-\left(\frac{t}{\tau}\right)^{\beta}\right]$

## Parameters of Kohlrausch exponent

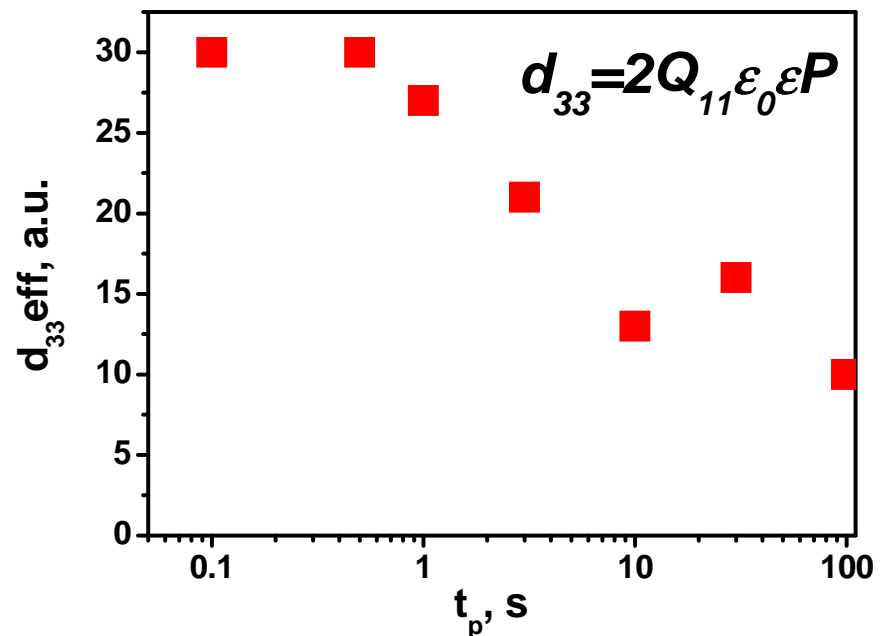
Voltage pulse height $V_{dc}$ , V	Parameters of the slow relaxation fitted with Kohlrausch exponent	
	$\tau$ , s	$\beta$
3	600	0.34
6	1400	0.5
9	1400	0.7
12	2000	0.7
15	1500	0.7

- Change of the relaxation time spectrum with increasing poling voltage

# $d_{33}$ suppression under long poling



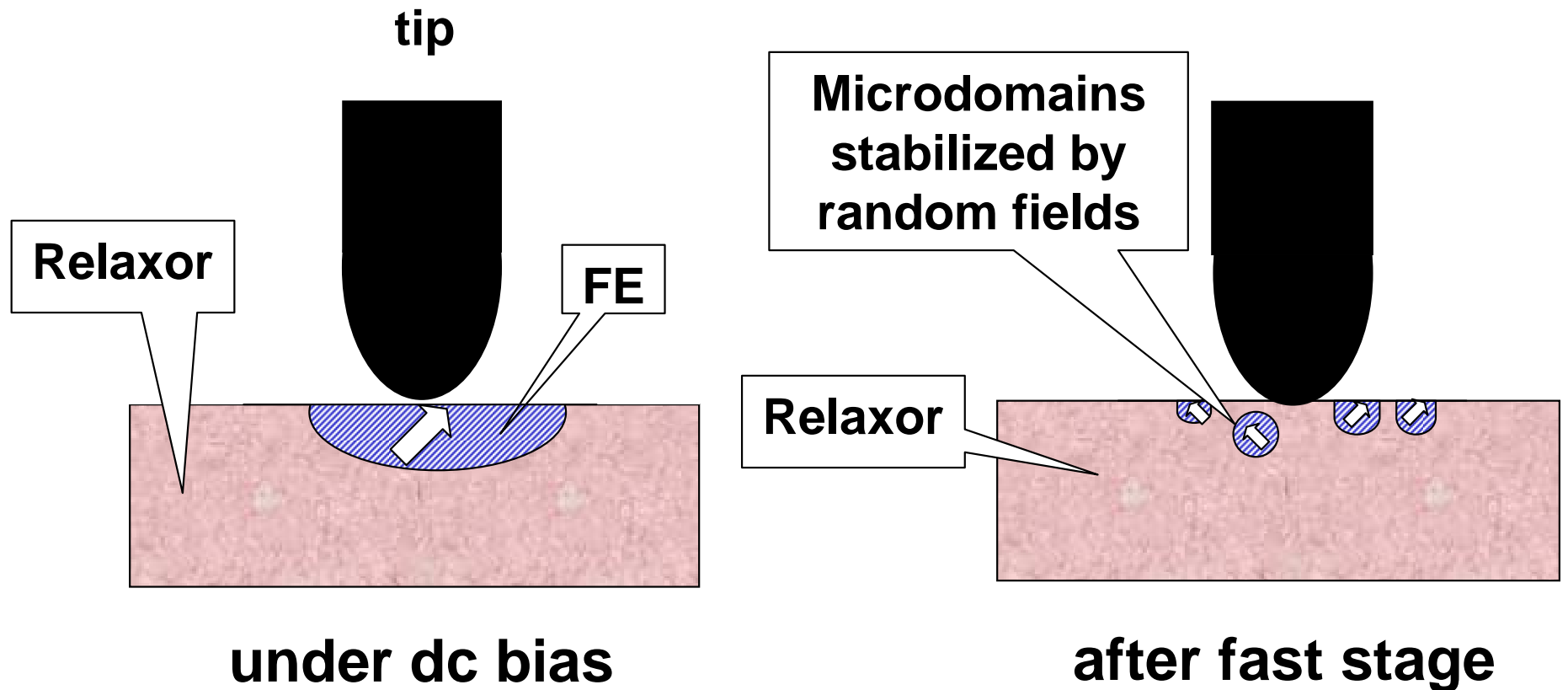
Slow stage disappears  
if  $t_p < 5$  s



Initial  $d_{33}$  is suppressed  
under long poling

- $d_{33}$  suppression under long poling could be due decrease of dielectric constant in polar area larger than the tip size.
- Fast relaxation after long poling is due to recovery of dielectric constant in the nearby-tip area.

# Model of polarization relaxation



- Fast stage: relaxation of internal bias that stabilizes polar state.  
Possible cause: drift of oxygen vacancies and pn-junction formation.
- Slow stage: thermal splitting of microdomains into nanoclusters.

# Conclusions

- Several hierarchical length scales accessible by PFM in several families of relaxors
- Apparent correlation length is several times greater than that expected from scattering and is sensitive to disorder, doping and temperature
- PNR coalescence and self-organization into regular ferroelectric domains demonstrated
- Nanoscale domains plays important role in switching and giant piezoresponse in PZN-PT
- Grain boundary effect in relaxor ceramics and films is demonstrated and explained on a local scale